Aus dem Institut für Pharmakologie und Toxikologie
des Universitätsklinikums Aachen
Direktor: Prof. Dr. Stefan Uhlig

vertreten in der Technisch-Naturwissenschaftlichen Fakultät
der Universität zu Lübeck
durch Prof. Dr. Jürgen Westermann

Gene regulation in the lungs by ventilatory stress and by TLR-ligands

Inauguraldissertation
zur
Erlangung der Doktorwürde
der Universität zu Lübeck
-Aus der technisch-naturwissenschaftlichen Fakultät-

vorgelegt von

Martina Barrenschee

aus Itzehoe

Lübeck, 2009

Erstberichterstatter: Prof. Dr. J. Westermann

Zweitberichterstatter: Prof. Dr. S. Uhlig

Vorsitz: Prof. Dr. E. Hartmann

Tag der mündlichen Prüfung: 12. April 2010

Durch unser Wissen unterscheiden wir uns nur wenig
in unserer grenzenlosen Unwissenheit aber sind wir alle gleich
Sir Karl R. Popper

Danksagungen

Die vorliegende Arbeit wurde am Forschungszentrum Borstel, Abteilung Immunchemie und Biochemische Mikrobiologie in der Laborgruppe Lungenpharmakologie und am Institut für Pharmakologie und Toxikologie des Universitätsklinikums Aachen angefertigt.

Ein besonderer Dank gilt Prof. Dr. Stefan Uhlig für die Möglichkeit meine Doktorarbeit sowohl innerhalb seiner Arbeitsgruppe am Forschungszentrum Borstel, als auch am Institut für Pharmakologie und Toxikologie in Aachen anfertigen zu können. Zusätzlich danke ich ihm für seine ständige Diskussionsbereitschaft, die Anregungen und Ideen, sowie die stete Unterstützung.

Herrn Prof. Dr. Jürgen Westermann sei herzlich für die Bereitschaft, die Erstberichterstattung zu übernehmen, gedankt.

Für eine erfolgreiche Kooperation möchte ich mich bei Dr. Tamás Dolinay und Prof. Dr. Augustine Choi aus Pittsburgh bedanken, für die Bereitstellung des LPS für diese Arbeit danke ich herzlich Prof. Dr. Helmut Brade aus Borstel.
Für die hilfreichen Ratschläge und Denkanstöße in der Anfangsphase meiner Promotion sei Dr. Heike Dombrowsky aus Borstel gedankt.
Für die Einarbeitung in das komplexe Modell der isoliert perfundierten Mauslunge bedanke ich mich bei Dörte Karp und Dag Friedrichs aus Borstel.
Durch die Kompetenz und Freundlichkeit von Kerstin Viertmann aus Borstel und Birgit Feulner aus Aachen entstand eine hervorragende Zusammenarbeit an der Real-Time PCR, für die ich mich ebenfalls herzlich bedanken möchte.

Für die netten Gespräche, die meinen Laboralltag in Aachen immer aufgelockert haben und stete Hilfsbereitschaft, danke ich herzlich Marion Peters.

Einen besonderen Dank gilt Dr. Eike Reppien, für die gute Arbeitsatmosphäre in Borstel und ihre Freundschaft, die mich durch die Jahre hinweg begleitet hat.

Danken möchte ich weiterhin allen Mitarbeitern der Laborgruppe von Prof. Dr. Helmut Brade aus Borstel und der Laborgruppe von Prof. Dr. Günther Schmalzing aus Aachen für die angenehme Arbeitsatmosphäre und Kollegialität im Laboralltag.

Familie Stickeler aus Kornelimünster danke ich für die freundliche Aufnahme in ihr Haus, die angenehme Nachbarschaft und liebevolle Fürsorge, die meinem Mann und mir in der Zeit in Aachen zuteil wurde.

Weiterhin möchte ich mich bei meinen Freunden und meiner Familie bedanken, die mich durch ihr Engagement und ihren Glauben an mich auch in schwierigen Zeiten der Promotion nach all ihren Kräften unterstützt haben.
Meinen Eltern und Schwiegereltern gilt hierbei ein besonderer Dank für die stete finanzielle und sachliche Unterstützung, insbesondere während der Endphase meiner Promotion.
Katrin, Judith, Heiko, Manfred, Simone, Martin, Nicole, Almut und Timbo, danke für eure Freundschaft und Unterstützung all die Jahre hindurch. Ich bin froh, wieder bei euch zu sein.

Mein größter Dank gilt jedoch meinem Mann Sven, der mich in allen Lebenslagen unterstützt, mir den Rücken stärkt und freihält, und auf den ich mich immer verlassen kann. Danke für deine Liebe.

Publications contributing to this study

Dolinay, T., N. Kaminski, M. Felgendreher, H. P. Kim, P. Reynolds, S. C. Watkins, D. Karp, S. Uhlig, and A. M. Choi. 2006. Gene expression profiling of target genes in ventilator-induced lung injury. *Physiol. Genomics 26:68-75.*

Spieth, P. M., A. R. Carvalho, P. Pelosi, C. Hoehn, C. Meissner, M. Kasper, M. Hubler, N. M. von, C. Dassow, M. Barrenschee, S. Uhlig, T. Koch, and M. G. de Abreu. 2009. Variable tidal volumes improve lung protective ventilation strategies in experimental lung injury *Am.J.Respir.Crit Care Med. 179:684-693.*

Dombrowsky, H., M. Barrenschee, M. Kunze, and S. Uhlig. 2009. Conserved responses to trichostatin A in rodent lungs exposed to endotoxin or stretch *Pulm.Pharmacol.Ther. 22:593-602.*

Barrenschee, M., S. Uhlig. 2009.
Effects of two TLR2 agonists in isolated mouse lungs
PLoS One, submitted

Abstracts

M. Barrenschee, S. Uhlig, U. Uhlig, Amphiregulin Induction of Proinflammatory Signaling Pathways in Isolated Perfused Mouse Lungs
Am. J. Respir. Crit. Care Med., Apr 2008;177: A101

C. Dassow, C. Martin, M. Barrenschee, S. Uhlig, Induction of Amphiregulin in Precision-Cut Lung Slices *Am. J. Respir. Crit. Care Med., Apr 2008;177:* A65

S. Uhlig, U. Uhlig, M. Felgendreher
From stretch to inflammation: Molecular mechanisms of biotrauma
Acta Physiologica 2007; Volume 189, Supplement 653

Table of Contents

Abbreviations

Akap12	A kinase anchor protein 12
ALI	Acute lung injury
AM	Alveolar macrophages
Angptl2	Angiopoietin-like 2
Anxa1	Annexin A1
AR	Amphiregulin
ARDS	Acute respiratory distress syndrome
Areg	Amphiregulin
B2m	Beta 2 microglobulin
BAL	bronchoalveolar lavage
C	Celsius
cDNA	Copy desoxyribonucleic acid
C_L	Lung compliance
Cldn4	Claudin 4
Cldn7	Claudin 7
cm H_2O	Centimetre water column
Cxcl1	Chemokine (C-X-C motif) ligand 1
Cxcl10	Chemokine (C-X-C motif) ligand 10
Cxcl2	Chemokine (C-X-C motif) ligand 2
Cyr61	Cystein rich protein 61
DMSO	Dimethylsulfoxide
DNA	Desoxyribonucleic acid
dsDNA	Double strand desoxyribonucleic acid
ECM	Cell extracellular matrix
EDTA	Ethylendiamin Tetraacetate
EEP	End expiratory pressure
EGFR	Epidermal growth factor receptor
EGFRI	Epidermal growth factor receptor inhibitor
EGTA	Ethylene glycol tetraacetic acid
EIP	End inspiratory pressure
E_L	Lung Elastance
ELISA	Enzyme linked immunosorbant assay
ERK	Extracellular regulated kinase
Fgfbp1	Fibroblast growth factor protein 1
GADD45	Growth Arrest and DNA Damage 45
GM-CSF	Granulocyte macrophage colony-stimulating factor

h	Hour
Hbegf	Heparin-binding EGF-like growth factor
HES	Hydroxyethyl starch
Hprt1	Hypoxanthine phosphoribosyltransferase 1
Hspb8	Heat shock 22kDa protein 8
ICAM-1	Inter-Cellular Adhesion Molecule 1
IKK	I kappa B kinase
IL	Interleukin
Il11	Interleukin 11
Il1b	Interleukin 1 beta
Il6	Interleukin 6
IPL	Isolated perfused mouse lungs
IRAK	IL-1 receptor-associated kinases
IRF-3	Interferon regulatory factor 3
IRF-7	Interferon regulatory factor 7
JNK	c-Jun N-terminal kinases
KDa	Kilodalton
Klf5	Krüppel-like zinc-finger transcription factor 5
LPS	Lipopolysaccharide
MALP-2	Macrophage activating protein 2 KDa
min	Minute
mmHg	millimetre mercury column
MODS	Multiple organ dysfunction syndrome
mOsm	miliosmole
mRNA	Messenger ribonucleic acid
MV	mechanical ventilation
MyD88	Myeloid differentiation primary response gene (88)
NaCl	sodium chloride
NF-κB	Nuclear factor-kappa B
NO	Nitric oxide
NOS	Nitric oxide synthase
Nr4a1	Nuclear receptor subfamily 4, group A, member 1.
P	Pressure
PAF	Platelet-activating factor
Parg	Poly (ADP-ribose) glycohydrolase
PBS	Phosphate buffered saline
pERK	phospho-extracellular regulated kinase
PI3K	Phosphoinositide 3 kinases
pJNK	Phospho-c-Jun N-terminal kinases
PKB	Protein kinase B
PMN	Polymorphonuclear neutrophilic leukocytes

PRR	Pattern recognition receptor
Ptgs2	Prostaglandin-endoperoxide synthase 2
qPCR	Quantitative real time polymerase chain reaction
R_L	Lung resistance
RNA	Ribonucleic acid
ROS	Reactive oxygen species
Rpl32	Ribosomal protein L32
RT	Room temperature
RTK	Receptor tyrosine kinases
RT-qPCR	Reverse transcriptase-quantitative real time polymerase chain reaction
s	second
SAPK	Stress-activated protein-kinases
SDS-PAGE	Sodium dodecyl sulfate polyacrylamide gel electrophoresis
SEM	Standard error of the mean
Slpi	Secretory leukoprotease inhibitor
SOCS	Suppressors of cytokine signalling
t	Time
T	Temperature
TBS	Tris buffered saline
TBS-T	Tris buffered saline-Tween®-20
TEMED	Tetramethylethylendiamin
TLR	Toll-like receptor
Tnc	Tenascin c
Tnf	Tumor necrosis factor
Tollip	Toll interacting protein
Traf1	TNF receptor-associated factor 1
TRAF6	TNF receptor-associated factor 6
TRIAP	Toll-interleukin 1 receptor (TIR) domain-containing adaptor protein
TV	Tidal volume
Tyk2	Tyrosine kinase 2
UV	Ultraviolet
V	Volume
VILI	Ventilator-induced lung injury

1.Introduction

1.1. The lungs

During the evolution of the predominantly oxidative earth atmosphere, organisms developed whose energy metabolism depends on O_2 as an oxidant. The oxidative metabolism requires a constant exchange of oxygen and carbon dioxide between organism and environment [1]. While in protozoa gases can cross the cell membrane directly, most higher metazoa developed special respiratory epithelia to ensure gas exchange. Land-living vertebrates developed lungs as the inversion of the body surface. This enlarged respiratory surface area exceeds the body surface by a multiple [1]. Thus, humans need a respiratory lung surface of approx. 100 m^2 [2] in order to be able to cover their oxygen demand of approx. 300 $ml \cdot min^{-1}$ at rest and of up to 3 $l \cdot min^{-1}$ at hard work [3].

1.1.1.Functional anatomy and physiology of the lungs

1.1.1.1. General arrangement

The lungs, located within the upper chest, behind the ribs and the sternum are part of the human respiratory system, which also includes the diaphragm and chest muscles, the nose and mouth, the pharynx and trachea and finally the bronchial tree. The two pary attached lung lobes are covered with a thin membrane, known as pleura which completes the pleura cavity except for the pleural space, where negative pressure prevent collapsing of the lungs at end expiratory state [4].

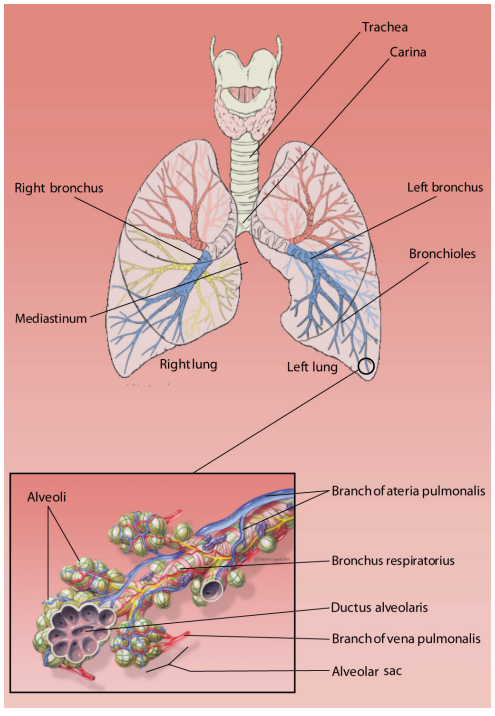

Figure 1 Overview of lung anatomy. Pictures created by Lynch *et al.* [5, 6].

The trachea divides into the left and right bronchus at the carina. The space between the lungs, in the middle portion of the upper chest (thorax) is known as the mediastinum. The lymph nodes are located within and around the lungs and the mediastinum. The trachea divides into two main airways called bronchi upon reaching the lungs; one bronchus serves the right lung and the other one the left lung. The bronchi subdivide up to 23 generations ending in the alveolar

ducts. Down to the terminal bronchioles, at the 16th generation, the airways are lined with cartilage. From the 17th generation of airway branching, alveoli can be observed with increasing density up to the final airway generation, the so called *Ductuli alveolares*. At the end of each alveolar duct, clusters of approx. 20 alveoli (alveolar sacs) are placed, where the oxygen transport occurs [2]. Whereas pulmonary stiffness of the respiratory tract due to trachea cartilages and plates decreases with each generation of branching, smooth muscle that coat the airways relatively increases [7]. Bronchioles miss cartilages and therefore smooth muscle closely surrounds the airways [4].

1.1.1.2. Blood supply of the lungs

Blood supply of human lungs occurs in two independent systems. First, bronchiolar vessels, that branch off from the aorta provides the lung tissue with blood from the lung hilum to the terminal bronchioli. This so called bronchial circulation is not involved in gas exchange. Venous blood of the bronchial circulation partly ends in veins of the systemic circulation, additionally to some extent blood is discharged by the pulmonary veins [8].

Second, pulmonary arteries, forming the pulmonary circulation arise from the *truncus pulmonalis*, leading along the airways and finally envelop alveoli as a capillary network. Lung capillaries with a diameter of approx. 13 µm represent the alveolo-capillary unit for gas exchange between blood and air. The alveolo-capillary unit is composed of the alveolar epithelium, a small interstitium and the capillary endothelium, allowing the diffusion of gases due to its thinness of 0.4 to 2 µm [9]. Pulmonary veins containing oxygenated blood lead along segmental septi to the hilum and finally back to the right atrium of the heart [10].

1.1.1.3. Composition of alveoli

It has been calculated that approx. 300 million alveoli contribute to the respiratory region of the lungs, each supplied by 1.000 capillary segments. The total number of cells that constitute the alveolar lining is about 19 x 10^9 [2], where two cell types are predominantly recognized. The flat type I cells (AT I) provide the oxygen transport and cover approx. 93 % of the alveolar surface area, forming the external part of the blood air barrier as a thinly single-layered squamous epithelium [11]. The cuboidal type II cells (AT II) making up 7 % of the alveolar surface area produce the pulmonary surfactant [12], that reduces the surface tension in alveoli and by that increases pulmonary compliance and prevents the lungs from collapse at the end of expiration [13]. In addition, AT cells are responsible for the transepithelial movement of ions [14] and water [15] and

furthermore AT II cells are responsible for the regeneration of alveolar epithelium via differentiation into type I cells [16].

1.1.1.4. Pulmonary defense

Due to their extended surface contact to the environment, lungs possess several defense mechanisms to protect themselves from inhaled particles, toxins and microorganisms, including airway, bronchioli and alveoli clearance. The clearance of airway secretions is generally realized by the filtering mechanism of the mucociliary escalator. Normally, mucus lines the respiratory tract. Due to continuous beating of cilia the mucus removed out of the lungs, hence any particles that penetrate into the lungs are trapped in the mucus and swept out up to the epiglottis where they can be swallowed [17].

Alveolar macrophages (AM) are located within the alveolar spaces and are found in close proximity to AT I cells within the alveolar surfactant film. AMs are essential for maintaining a sterile environment in the pulmonary compartment by eliminating invading pathogens and pollutants through phagocytosis of microorganisms or particles that enter the alveolar space [18,19].

Since clearance of invading pathogens and foreign particles becomes more difficult with increasing amounts, high exposition additionally induces a modest influx of polymorphonuclear neutrophilic leukocytes (PMNs). PMNs are attracted by macrophage-derived substances including leukotriene B4 (LTB4) and chemotactic peptides such as interleukin-8 (IL-8) and related chemokines [20]. In addition, excessive exposition of foreign material triggers the adaptive immune system, hence lymphoid aggregates develop containing loose clusters of T-lymphocytes, B-lymphocytes, plasma cells and macrophages [21] to eliminate contaminants.

1.1.1.5. Respiratory mechanics

Pulmonary diseases changes the physiology of the lungs, hence respiratory mechanics changes. Therefore, measurement of respiratory mechanics is necessary during clinical trials as well as animal experiments, dealing with ventilatory settings. Below, some parameters, that are useful for understanding this work are summarized, for deeper understanding excellent books and reviews explain this topic more closely [22,23,24,25].

1.1.1.5.1. Tidal volume (V_T)

The term tidal volume (V_T) is described as the total volume of inspiration or expiration during one breath. V_T is determined by the difference of pressure between thoracic and atmosphere (transpulmonary pressure, P), the airway resistance (pulmonary resistance, R_L) and the distensibility of the lungs (pulmonary compliance, C_L). Mathematical pulmonary mechanics can be expressed as

$$P = \frac{1}{C_L} V + R_L \frac{dV}{dt}$$

where V is the volume of inspiration and dV/dt describes the velocity of airflow.

1.1.1.5.2. Pulmonary resistance (R_L)

The pulmonary resistance (R_L) represents the total inelastic resistance that the air has to overcome during inspiration and expiration. It is composed of the frictional resistance, that develops during breathing and the flow resistance of the airways (airway resistance). The flow resistance can be described by Poiseuille's Law. Therefore the resistance depends primarily on the cross section of the respiratory system. Regarding the total cross section area of the airways, under normal conditions the minimum total diameter is in the upper airways, so that these airways normally dominate air flow resistance.

1.1.1.5.3. Pulmonary compliance (C_L)

Pulmonary compliance (C_L) refers to the distensibility of the lungs as elastic structures and is defined as the change in lung volume produced by a change in transpulmonary pressure during one breath. Typically C_L is constant for a certain range (increased volume correlates with pressure augmentation), but drops against zero when reaching the limit of tissue elasticity (even small increases in volume produces large increases of pressure). C_L is determined by volume increase (ΔV) per increase of the applicator transpulmonary pressure (ΔP) expressed as

$$C_L = \frac{\Delta V}{\Delta P}$$

In general, flexible structures posses high compliances, whereas rigid structures show low values. The reciprocal value of compliance is referred to as elastance (E_L), where E_L describes the stiffness of the lung.

Compliance can also change in various disease states. For example, in fibrosis the lungs become stiff, making a large pressure necessary to maintain a moderate volume. Such lungs would be considered poorly compliant. However, in emphysema, where many alveolar walls are lost, the lungs become loose and floppy so that only a small pressure difference is necessary to maintain a large volume. Thus, the lungs in emphysema would be considered highly compliant [3].

1.2. Clinical manifestations of inflammation-associated lung dysfunctions

1.2.1. Acute respiratory distress syndrome (ARDS)

Acute respiratory distress syndrome (ARDS), first described in 1967 by Ashbaugh *et al.* [26] is a devastating disease of the lungs. ARDS is caused by a variety of direct and indirect causes (table 1) and characterized by inflammation of the lung parenchyma leading to impaired gas exchange with concomitant systemic release of inflammatory mediators causing inflammation, hypoxemia and frequently resulting in multiple organ dysfunction syndrome (MODS)[27,28]. A less severe form of ARDS is called acute lung injury (ALI).

First Ashbaugh and colleagues described ARDS as an acute symptom of severe dyspnea, refractory hypoxemia, diminished lung compliance as well as diffuse bilateral alveolar pulmonary infiltrates evident on the chest radiograph [26]. To provide specific criteria to identify patients systematically, in 1988 an expanded definition was proposed that quantified the physiologic respiratory impairment with a four point system. This was based on the level of the ratio of the partial pressure of arterial oxygen (PaO_2) to the fraction of inspired oxygen (FiO_2), positive end-expiratory pressure (PEEP), lung compliance (C_L) and the degree of infiltration evident on the chest radiograph with additional consideration of the acute onset of ARDS/ALI and the presence or absence of systemic disease [30].

Table 1 Clinical disorders associated with the development of ARDS. Ware *et al. 2000* [29]

Direct lung injury	Indirect lung injury
Common causes	***Common causes***
Pneumonia	*Sepsis*
Aspiration of gastric contents	*Severe trauma with shock and multiple transfusions*
Less common causes	***Less common causes***
Pulmonary contusion	*Cardiopulmonary bypass*
Fat emboli	*Drug overdose*
Near-drowning	*Acute pancreatitis*
Inhalational Injury	*Transfusion of blood products*
Reperfusion pulmonary edema after lung transplantation or pulmonary embolectomy	

In 1994 the *American-European Consensus conference* recommended a new definition by considering patients with less severe hypoxemia ($PaO_2/ FiO_2 \leq 300$ mmHg) to have acute lung

injury (ALI), while patients with more severe hypoxemia (PaO_2/ $FiO_2 \leq 200$ mmHg) are considered to have the acute respiratory distress syndrome (ARDS) [31].

1.2.1.1. Clinical disorders and risk factors for ARDS/ALI

The strongest risk factor for ARDS is sepsis, with approx. 40 % of all causes [32, 33]. Other risk factors are pneumonia, aspiration of gastric contents, severe trauma with shock, multiple transfusions and smoke inhalation. Weaker evidence was identified for pulmonary contusion, fat embolism, drug overdose, cardiopulmonary bypass, acute pancreatitis and transfusion of blood products [34, 35, 32, 33]. In addition, new studies observed, that ventilatory settings rise the risk of new-onset ARDS [36].

1.2.1.2. Incidence and mortality for ARDS/ALI

Probably due to the difficulty in finding a consensus for ARDS/ALI over the past years several studies found a fluctuation in incidence rates [37,38,35,39,40]. In 2003 Goss e*t al*. reviewed recent estimates of ARDS/ALI in the USA and reported that incidence ranging from 1.3 to 22 per 100.000 person · $years^{-1}$ as well as from 17.9 to 34 per 100.000 person · $years^{-1}$ for ALI [41]. A more recent study, performed by Rubenfeld *et al*. in 2005 determined the evidence of ALI in the USA to be 78.9 per 100.000 persons · $years^{-1}$ [42]. However, prognoses of ARDS/ALI depends on the kind and number of insults and risk factors thus highly complicating the determination of incidence in ARDS/ALI.

In spite of modern intensive care medicine ARDS is still associated with a high mortality rate. Mortality rates also differ over time perhaps due to different definitions of this syndrome [43, 39, 44, 45, 46]. In 2008 Zamboon *et al.* performed a systematic analysis of the ARDS/ALI literature to document possible trends in mortality between 1994 and 2006. The overall pooled mortality rate for all 72 studies was 43% [47], showing a wide variation from 15 % to 72 %. Most patients with ARDS/ALI are reported to die due to sepsis [37,48].

1.2.1.3. Pathophysiology of ARDS/ALI

The pathophysiology of ARDS/ALI is driven by an aggressive inflammatory reaction. Histophatologically, ARDS/ALI is divided in three phases, the early phase that is described as being exudative and lasts typically for the first week after the onset, the proliferate phase, typically occurring the second two weeks after the onset of respiratory failure, and finally the fibrotic phase, beginning from day 10 [49].

The early phase of ARDS/ALI is characterized by an increase in the permeability of the alveolocapillary barrier, which in turn leads to an influx of proteinaceous edema fluid into the alveolar space. Damage to the alveolocapillary barrier causes the accumulation of pulmonary edema [50].

The proliferative phase is characterized by endothelial proliferation of the capillaries and by fibrosis and at least, the fibrotic phase is characterized as a chronic state with fibroproliferative character while morphological remodelling of the lung occurs [51]. AT I cells are easily injured and damage to them disrupts the removal of edema fluid and by that leading to accumulation of pulmonary edema [52]. Damage to AT II cells leads to decreased lung compliance, collapsing of alveoli, diminished ion transport [53] and impaired repair of the epithelium, which in turn can lead to fibrosis [54]. It is known that the extent of fibrosis correlates with mortality in ARDS [55].

ARDS/ALI is characterized by a complex interaction of inflammatory mediators forming and boosting the inflammatory response. Alveolar macrophages (AM), known to be responsible for clearing inhaled particles and lung surfactant [19], secrets inflammatory cytokines/chemokines e. g. interleukin-1, 6, 8 and 10 (IL-1, IL-6, IL-8, IL-10) into the alveolar space [56, 57]. In addition, AM secrete tumor necrosis factor-α (TNF-α) which is known to stimulate chemotaxis and activate neutrophils [57]. Neutrophils (also referred to as polymorphonuclear neutrophilic leukocytes (PMNs)) accumulate, so that PMNs can become the predominant leukocytes in the alveolar spaces [58, 59] which in turn can increase the amount of oxidants [60], proteases [61], leukotrienes (LTC) [62] and other inflammatory molecules, such as platelet activating factor (PAF) [63].

Critical roles in the inflammatory network developing during ARDS/ALI have been described for various other stimuli e.g. TGF-ß , GM-CSF, ICAM-1, substance P [27] and in response to these stimuli also for reactive oxygen species (ROS)[64] and nitric oxide (NO)[65].

1.2.2. Ventilator-induced lung injury (VILI)

Mechanical ventilation is a mainstay in the therapy of patients with ARDS/ALI. Established to guarantee continued sufficient oxygen in the blood the use of this life-saving technique has well documented side-effects, including increased risk of pneumonia [66], diminished cardiac performance [67] and difficulties associated with sedation and paralysis [68].

Moreover, mechanical ventilation can cause damage of the lung known as ventilator-induced lung injury, a term, which summarizes different types of injury [69]: Barotrauma, volutrauma and atelectrauma are types of injury emphasizing on the mechanical part, whereas another type of

injury, the so called biotrauma describes the process, by which stretch, alternatively overstretching the alveolar units (overventilation) leads to an inflammatory response in the lungs. It is suggest, that biotrauma may play a more fundamental part in the development or worsening of ARDS/ALI as formerly assumed [69,70,71,72].

In 2000 the ARDSnet publicized a study in which 861 patients with ARDS/ALI were enrolled to a multicenter, randomized trial. This first phase III study that shows an effect of treatment on mortality in ALI, compared traditional ventilation treatment (12 ml · kg^{-1} body weight, and mean plateau pressure (P_{plat} of < 35 cm H_2O) with ventilation with lower tidal volume (6 ml · kg^{-1} body weight and mean P_{plat} of < 25 cm H_2O). The study showed that mortality was lower in the group treated with lower tidal volumes (mortality rate was 31%) compared to the group treated with traditional tidal volumes (mortality rate was 39. 8 %)[73], demonstrating the importance of protective ventilatory strategies to prevent ventilator-induced lung injury.

A remakle finding of this and another clinical study was the fact, that ventilation with lower tidal volumes were associated with reduced markers of inflammation, among them proinflammatory cytokines [74,75].

1.2.3. Biotrauma

Biotrauma describes the process by which stretch produced by overventilation (overstretching of alveolar units by ventilation with high volumes or pressures) or shear forces generated during repetitive opening and closing of lung units initiates or triggers lung injury and inflammation [69].

Inflammatory responses in the lungs due to overventilation/overdistension were found *in vitro*, in perfused organs, *in vivo* and in ARDS patients over the past years, corroborating the hypothesis of biotrauma [76]. Additional experiments with excluding necrosis *in vitro* [77,78] and in intact organs [79,80] raise the hypothesis that mechanotransduction (i.e. transformation of an extracellular mechanical stimulus (e.g. stretch) in an intracellular biochemical responses is an important mechanism in biotrauma [75].

1.2.4. Ventilator-associated pneumonia (VAP)

Pneumonia, a well described infectious inflammatory lung disease is characterized by lung parenchymal and alveolar inflammation with abnormal alveolar filling with fluid. Pneumonia is caused by a multiplicity of insults, most commonly by microorganisms colonizing the lower respiratory tract, leading to inflammatory lung reactions [81,82].

Formerly, pneumonia was classified by the causative organism, such as bacteria, viruses, fungi, or protozoa but clinically it may be more useful to classify this illness with respect to a person's risk factor. So the most commonly used classification scheme today divided pneumonia in community-acquired pneumonia (CAP) and hospital-acquired pneumonia (HAP), also called nosocomial pneumonia [83,84].

Where CAP refers to infectious pneumonia, that develops in persons with limited or no contact with medical institutions or settings, nosocomial pneumonia refers to any pneumonia contracted within 48-72 hours of being admitted in hospital [84].

Within hospital-acquired infections, nosocomial pneumonia is the leading cause of mortality [85], most commonly due to mechanical ventilation, whereas duration of mechanical ventilation plays a fundamental role in developing this so called ventilator-associated pneumonia (VAP). For example, nosocomial pneumonia can be observed in 5 % of all patients after 5 days of mechanical ventilation but in 65 % after 30 days [86].

In most cases nosocomial pneumonia is the result of microaspiration of bacteria, which colonize the upper respiratory tract (e.g. oropharynx and trachea) [84]. In ventilated patients, oropharyngeal secretions accumulate subglottic above the endotracheal cuffs thus leading to microaspiration of pathogens into the lower airways with subsequent colonization of the tracheobronchial tree [87] and in turn to infection [88,89].

However, there are various microbiological causes of nosocomial pneumonia [84]. Taken together all microorganisms share the ability to use defects of the lung defense caused by pulmonary or systemic consequences of the underlying diseases.

In many cases, the microbial flora of affected patients is modified by the basic disease or the accompanying antibiotic therapy. The spectrum of pathogens differs from typical pathogens for respiratory infections, including Gram-positive and Gram-negative bacteria [84] to atypical organisms and finally symbiotic commensales. Also viruses and fungi have been observed to promote nosocomial pneumonia [90,91].

The incidence of VAP-attributable mortality is difficult to quantify due to the possible confounding effects of associated conditions, but VAP is known to increase the mortality of the underlying disease by about 30 % [92]. Since ARDS patients have to be mechanical ventilated, the risk of VAP is high.

As leading pathogens within VAP, Gram-negative bacteria such as *Pseudomonas sp.* and diverse Enterobacteriaceae as well as Gram-positive bacteria, especially *Streptococcus pneumoniae* and *Staphylococcus aureus* are common [84]. Bacteria are known to mobilize the host's innate immune

system through different cell-wall components via activating different toll-like receptors (TLR, introduced in 1.4.2) thus leading in turn to inflammatory responses.

1.3. Cellular mechanisms of inflammation-associated lung dysfunctions

1.3.1. Extracellular mechanosensation

Among the potential mechanosensor pathways, that are proposed for stretch-activated ion channels [93,94] and the extracellular matrix (ECM)-integrin-cytoskeleton complex [95,96], evidence suggests, that receptor tyrosine kinases (RTKs) can also serve as mechanosensors [97]. It has been demonstrated that mechanical forces can activate platelet-derived growth factor (PDGF) in vascular smooth muscle cells, that could not be blocked by antibodies against PDGF receptors, leading the authors to speculate, that physical forces may be absorbed by the receptor, followed by transfer of the signal to the plasma membrane [98]. In addition, PDGF and its receptors were also found to be involved in stretch induced proliferation of fetal rat lungs [99]. Furthermore it has been reported, that compressive stress shrinks the lateral intracellular space surrounding airway epithelial cells, increasing local ligand concentrations, which triggers cellular signalling via autocrine binding of epidermal growth factor (EGF) family ligands to the epidermal growth factor receptor (EGFR) in airway epithelial cells [100]. Additional evidence for the involvement of the EGFR were found in alveolar epithelial and endothelial cells in response to cyclic stress [101,102]. Furthermore in cooperation with T. Dolinay (Division of Pulmonary, Allergy and Critical Care Medicine, University of Pittsburgh, Pittsburgh, Pennsylvania, USA) we found the EGFR ligand amphiregulin (AR) to be high expressed in lungs subjected to overventilation [103].

1.3.2. Intracellular signalling

Intracellular signal transduction pathways initiated by mechanical ventilation and the canonical inflammation pathway initiated by microorganisms share similarities [70]. Thus, differentiation of VILI-specific genes or proteins and microorganism-induced inflammatory responses of the lungs may help to design specific treatment strategies, that block either overventilation-specific or microorganism-dependent signal transduction pathways. Proinflammatory pathways due to overventilation or microorganisms includes the activation of mitogen activated protein kinases (MAPK), such as JNK/SAPK and ERK1/2 (introduced in 1.3.2.1) with subsequent activation of transcription factors. In addition, gene induction of several inflammatory genes (see chapter 1.3.2.4 and 1.3.2.5) is observed and release of cytokines, chemokines and adhesion molecules (1.3.3) which in turn forms and boosts bactericidal effects or ventilator-induced lung injury, which both participate in the development and worsening of ARDS/ALI, as summarized in figure 2.

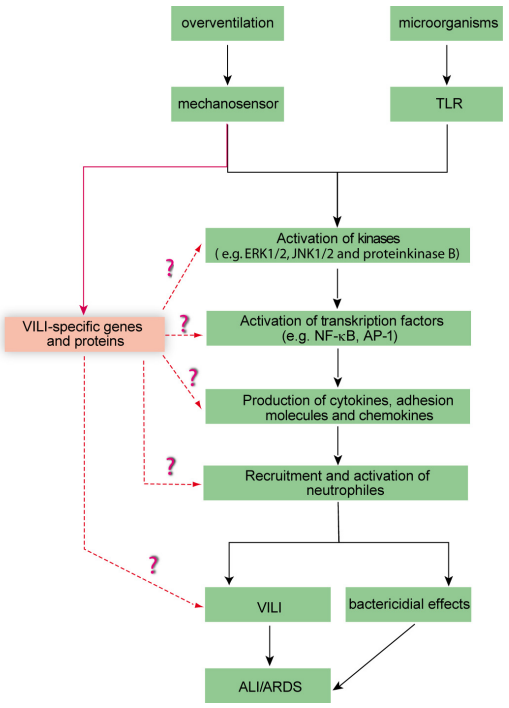

Figure 2 Activation of canonical inflammatory responses due to overventilation and microorganisms. Red lines refers to important, unsolved questions. Adapted from *Uhlig et al. 2004* [70].

1.3.2.1. Mitogen-activated protein kinases (MAPK)

Mitogen-activated protein kinases (MAPK) represent an evolutionally conserved and ubiquitous superfamily of serine/threonine specific protein kinases that regulate multiple cellular processes, including apoptosis, growth and differentiation by transducing extracellular stimuli (mitogens) to the nucleus [104].

The MAPK superfamily includes three primary signalling cascades: the extracellular signal regulated kinases (ERK 1/2), the c-Jun NH_2-terminal kinases (JNK, JNK is also called stress-activated protein kinase (SAPK) and the p38 MAPKs ; the latter two belong to the group of stress-activated protein kinases (SAPKs) [105, 106]. MAPKs are associated with various forms of inflammatory

injury [107]. Therefore recent research has focused on intracellular signalling pathways in the development of VILI, among which include the MAPK pathways [108,109].

1.3.2.1.1. ERK

Several extracellular-regulated kinases (ERKs) have been discovered. The best characterized kinases are the 44-kDa MAPK (ERK1) and the 42-kDa MAPK (ERK2) [110]. ERK1 and ERK2 (now referred to as ERK1/2) have a wide diversity of potential substrates including other protein kinases (MAPKAP, c-Raf, MEK) transcription factors (c-Jun, c-Fos, Elk1) and cell surface substrates ($cPLA_2$, EGFR) [111]. Activation of ERK1/2 in response to stretch has been described in pulmonary epithelial cells [112] as well as in perfused rat lungs during high pressure ventilation [113]. In addition, activation of ERK1/2 was found to be located in AT II cells in isolated perfused mouse lungs. Furthermore detection of active levels of the transcription factor Elk1 provides evidence that ERK1/2 was effectively activating their commonly known targets. Moreover the MAPK/ERK inhibitor U0126 prevented ventilator induced activation of ERK1/2 and Elk1 in isolated perfused mouse lungs [114]. Increased activation of ERK1/2 was also described in a model of VILI [108].

1.3.2.1.2. JNK/SAPK

The members of the c Jun N-terminal protein kinase (JNK/SAPK) pathway and the p38 MAPK pathway were initially identified as stress-activated protein kinases (SAPKs), since they were preferentially activated by environmental stress [115]. It has now become clear that they belong to two different pathways due to differences in their dual phosphorylation motif in their upstream activators and their down-stream targets [116]. The c-Jun N-terminal kinases (JNK/SAPKs) are named after the first substrate identified, the gene *c-jun* [117].

JNK/SAPK activates transcription of c-jun, c-fos and transcription factor (ATF)-2, which in turn activates transcription at sequences that bind the AP-1 transcription factor [118]. In isolated perfused lungs both increased amount of activated JNK/SAPK and enhanced phosphorylation of transcription factors ATF-2 and c-jun during overventilation were detected. Moreover activated JNK/SAPK were found to be located to cells resembling AT II cells [114]. In addition, increased activation of JNK/SAPK were observed in a model of VILI with altered neutrophil sequestration in the lung tissue in *JNK/SAPK*$^{-/-}$ mice during mechanical ventilation with high tidal volumes [119]. Also *JNK/SAPK*$^{-/-}$ mice were found to be less susceptible to ventilator-induced lung injury than their wild type counterparts [120].

1.3.2.1.3. P38

P38 mitogen-activated protein kinases are a class of mitogen-activated protein kinases, that regulate a variety of cellular processes including growth processes, differentiation, apoptosis and responses to inflammation. The P38 MAP kinases are regulated by cytokine receptors and can be activated in response to bacterial pathogens [121].

The P38 MAPK consists of the four known isoforms, p38α, p38β, p38 δ, p38γ, whereas p38α was discovered first in 1994 and cloned while studying intracellular signalling pathways [122]. The other closely related proteins were later identified and classified with p38 as a new MAP kinase group [123]. Similar to the JNK/SAPK pathway, the p38 MAP kinases are activated by a variety of cellular stresses including osmotic shock [124], inflammatory cytokines [125], lipopolysaccharides (LPS) [126], ultraviolet light [127] and growth factors [128].

As known for ERKs and JNK/SAPKs, P38 MAP kinases are phosphorylated on the threonine and tyrosine residues shared TxY motif within minutes after Toll-like receptor (TLR) stimulation of macrophages or dentritic cells (DC) [129]. Since p38 MAPK signalling is known to be involved in adaptive and innate immunity [130, 131] recent publications also have implicated p38 MAPK in the pathogenesis of VILI [120, 132]. Activation of the p38 MAPK signalling pathway plays essential roles in production of proinflammatory cytokines such as Il-1β, TNF-α and IL-6 and induction of enzymes such as cyclooxygenase-2 (COX-2), which control connective tissue remodelling in pathological conditions and expression of intracellular enzymes such as inducible nitride oxide synthase (iNOS) and many other inflammatory molecules [121].

1.3.2.2. AKT/Protein kinases B (PKB)

The serine/threonine kinases AKT, also referred to as protein kinase B (PKB) [133,134] are thought to play important cellular roles during cell survival, growth, proliferation, angiogenesis, metabolism and migration [135]. In humans, there are three genes encoding enzymes of the AKT-protein family referred to as Akt1, Akt2 and Akt3 [133].

Akt1 (now referred to as AKT/Protein kinase B), originally identified as oncogene [134] is involved in cellular survival pathways, by inhibiting apoptotic processes [136] and is also able to induce protein synthesis pathways, and therefore considered as a key signalling protein in the cellular pathways that lead to skeletal muscle hypertrophy [137] and general tissue growth [138]. Since it can block apoptosis, and thereby promote cell survival, AKT/Protein kinase B has been implicated as a major factor in many types of cancer [139]. In addition, AKT/Protein kinase B has been shown to activate nuclear factor 'kappa-light-chain-enhancer' of activated B-cells (NF-κB) via regulation

of I-κB kinase α (IKKα), resulting in transcription of prosurvival genes [140]. PKB posses a protein domain known as the PH domain, or Pleckstrin Homology domain, that binds to phosphoinositides with high affinity [141]. In the case of the PH domain of PKB, it binds either phosphatidylinositol (3,4,5)-trisphosphate (PI(3,4,5)P3) or phosphatidylinositol (3,4)-bisphosphate (PI(3,4)P2), products of phosphoinositide 3-OH kinases (PI3Ks) [142].

1.3.2.3. Phosphoinositide 3-OH kinases (PI3Ks)

Phosphoinositide 3-OH kinases (PI3Ks) are a large family of intracellular signal transducers that are divided in three classes depending on the basis of their primary structure, regulation and *in vitro* lipid substrate specificity [143]. PI3Ks are known to generate lipid second messenger molecules that results in the activation of multiple intracellular signalling cascades involved in the regulation of cell proliferation, survival metabolism, cytoskeletal reorganisation and membrane trafficking [144,145]. Central roles of the PKB- dependent activation of PI3K in response to mechanical stretch were demonstrated in pulmonary epithelial and endothelial cells [146, 102], in cardiac myocytes [147] and skin keratinocytes [148]. In response to overventilation the attenuation of PKB and NF-κB activation with subsequently diminished cytokine release due to inhibition of PI3K in isolated perfused mouse lungs was found [113]. Additional modulations of vascular permeability due to PKB dependent activation of PI3K during high tidal volume ventilation was observed [149].

1.3.2.4. Gene induction

Increased levels of mRNA of MIP-2 [150,80,151], MCP-1 [80], MIP-1 [80], KC [80], IL-6 [113,151] and TNF-α [152, 151] due to mechanical ventilation with high tidal volumes were detected in different animal models. In addition, high mRNA levels of IFN-γ and transcription factor c-fos [150] as well as NFκ-B [153] were found during overventilation. Furthermore increased mRNA levels of components of the extracellular matrix (procollagen, fibronectin), growth factors (FGF) and TGF-β already indicate that inappropriate ventilation strategies may promote the development of pulmonary fibrosis and airway remodelling [154].

1.3.2.5. Gene expression profiling

New insights into the understanding of the physiologic and molecular mechanism of acute lung injury due to mechanical ventilation could be obtained by the microarray-based gene expression analysis approach providing an unbiased view of the transcriptional state of cell populations. As

mentioned above (1.2.2) VILI is a complex pathophysiologic process that involves a variety of molecular pathways, thus differential activation of genes in the context of VILI is expected to explain the molecular mechanisms underlying VILI.

Thus, Copland and colleagues found immediate-early response genes like *Nur77*, *Erg1*, *Btg2*, *Il1b*, *Hsp70* and *c-Jun* in a rat model of VILI [155], suggesting an involvement of protein kinase c (PKC)-mediated pathways [156], growth factor production [156], inflammation [157,158], cell death pathways [159,160] and cytoprotection [161] in the context of VILI.

Since ALI and ARDS can occur in the setting of several risk factors that are characterized by systemic (e.g. sepsis) or local (e.g. pneumonia) inflammation, some studies in animal models have examined whether induction of systemic inflammation with intravenous bacterial lipopolysaccharide (LPS) can cause a synergistic increase in lung injury in ventilated animals**.**

Altemeier and coworkers and Gharib *et al.* addressed the issue of interaction between innate immune inflammation and VILI using microarray based analysis [162,163]. Altemeier *et al.* confirmed a gene- pattern of increased expression (mechanical ventilation (MV) < LPS < MV+ LPS) in genes for CXCL-2, CCL-3, IL1-b, IL-6, GADD45-γ, and IRF-7 by quantitative real time PCR (qPCR). In addition, they confirmed the finding of GADD45-γ on a protein level using immuno-histochemical approaches, demonstrating increased expression of GADD45-γ protein in the alveolar wall of mice in groups treated with LPS and MV relative to either condition alone. Notably, GADD45-γ expression had never been before associated with LPS-induced inflammation or VILI before this report, suggesting that molecular-based analysis can identify novel candidate genes in VILI [162]. Ghaib *et al.* focused on putative transcription factor binding sites that were overrepresented in the promotor of genes found to be differentially regulated by MV and LPS. Additional genes upregulated by the combination of both conditions presented a fusion of the list found in either condition alone, suggesting an additive effect of LPS and MV on lung injury and gene expression [163].

Across species, Grigorey *et al.* used different study designs to identify genes important to the pathophysiology of VILI [164]. The authors had looked for common gene expression signatures in models of VILI performed in four different species (rat, mouse, canine and human), with the objective to find expressed genes that are conserved between species. 69 genes regulated by mechanical ventilation with high tidal volumes were found. Functional annotation of these genes revealed an overrepresentation of genes, involved in immunity, inflammation, regulation of proliferation and cell cycle, coagulation, antimicrobial response, apoptosis, cell-cell-signalling and

chemotaxis. Literature searches of Pub Med database identifed 12 of the 69 genes previously linked with lung injury [164].

Within all these studies, the authors generated RNA samples from the whole lung tissue to study differential gene expression. By that, an increase or decrease of transcript levels due to the influx of inflammatory cells such as neutrophils could not be excluded.

One way to avoid this problem is, to study gene expression changes in a purer cell population. So in cooperation with T. Dolinay and A. Choi (University of Pittsburgh, USA) we performed studies of differential gene expression in isolated perfused mouse lungs (IPL,1.5). In this model interactions with the systemic circulation are excluded via eliminating peripheral leukocytes through blood-free perfusion *ex vivo*. Thus, the model of isolated perfused mouse lungs allows the determination of lung-specific changes in gene expression during different treatments [153].

1.3.3. Mediator release

In line with gene induction, cytokine and chemokine release associated with overventilation were found *in vitro* (macrophages, Il-8, [78]), in isolated lungs (rats and mice: TNF-α, Il-1, Il-6, Il-10, MIP-2, KC, [150,80,79]) and *in vivo* (rats: TNF-α, Il-1, Il-6, MIP-2 [150,165]). In addition, *et al.* found increased amounts of IL-1, IL-6 and Il-1α in bronchoalveolar liquid (BAL) and blood of patients with ARDS [74]. Furthermore the ARDSnetwork reported in 2000 an induction of *TNF-R55* and *TNF-R75* during mechanical ventilation with high tidal volumes [166].

1.4. Cellular receptors and pathways of inflammation-associated lung dysfunctions

1.4.1. The epidermal growth factor receptor family (ErbB)

Tyrosine kinase receptors (RTKs) such as insulin, epidermal growth factor (EGF) and platelet derived growth factor (PDGF) are characterized by their intracellular tyrosine kinase domain, which is known to process proteins via phosphorylation on its tyrosine residues [167].

The epidermal growth factor receptor (EGFR) belongs to the ErbB family of receptor tyrosine kinases (RTK), and has been found in many cell types, including lung cells [168]. At present 4 ErbB receptors are known,.ErbB1 (EGFR), ErbB2, ErbB3 and ErbB4. ErbBs are transmembrane receptors composed of a large extracellular ligand binding region, a single membrane spanning α-helix and

an intracellular amino acid region, that contains a juxtamembrane region followed by a tyrosine kinase domain and carboxyterminal regulatory sequences [169]. The receptors are activated when the extracellular domain undergoes a conformational change due to ligands which facilitate either homo- or heterodimerization with other family members [170]. In turn receptor dimerization leads to activation of downstream signalling pathways involved in cell proliferation, migration, differentiation and apoptosis [171].

ErbB1 and ErbB2 are often overexpressed, amplified or mutated in many forms of cancer (e.g. lung cancer, breast cancer, leukaemia), correlating with poor prognosis thus making them important therapeutic targets [172,173]. Amplification or overexpression of ErbB3 correlates with prostate, bladder and breast malignancies [174], while ErbB4 polymorphisms have been associated with schizophrenia [175].

Whereas ErbB1 and ErbB4 are fully functional as ligand-dependent tyrosine kinases, it should be noted, that ErbB2 does not bind any known ligand, but it is known to amplify signalling of growth factors as a coreceptor for other ErbBs [176]. In addition ErbB3 is known as an impaired kinase due to substitutions in critical residues in its kinase domain thus it is only activated through heterodimerization with other ligand occupied ErbBs [177].

Generally the initial step in ErbB mediated signalling is activation of receptors through ligand binding but it also has been shown, that ligand-independent stress stimuli can activate ErbB receptors. UV radiation, arsenite or oxidative stress increase the level of tyrosine phosphorylation on ErbB receptors [178]. Moreover, activation of the EGFR was found in lung epithelial cells in response to distension due to cyclic stress [102,101] or tissue compression [100].

Common therapeutic strategies of diseases where ErbB receptors are involved deals with blocking of ErbBs due to special inhibitory agents [179,180,181]. For example, the first molecular-targeted agents to be approved for the treatment of lung cancer are tyrosine kinase inhibitors that are directed against the EGFR [179].

1.4.1.1. ErbB-ligands

Under physiological conditions, activation of ErbBs are controlled by the expression and post-translational processing of their ligands [183]. In that process, proteases of the ADAM (a disintegrin and metalloproteinase) family take central roles by generating soluble and thus active forms of ErbB ligands due to limited proteolytic cleavage of their extracellular domain from integral membrane precursors, a process, known as ectodomain-shedding [184,185,186]. The metallo-proteinase TACE/ADAM 17 is generally considered to be responsible for shedding of inactive proforms of ligands, that activate ErbB1/EGFR [187]. At present, 11 polypeptide extracellular ligands of ErbB receptors are known. Each of them contains a conserved three-loop epidermal growth factor (EGF) domain that confers binding specificy [188], allowing them to be divided into three groups. The first group includes epidermal growth factor (EGF), transforming growth factor-β (TGF-β) and amphiregulin (AR) and bind specifically to ErbB1; the second group includes heparin-binding EGF-like growth factor (HB-EGF), betacellulin (BTC) and epiregulin (EPR) with dual specificity to bind even to ErbB1 or ErbB4. The third group includes the neuregulins, neuregulin-1 (NRG-1), NRG-2, NRG-3 and NRG-4, which bind ErbB3 and ErbB4 (NRG1 and NRG2) or only ErbB4 (NRG-3 and NRG-4) [182] (figure 4).

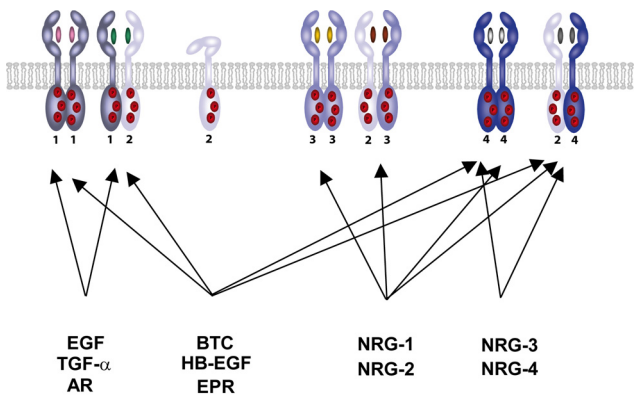

Figure 3 Binding specificity of epidermal growth factor (EGF)-related peptide growth factors allows them to be divided into three groups. ErbB2 has no direct ligand and needs to heterodimerize with another ErbB receptor to acquire signalling potential (indicated by phosphoresidues). ErbB3 lacks kinase activity, thus homodimers do not signal. According to Holbro *et al.* [182].

1.4.1.1.1. The epidermal growth factor like ligand amphiregulin (AR)

One member of the ErbB family of growth factors, that predominantly activate the EGFR is amphiregulin (AR). AR, originally isolated from conditioned medium of the human breast carcinoma cell line [189] is a 252-amino acid transmembrane glycoprotein with two major soluble forms of 78 and 84 amino acids [190].

AR is known to promote the growth of many cell types, including epithelial cells, fibroblasts, and keratinocytes [191,192,193]. Furthermore, AR has been shown *in vitro* to drive the proliferation of malignant cells in an autocrine/paracrine manner [194]. In addition, AR is commonly

overexpressed in many human cancers, in which AR levels correlate with tumor progression and diminished survival of patients [195,196] and recently amphiregulin is discussed as target for breast cancer therapy [197].

In contrast to all these reports, the literature is virtually void of data regarding the possible functions of AR in the lungs. It is reported, that amphiregulin secretion is induced on exposure to tobacco smoke and fine particulate matter in human pulmonary epithelial cells [198]. In addition, there are a few reports where upregulated amphiregulin expression in mast cells of asthmatic patients significantly correlated with the goblet cell hyperplasia in their mucosa [199]. Furthermore, mast cell secreted amphiregulin promoted the proliferation of primary human lung fibroblasts and induced lung fibrosis [200].

Finally Dolinay *et al.* observed the upregulation of amphiregulin mRNA expression and increase of amphiregulin protein levels in the distended tissue of overventilated mouse lungs [103].

1.4.1.2. ErbB-signalling pathways

Concomitant with ligand binding, ErbB receptors dimerize and undergo transphosphorylation on residues in their cytoplasmic tails, thereby creating docking sites for SH2-containing proteins, such as phospholipase c-Shc, Grb2 and PI3K. These interactions lead to the activation of multiple functionally interlinked signalling pathways, notably MAPK pathways (e.g. ERK1/2 and JNK/SAPK), the PI3K/AKT pathway, the STAT-pathway and the phospholipase-γ pathway [201], which in turn leads to the translocation of proteins in the nucleus, activation of transcription factors with concomitant gene expression of several genes involved in cell proliferation, migration, differentiation and apoptosis. [171] (Figure 4).

In addition, receptor transactivation enhances the diversification of ErbB-mediated signal transduction. For example, inter-receptor communication of EGFR with G-protein-coupled receptors (GPCRs) mediated by Src, PI3K, Ca^{2+}/calomoduline and small GTPases were reported. Moreover members of the cytokine superfamily as well as cell adhesion molecules of integrins were found to activate ErbB receptors [202]. Negative regulation of ErbB receptors effects primary through receptor degradation., where numerous endogenous regulatory proteins have been identified over the past years, that suppress the signalling activity of ErbB receptors [203].

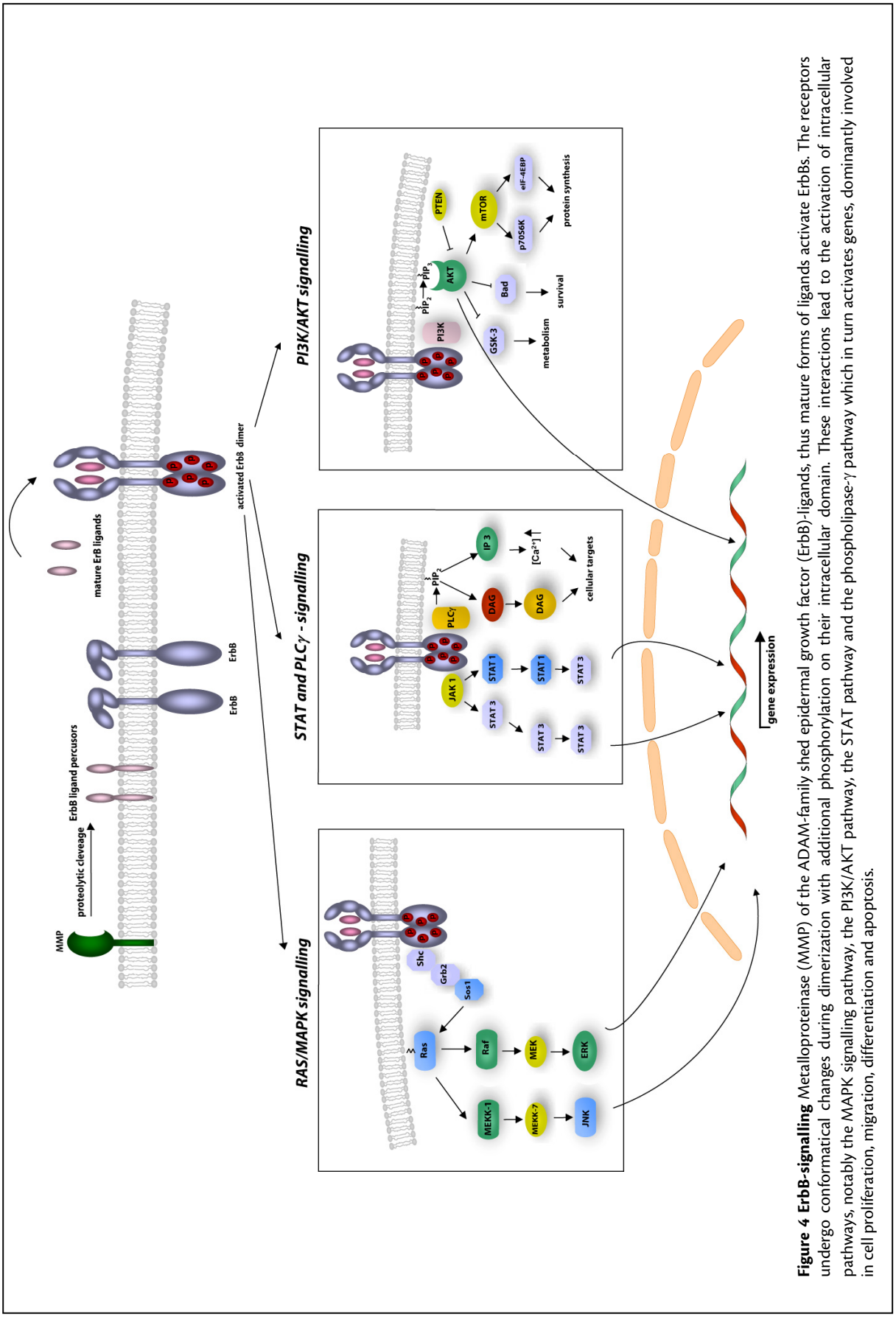

Figure 4 ErbB-signalling Metalloproteinase (MMP) of the ADAM-family shed epidermal growth factor (ErbB)-ligands, thus mature forms of ligands activate ErbBs. The receptors undergo conformatical changes during dimerization with additional phosphorylation on their intracellular domain. These interactions lead to the activation of intracellular pathways, notably the MAPK signalling pathway, the PI3K/AKT pathway, the STAT pathway and the phospholipase-γ pathway which in turn activates genes, dominantly involved in cell proliferation, migration, differentiation and apoptosis.

Taken together, the ErbB family of receptors initiates, influences and forms a complex network of signalling pathways, involved in growth, differentiation and apoptosis. Thereby activating of ErbBs by ErbB ligands plays a fundamental role and diversity of ErbB-mediated signaltransduction is enhanced by receptor transactivation. In addition, unphysiological conditions e.g. UV-light and mechanical stress were reported to activate ErbBs.

1.4.2. The toll-like receptor (TLR) family

The primary response to pathogens in the innate immune system is generally triggered by the unique family of germline-encoded pattern recognition receptors (PRR), that recognize extracellular or endosomal pathogen-associated molecular patterns (PAMPs) found in broad types of organisms including plants, invertebrates and vertebrates [204]. Toll-like receptors (TLRs) are single membrane-spanning non-catalytic receptors of the innate immune system, belonging to this family [205].

PRRs are classified according to their ligand specificity, function, localization and/or evolutionary relationships. Together with the cytoplasmic NOD-like receptors, the large family of TLRs form the class of signalling PRRs [206]. Within that, together with the Interleukin-1 receptors, TLRs compose a receptor superfamily known as "Interleukin-1 Receptor/Toll-like Receptor Superfamily" where all members of this family are characterized by its highly conserved cytoplasmatic TIR (Toll-IL-1 receptor) domain [207]. Despite this similarity, the extracellular portions of both types of receptors are structurally unrelated. The IL-1 receptors possess an immunoglobulin-like domain, whereas TLRs bear leucine-rich repeats (LRRs), where each extracellular domain contains 19-25 tandem copies of the LRR motif related to ligand recognition [208]. TLRs are known to recognize a broad spectrum of microbial components, including cell wall components of Gram-positive and Gram-negative bacteria, depending on ligand binding specificity, which in turn leads to distinct anti-pathogen responses, including anti-microbial peptides [209], cytokines [210] or apoptotic signals [211,212]. Among them, TLRs are capable of sensing organisms ranging from bacteria to fungi, protozoa and viruses [213].

1.4.2.1. TLR ligands

In mammals, at present 11 TLRs are known [214]. TLR1-9 are conserved between human and mouse. However, although TLR10 is presumable functional in humans, the c-terminal half of the mouse *tlr10* gene is substituted to an unrelated and non-productive sequence [214].

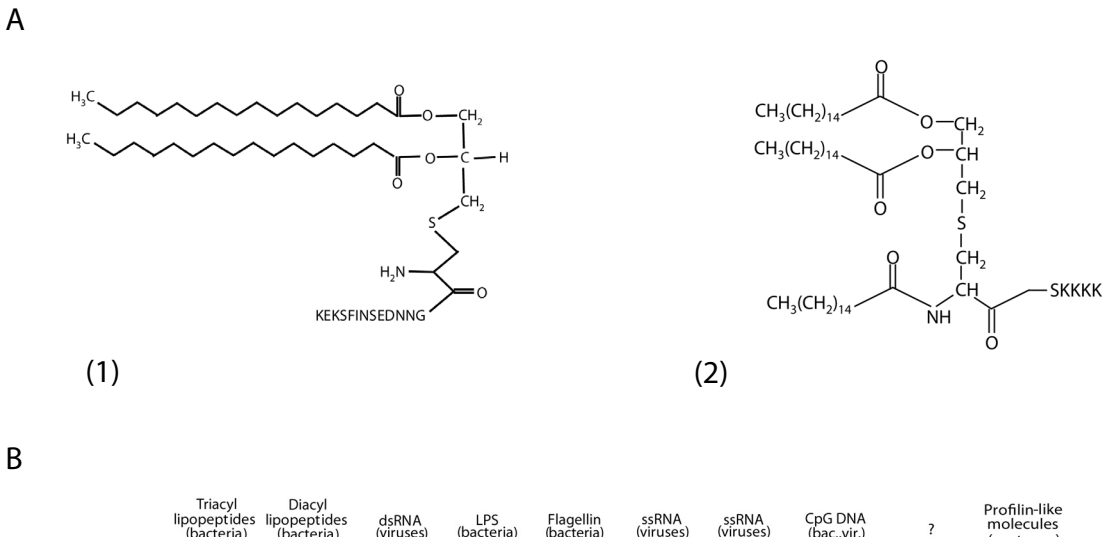

Figure 5 (A) Structural formula of the active stereoisomers of synthetic (1) MALP-2 and (2) Pam_3CysSK_4 which dimerize either with TLR2/6 or TLR1/2 to form host defense reactions. **(B) Members of the Toll-Like Receptor-(TLR) family**. In general, TLRs contain extracellular tandem-like leucine-rich ligand binding regions (LRRs) and a highly conserved cytoplasmatic TIR (TLR-IL-1 receptor) domain characterized by the presence of tree homologous regions (Box 1, 2, 3). TLRs dimerize upon binding to specific pathogen associated molecular patterns (PAMs), mostly components of bacteria and viruses. Since the *tlr10* mouse gene is not functional, so far no ligand was found.

Furthermore, mouse TLR11 is functional, but there is a stop codon in the human TLR11 gene, which results in a lack of producing human TLR11 [215].

In general, TLRs are known to undergo receptor homodimerization upon binding different ligands [216]. TLR2 heterodimerize with TLR1 upon binding triacetyl lipopeptides [217] or TLR6 upon binding diacetyl lipopeptides [218] originated from bacteria. Presently, a broad spectrum of TLR2 agonist are known. Besides lipopeptides/lipoproteins (LP)[219,220] also peptidoglycans (PG) [221] and lipoteichonic acid (LTA) [222] as well as lipoarabinomannan from *Mycobacteria sp.* [223], phenol-soluble modulin from *Staphylococcus sp.* [224], zymosan from fungi [225] and glycosylphosphatidylinisitol from *Trypanosoma cruzi* [226] are reported to be TLR2 agonist, but

these variety of PAMPs recognized by TLR2 has recently been explained as inadequately purification of ligand fractions and thus contamination with lipopeptides/lipoproteins, as especially discussed at present for LTA [227,228,220] and PG [229,220].

One of the best characterized TLR2 ligand is macrophage-activating lipopeptide 2KDa (MALP-2) originally isolated from a clone of *Mycoplasma fermentas* [230]. Today it is able to produce synthetically, thus avoids purification problems. MALP-2 forms host defense signalling via dimerization of TLR2 with TLR6 and uses CD36 as a coreceptor [231]. It has been observed to induce chemoattractant proteins such as macrophage inflammatory protein (MIP)-1 , and MIP-2 and by that promote pulmonary leucocyte infiltration [232] as well as reducing lung metastasis [233]. In addition, pulmonary application of MALP-2 was reported to improve vaccination [234] and survival in pneumonia [235]. But other than this, little is known about the pulmonary effects of MALP-2 in the lungs.

Another frequently used TLR2 -ligand is the synthetic bacterial lipopeptide analogon Pam_3CysSk_4 ((S)-(2,3-bis(palitoyloxy)-(2RS)-propyl)-N-palmitoyl-Cys-(S)-Ser(S)-Lys4-OH), which is known to mediate signalling through dimerization of TLR2 with TLR1 [236]. It has been observed that TLR2 activation through Pam_3CysSK_4 (now referred to as Pam_3Cys) impairs hypoxic pulmonary vasoconstriction (HPV) and induces deleterious systemic effects in a mouse model [237]. In intact lungs Pam_3Cys has been observed to cause cytokine and chemokine release [238] and in human bronchial epithelial cells (hBE) and human alveolar macrophages it stimulated release of TNF-α, IL-1,IL-6 and IL-8 [239,240]. In line with MALP-2 effects in the case of Pam3Cys, there is also little known about its pulmonary effects *per se*.

The importance of TLR4 in innate immune response was initially demonstrated in the C3H/HeJ mouse stain that is resistant to endotoxin shock, by finding specific mutations in the TLR4 gene [241]. TLR4 dominantly recognize lipopolysaccharides, characteristic parts of the cell walls from Gram-negative bacteria. In addition, TLR4 is known to recognize taxol (a strong antitumor agent in humans) derived from *Taxus brevifolia* [242] and furthermore endogenous ligands, such as heat shock protein 60 (HSP 60), HSP 70, fibronectin, hyaluronic acid, fibrinogen and heparan sulfate [243]. LPS recognition via TLR4 requires the formation of a protein complex containing accessory molecules. Generally LPS is bound to LPS-binding protein (LBP), that is present in the serum and initially recognized by the CD14 receptor. Once bound to CD14, LPS comes in close proximity with TLR4, however the efficient triggering of an inflammatory response additionally requires the expression of the secreted protein MD-2 [244].

While TLR5 mediated signalling in dominantly induced by flagellin, a component of the bacterial flagellum complex, responsible for bacterial motility [245], TLR3, TLR7, TLR8 and TLR9 are

dominantly responsible for adequate host defense against viral infections via recognizing viral PAMs [246]. By that, the family of TLR receptors recognizes a multiplicity of different pathogen structures and enables tissue cells to react specifically to invading pathogens.

1.4.2.2. Signalling pathways via TLRs

The activation of TLR signalling pathways originates from the cytoplasmic TIR domains, whose crucial role was first revealed in the C3H/HeJ mouse strain, observing a point mutation within the TIR domain to be responsible for defective LPS signalling [241,247]. Signalling pathways downstream of the TIR domain are specified by TIR domain-containing adaptor proteins, of which MyD88 was discovered first [248]. MyD88 forms the initial step in the MyD88- dependent signalling pathway and thus is essential for the inflammatory responses mediated by all receptors of the TLR family members [208].

Additional adaptor proteins that form initial steps in MyD88-independent pathways were later identified, peculiar to TLR3- and TLR4 signalling pathways [8]. Signalling from specially TLR4 is transferred to (TIRAP)/MyD88-adaptor-like (Mal) [249, 250] where TLR3 signalling is generally mediated through TIR domain-containing adaptor inducing IFN-γ(TRIF)/TIR domain-containing adaptor molecule (TICAM-1) [251] as summarized in Figure 6.

1.4.2.2.1. MyD88-dependent pathway

MyD88 possess the TIR domain in the C-terminal portion, as well as a death domain in the N-terminal portion [252] a conserved sequence motif, known to be present in several proteins involved in apoptotic signal transduction [253]. MyD88 serves as major adaptor protein in TLR signalling upon associating with the TIR domain of TLRs and recruits members of the IL-1 receptor-associated kinases (IRAKs) to TLRs via interaction of the death domains of both molecules classes [208].

Once phosphorylated, IRAKs associates with TRAF6 to phosphorylate the IKK complex which in turn mediates translocation of NF-κB into the nucleus and by that activation of gene transcription of several inflammatory mediators forming the host defense response [208]. In addition, TLRs bridge the signalling pathway via ECSIT (for 'evolutionarily conserved signalling intermediate in Toll pathways') to TRAF 6 for the MAPKs ERK1/2, p38 and JNK/SAPK in response to specific bacterial products [254]. Furthermore, toll-interacting protein (Tollip) plays an inhibitory role in TLR2/4-mediated cell activation by suppressing the activity of IRAKs [255] and by that controlling the magnitude of inflammatory cytokine production in response to endotoxin [256]. In addition TIRAP/Mal involved in the MyD88 signalling pathway through TLR2 and TLR4 [257] is known to activate the dsRNA-binding protein kinase PKR [258], that is proposed to be an other central downstream component of MyD88-dependent signalling pathways [259].

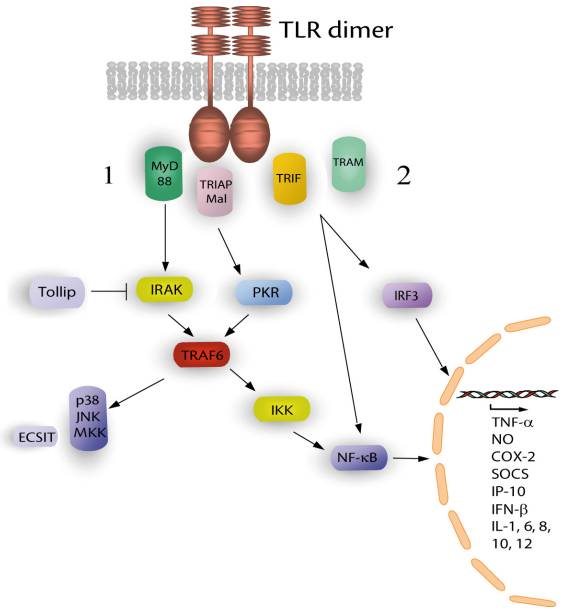

Figure 6 Toll-like receptor signalling. (1) *MyD88-dependent pathway*. Major adaptor protein MyD88 interacts with IL-1 receptor-associated kinases (IRAKs), IRAKs phosphorylates and associates with TRAF-6, thus leading to NF-κB activated gene transcription. TLRs bridge signalling via ECSIT (for evolutionarily conserved signalling intermediate in Toll pathways) for MAPKs. In addition, TRIAP/MAL adaptor protein, involved in TLR2 and TLR4 signalling pathway is known to activate protein kinase PKR, whereas TOLLIP (toll-interacting protein) plays an inhibitory role. (2) *MyD88-independent pathway* appears to utilise both IFN-regulatory factor 3 (IRF3) and NF-κB, thus results in additional expression of IFN-inducible genes, but only in the case of TLR4 activation.

1.4.2.2.2. MyD88-independent pathway

MyD88-independent TLR signalling was further characterized by determining genes expressed in MyD88-deficient macrophages following exposure to LPS [260]. With this approach, a number of genes known to be interferon (IFN)-inducible were identified, such as glucocorticoid-attenuated response gene 16 (GARG16), immuno-responsive gene 1 (IRG1) and the gene encoding CXC-chemokine ligand 10 while genes encoding inflammatory cytokines, such as TNF-α , IL-6 and IL-1b were not expressed [208]. The MyD88-independent pathway appears to utilise both IFN-regulatory factor 3 (IRF3) and NF-κB, thus resulting in the expression of IFN -inducible genes including CXCL10 in the case of TLR4 stimulation [261]. TLR4 engages TRIF (Toll-IL-1R-containing

adaptor inducing IFN-β) via a bridging adaptor molecule (TRAM) to signal IFN regulatory factor (IRF) 3 activation (Figure 6) and expression of type I IFNs [262]. Since stimulation with TLR2 failed to upregulate the expression of IFN-inducible genes, it is suggested, that activation of TLR2 is not mediated in a MyD88 independent manner [260].

1.5. The model of isolated perfused mouse lungs (IPL) to study mechanisms of inflammation-related lung dysfunctions

The lungs as complex organ is in the constant exchange of information and substances with other organs of the body, so that in total an extremely complex system exists. In order to study this system, it is important to eliminate some of its complexity. In this sense, the model of isolated perfused lungs represents a much less complicated system than the whole animal with maintaining a majority of the completeness of the organ.

As experimental approach the isolated perfused lung stands in between experiments *in vivo* with whole animals and *in vitro* with cultured cells [263], where the isolated perfused mouse lungs represents the organ model to perform studies with the mouse as classic and commonly used model organism of vertebrates [79,80,153].

Advantages of this model are the ability to measure lung-borne mediators by eliminating the involvement of the systemic circulation via blood free-perfusion and the possibility to collect molecular biological data of proteins and genes in lung tissue [114,113,151]. Furthermore, we successfully performed a detailed analysis of ventilator-induced activation of inflammatory genes by gene array measurements [103]. All experiments in this work were obtained in this model. Nevertheless it should be noted, that the IPL is not a model of VILI, as during overventilation the lung structure remains largely intact [80]. However, since an intact pulmonary microanatomy can be considered as prerequisite for (patho) mechanotransduction processes [75], the model of IPL can be regarded to be qualified for mechanotransduction studies.

2. Aim of the study

The acute respiratory distress syndrome (ARDS) is characterized by aggressive inflammatory reactions in the lungs. It was the aim of this thesis to further examine the responses of the lungs to three major causes of ARDS, namely TLR2 receptor ligands, TLR4 receptor ligands and mechanical ventilation.

Sepsis due to infection with Gram-negative or Gram-positive bacteria represents one of the main causes of ARDS. Furthermore, ventilator-induced pneumonia may complicate ARDS. While the pulmonary consequences triggered by the activation of the TLR4 ligand lipopolysaccharide (LPS) have been extensively studied, relatively little is known about the pulmonary responses caused by TLR2 activation. Therefore it was a major aim of this work to examine the pulmonary consequences of TLR2 activation during mechanical ventilation.

Mechanical ventilation (MV), a mainstay in the therapy of patients with ARDS, is known to have several side-effects. Over the past years it has become evident that overstretching of alveolar units even without physical tissue destruction (overventilation) may result in a response called biotrauma via triggering canonical inflammatory pathways that contribute to the development of ventilator-induced lung injury (VILI). Because the inflammatory responses induced by mechanical ventilation are similar to that induced by other well known causes such as sepsis, it was one aim of this study to use a gene expression profiling approach to identify genes specifically induced by overventilation, but not by LPS. One of the candidate genes identified was the epidermal growth factor receptor (EGFR) ligand amphiregulin (AR), and another aim of this thesis was to examine its effects in the lungs.

3. Material and Methods

3.1. Animals

Lungs were taken from female BALB/C (OlaHsd) obtained from Harlan Winkelmann (Borchen, Germany) or from the breeding house of the FU Berlin (origin line was OlaHsd from Harlan). All animals were used at a weight of 20-25 g and kept under controlled conditions (22°C, 55% humidity, 12 h day/night rhythm) on a standard laboratory chow.

3.2. Material

3.2.1.Instruments and equipment

3.2.1.1.The isolated perfused mouse lung (IPL)

If not otherwise noted the following instruments were purchased from Hugo-Sachs-Electronics (March-Hugstetten, Germany).

Table 2 Instruments used for the isolated perfused mouse lung

Instruments	
	Perspex-perfusion-chamber I (mouse), type 839
	Water bath Lauda ecoline 003 with immersion circulator E 100.
	Peristaltic pump Ismatec MS reglo-analog
	Oscilloscope HAMEG Typ HM 407
Pressure transducer	
	Differential pressure transducer Validyne DP-45-14 (*for measuring the velocity of airflow in conjunction with a silicon tube (inner diameter 0.9 mm)*)
	differential pressure transducer MPX-399/2 (*for measuring the pressure in the ventilation chamber*)
	Perfusion pressure transducer ISOTEC (*for measuring the pulmonary artery pressure*)
Plugsys-Unit with	
	Ventilation control module VCM
	Timer Control Module (TCM)
	2 Digital bridge amplifier (DBA) (*for amplifying the signals from the ISOETC pressure transducer and MPX 399/2*)
	2 carrier frequency bridge amplifier (CFBA) (*for amplifying the signals from the Validine DP 45-14 pressure transducer*)
	Internal data bus for control- and data signals
	Gateway for transferring the data signals to a personal Computer (hard disc, ROM)

Personal computer Pentium 300 Mhz with Mehlhaus A/D converter to supply the raw data from the Plugsys-Unit and HSE Pulmodyn® W software for Microsoft® Windows® 95/98/NT/XP (for calculating the physiological parameters from the measured raw data and displaying as well as saving of all data during the experiments).

3.2.1.2.Other instruments and equipment

Other instruments, used in this thesis are listed in the following table.

Table 3 Instruments and Equipment.

equipment	description	company
96-well plates		*VWR International GmbH, Darmstadt, Germany*
Accu-jet pipette controller		*Brand GmbH & Co. KG, Wertheim, Germany*
Bath thermostat	*ED-19A*	*Julabo, Seelbach, Germany*
Centrifuge	*Megafuge 1.0R*	*Heraeus Instruments, Osterode, Germany*
Centrifuge	*5417 R*	*Eppendorf, Hamburg, Germany*
Electrophoresis power supply	*Consort E802*	*Consort, Thurnhout, Belgium*
EU frosted Non-skirted Thin-wall plates	*96 x 0.2 ml (low profile) white*	*BIOplastics Landgraaf, Netherlands*
EU Opti-Seal Optical Disposable Adhesive		*BIOplastics Landgraaf, Netherlands*
Fluorescence and Absorbance Reader	*GENios*	*Tecan Trading AG, Grailsheim,Germany*
Gel blotting paper		*Whatman, Dassel, Germany*
Glass plates		*Amersham Biosciences, Freiburg, Germany*
Light Cycler® 480		*Roche Applied Science, Mannheim, Germany*
Microtiter-adhesive foil		*Neolab, Heidelberg, Germany*
Nitrocellulose transfer membrane		*Schleicher & Schnuell, Marienfeld, Germany*
Nunc-Immuno Plate	*F96 Maxissorp*	*Nunc, Langenselbold, Germany*
Odyssey Infrared Imaging system		*LI-COR, Bad Homburg, Germany*
Osmomat 030		*Gonotec GmbH, Berlin, Germany*
Parafilm		*Roth, Karlsruhe, Germany*
PCR Cabinet		*Karl-Heinz Breidbach, Aachen, Germany*
pH-Meter		*Knick, Berlin, Germany*
Pipette tips	*Biosphere (PCR-clean) 10µl, 100µl*	*Sarstedt AG & C, Nümbrecht, Germany*
Pipette tips	*1000µl (PRR-grade)*	*Greiner bio-one GmbH, Frickenhausen, Germany*
Pipette tips	*serological pipettes 1ml, 5ml, 25ml*	*Greiner bio-one GmbH, Frickenhausen, Germany*
Pipettes	*Research (10µl, 100µl, 1000µl)*	*Eppendorf, Hamburg, Germany*
Pipettes	*Multichannel Research (100µl,300µl)*	*Eppendorf, Hamburg, Germany*
Pipettes	*Mulitpette® Xtream*	*Eppendorf, Hamburg, Germany*
Sterile reaction tubes	*1.5 ml*	*Eppendorf, Hamburg, Germany*
Semi-Dry Transfer Unit	*Hoefer TE77*	*Amersham Biosciences, Freiburg, Germany*
Semi-Dry Transfer Unit	*TE 77 PWR*	*Amersham Biosciences, Freiburg, Germany*
Standard vertical electrophoresis unit	*Hoefer, SE 600 Ruby*	*Amersham Biosciences, Freiburg, Germany*
Sterile reaction tubes	*0.5 ml*	*Eppendorf, Hamburg, Germany*
Thermoblock	*Biometra TB1*	*Biometra, Göttingen, Germany*
Thermoblock	*Triblock DB1A*	*Techne, Cambridge, England*
Vertical laminar airflow	*BH-EN 2003*	*Faster, Ferrara, Italy*
Vortexer		*IKA Janke & Kunkel, Staufen, Germany*

3.2.2. Chemicals

All chemicals, e.g. salts and solvents, were of lab grade and if not otherwise noted, usually purchased from Sigma (Deisenhofen, Germany), SERVA Electrophoresis GmbH (Heidelberg, Germany), Roth (Karlsruhe, Germany) or Merck (Darmstadt, Germany). TEMED was purchased from Gibco BRL (Karlsruhe, Germany), Sodium dodecyl sulfate (SDS) was purchased from INC Biomedicals Inc. (Costa, Mesa, CA).

3.2.3. Inhibitors and substances

The following table lists pharmacological agents, used in the isolated perfused mouse lung (IPL)

Table 4 Pharmacological agents used in the isolated perfused mouse lungs (IPL)

substances	supplier
Bovine Albumine (cryst./lyophil.)	*SERVA Electrophoresis GmbH, Heidelberg, Germany*
Recombinant mouse amphiregulin	*R&D Systems, Wiesbaden, Germany*
Pam_3CysSK_4	*EMC microcollections, Tübingen, Germany*
Macrophage-activating-lipopeptide-2 KDa (MALP-2)	*Alexis Biochemicals, Grünberg, Germany*
Lipopolysaccharide (LPS) from Salmonella abortus equi	*Helmut Brade, Research Center Borstel, Germany*
Dimethylsulfoxide (DMSO)	*Sigma Aldrich, Deisenhofen, Germany*
AG1478-in Solution	*Calbiochem/ Novabiochem, Bad Soden, Germany*
PD153035-in Solution	*Calbiochem/ Novabiochem, Bad Soden, Germany*

3.2.4. Antibodies

Antibodies for western blot analysis are listed in table 5. Primary antibodies were purchased from Cell Signalling Technology (Boston, USA) whereas secondary antibodies were obtained from LI-COR (Bad Homburg, Germany).

Table 5 Antibodies used for western blot analysis. [P] primary antibody, [S] secondary antibody

antibody
Rabbit-anti- ERK1/2, polyclonal[P]
Mouse- anti-phospho-ERK1/2, polyclonal[P]
Rabbit- anti-AKT, monoclonal[P]
Mouse-anti-phospho-AKT, monoclonal[P]
Rabbit -anti-mouse-SAPK/JNK, monoclonal[P]
Mouse-anti-phospho-SAPK/JNK, monoclonal[P]
Rabbit-anti-mouse-p38 MAPK, polyclonal[P]
Mouse-anti-phospho-p38 MAPK, monoclonal[P]
LI-COR IRDYE 680-goat-anti- rabbit[S]
LI-COR IRDYE 800-goat-anti -mouse[S]

3.2.5. Oligonucleotides

Oligonucleotides were used in this thesis as primers for quantitative Real-Time PCR (qPCR) analysis. All nucleotides were purchased from MWG Biotech (Ebersberg, Germany). Primer design was performed

via the free available software Oligo Analyzer 3.0 (©2000-2002Teemu Kuulasmaa) and Oligo Calculator (website of the University of Pittsburgh).

Table 6 Primer for mouse-target-genes used in quantitative-real-time PCR (qPCR). Reference : [1](this work), [2](Weisberg *et al.*, [264]), [3](Hu *et al.* [265]), [4](Ehlers *et al.* [266]).

target gene	Primer (sense)	Primer (antisense)
Akap12[1]	*5´-CCAAGAGGAAAGCCAGGATG-3´*	*5´-CTGCCATTTCTTTAGCTCGGT-3´*
Angptl2[1]	*5´-GAGAATACCAACCGCCT-3´*	*5´- ATAGGTCTCCCAGTTCC-3´*
Anxa1[1]	*5´-CGCTCAGTTTGCTCATATTC-3´*	*5´-TTACCAAGAGGACCAATGCT-3´*
Areg[1]	*5´-CTATCTTTGTCTCTGCCATCA-3´*	*5´-AGCCTCCTTCTTTCTTCTGTT-3´*
B2m[4]	*5´-TGACCGGCTTGTATGCTATC-3´*	*5´-CAGTGTGAGCCAGGATATAG-3´*
Cldn4[1]	*5´-CCTTCATCGGCAGCAACAT-3´*	*5´-AGAGCACCCACGATGATG-3´*
Cldn7[1]	*5´-CAACATCATCACAGCCCAGG-3´*	*5´-CACCAGGGACACCACCAT-3´*
Cxcl1[1]	*5´-CAAACCGAAGTCATAGCCAC-3´*	*5´-TGGGGACACCTTTTAGCATC -3´*
Cxcl10[1]	*5´-GCCGTCATTTTCTGCCTCAT-3´*	*5´-GCTTCCCTATGGCCCTCATT-3´*
Cxcl2[3]	*5´-AGTGAACTGCGCTGTCAATGC-3´*	*5´-AGGCAAACTTTTTGACCGCC-3´*
Cyr61[1]	*5´-TCCAGAATCTACCAAAACG-3´*	*5´-AAACCCACTCTTCACAGC-3´*
Fgfbp1[1]	*5´-TGGCTACTCAGGCGTTCTCA-3´*	*5´-CTTCTCTGCTTATTCTGGGC-3´*
Hbegf[1]	*5´-GTGTTGTCCGCGTTGGT-3´*	*5´- TGTCCCTTCCAAGTCCT-3*
Hspb8[1]	*5´-AAGCAGCAGGAAGGTGGGAT-3´*	*5´-TCGTTGTTGAAGCTGCTCTCT-3´*
Hprt1[1]	*5´-TTATGGACAGGACTGAAAGA-3´*	*5´-TGTAATCCAGCAGGTCAGCA-3´*
Il11[1]	*5´-AGAGACAAATTCCCAGCTGAC-3´*	*5´-TCTACTCGAAGCCTTGGCAG-3´*
Il1b[1]	*5´-GAAAGCTCTCCACCTCAATG-3´*	*5´-GCCGTCTTTCATTACACAGG-3´*
Il6[2]	*5´-CCAGAGATACAAAGAAATGATGG-3´*	*5´-ACTCCAGAAGACCAGAGGAAA-3´*
Klf5[1]	*5´-ACAACAGAAGGAGTAACCCG-3´*	*5´-TGCACTTGTAGGGCTTCTCG-3´*
Nr4a1[1]	*5´-CTTCAAAACCCAAGCAGC-3´*	*5´-AGGCAGACTCTAGCAACAGG-3´*
Parg[1]	*5´-GTGACTGTTCGGGTAGAC-3´*	*5´- GTTCGCTCACCATTCTCATC-3´*
Ptgs2[1]	*5´-AGATGACTGCCCAACTCCCAT-3´*	*5´-CAGGGATGAACTCTCTCCGTA-3´*
Rpl32[1]	*5´-AGCGAAACTGGCGGAAAC-3´*	*5´- GACCAGGAACTTGCGGAA***-3***´*
Slpi[1]	*5´-TGAGAAGCCACAATGCCG-3´*	*5´- CACTGGTTTGCGAATGGG-3´*
Tnc[1]	*5´-CTTCATTCGTGTGTTCGCCA-3´*	*5´-ATCCCACTCTACTTCCACAG-3´*
Tnf[1]	*5´-TCTCATCAGTTCTATGGCCC-3´*	*5´-GGGATGAGACAAGGTACAAC-3´*
Traf1[1]	*5´-TGAGAACCTGAGAGATGATG-3´*	*5´- TGAAGGAACAGCCAACACC-3´*
Tyk2[1]	*5´-AGTGTTCTGGTATGCCC-3´*	*5´- TGGTTAGAGTCACAGTATG-3´*

3.2.6. Buffers

3.2.6.1. Perfusion buffer (Mouse IPL)

3.2.6.1.1. Mouse IPL-perfusion buffer I

RPMI 1640 w/o phenol red, (Cambrex, Charles City, Iowa, USA), completed with 1 % glutamine, (Cambrex, Charles City, Iowa, USA), 4 % low endotoxin bovine serum albumine (Albumin Bovine Fraction V, Serva Electrophoresis GmbH, Heidelberg, Germany) ad NaCl to 335-340 mOsm · kg^{-1};.pH 7.3, 37°C.

3.2.6.1.2. Mouse IPL-perfusion buffer II

HES-Medium (Serag Wiessner, Naila, Germany, for composition see table 7) was completed with 1 % Ultraglutamine (Cambrex, Charles City, Iowa, USA), 1 x essential amino acids (MEM-aminoacidconcentrate (50x), PAA Laboratories, Pasching, Austria), 1 x nonessential amino acids, (MEM-NEAA-aminoacidconcentrate (100x), PAA laboratories, Pasching, Austria), 1 x vitamins (MEM-vitamins (100x), PAA Laboratories, Pasching, Austria), 0.001% bovine albumine (Crystalized powder, SERVA Electrophoresis GmbH, Heidelberg, Germany) ad NaCl to 335-340 mOsm/kg. After completion pH was adjusted to 7.5 at 37°C.

Table 7 Composition of HES-Medium (content of 1l, pH 8.0)

substance	content [g]
poly(O-2-hydroxyethyl)starch (200/0.5)	*40000*
substitution grade 0.5; median M_W = 200000	
calcium nitrate 4 H_2O	*0.1*
potassium chloride	*0.4*
magnesium sulfate 7 H_2O	*0.1*
sodium chloride	*6*
sodium hydrogen carbonate	*2000*
Disodium hydrogen carbonate 12 H_2O	*2020*
Glucose-monohydrate	*2200*
Gluthatione (red.)	*0.001*

3.2.6.2. Cell lysis buffer

Cell extraction-(CE)-buffer (containing 10 mM Tris, pH 7.4, 100 mM NaCl,1 mM EDTA, 1mM EGTA,1 mM NaF, 20 mM Na_4PO_7, 2 mM Na_3VO_4, 1% Triton X-100, 10% glycerol, 0.1% SDS, 0.5% deoxycholate (Biosource, Solingen, Germany)) was completed with 1 mM Pefabloc SC (4-(2-

aminoethyl)-benzosulfonylfluoride, Roche Diagnostics, Mannheim, Germany) and 1 x Complete Mini (protease inhibitor cocktail, Roche-Diagnostics, Mannheim, Germany).

3.2.6.3. Buffer for sodium dodecyl polyacrylamide gel electrophoresis (SDS-PAGE)

SDS-PAGE buffer contained 25 mM Tris, 192 mM glycine and 0.1% SDS (Biorad, Munich, Germany).

3.2.6.4. Blot transfer buffer

Blot transfer buffer contained 25 mM Tris, 192 mM glycine and 20 % methanol (pH 8.5) (Biorad, Munich, Germany).

3.2.6.5. Buffers for antibody incubation

3.2.6.5.1. TBS-buffer

TBS (Tris-buffered saline)-buffers contained 10 mM Tris,.50 mM NaCl (pH 7.6 (Sigma-Aldrich, Deisenhofen)).

3.2.6.5.2. TBS-T-buffer

TBS-T (Tris-buffered saline)-buffer contained 10 mM Tris and 50 mM NaCl (pH 7.6 (Sigma-Aldrich, Deisenhofen)) and 0.1% polysorbate 20 (Tween®-20, Sigma-Aldrich, Deisenhofen, Germany).

3.2.7. Additional solutions for enzyme-linked immunosorbent assay (ELISA)

Additional solutions for CXCL10 DuoSet ELISA Kit (R&D Systems) were developed in our laboratory .

PBS – Buffer contains 137 mM NaCl, 8 mM $Na_2HPO_4 \cdot 2\ H_2O$, 1,5 mM KH_2PO_4 and 2. 7 mM KCl.

Wash – Buffer – 0.005% polysorbate 20 (Tween®-20, Sigma-Aldrich, Deisenhofen, Germany) in 1 l PBS–buffer, pH 7.2-7.4.

Stop solution – 2 N H_2SO_4- sterile filtered

Reagent diluent – 1% BSA low endotoxin biotechnologie grade (SERVA Electrophoresis GmbH, Heidelberg, Germany) in 1 l PBS, pH 7.2-7.4.

3.3. Methods

3.3.1. The isolated perfused mouse lung (IPL)

3.3.1.1. Preparation of mouse lungs

Mice were anaesthetized with 200 mg · kg^{-1} body weight pentobarbital sodium (Narcoren, Pharmazeutische Handelgesellschaft mbH, Hamburg, Germany) and weighed. After the absence of the toe -and eyelid reflexes, mice were fixed in dorsal position on a cork plate inside the ventilation chamber and sprayed with 70% ethanol. After opening the peritoneum along the body centre line the trachea was freed by removing muscle and adenoid tissue. Subsequently, a ligature was place around the trachea and the trachea was opened with a diagonal cut. After inserting the tracheal cannula, the trachea was fixed and the lungs were ventilated with room air by positive pressure ventilation (3 cm H_2O to 10 cm H_2O) at a rate of 90 breaths · min^{-1} resulting in a tidal volume (V_T) of about 100 µl. After laparotomy the diaphragm was removed, blood coagulation was stopped with 1200 U · kg^{-1} body weight heparin (Sigma-Aldrich, Deisenhofen, Germany) and mice were bled with a cut through the *vena renalis*. After the abdomen was removed the chest was opened along the sternum and both costal arch's were laid aside and fixed with needles. Thymus and pericardium were completely removed, whereby the heart became accessible for positioning the perfusion catheter. A ligature was placed around the pulmonary artery and the aorta. The right ventricle was opened with a cut and subsequently the arterial cannula was inserted into the pulmonary artery and fixed with the ligature. The perfusion flow was adjusted to 0.5 ml · min^{-1}. Immediately the left ventricle was opened by cutting off the *apex cordis,* and the venous catheter was placed into the left atrium by piercing the mitral valve. The venous perfusate was removed by the perfusion pump. Finally the chamber cover of the ventilation chamber was closed and negative pressure ventilation (oscillatory ventilation pressure between –3 cm H_2O and -9 H_2O to -10 cm H_2O, negative pressure to prevent edema formation) was started and the perfusion rate adjusted to 1 ml · min^{-1}. To open atelectatic lung parts and to promote release of surfactant, deep breaths (end inspiratory pressure of –25 cmH_2O) were automatically initiated every 5 min.

3.3.1.2. Technical configuration and control of experimental parameters

Figure 7 illustrates the technical configuration of the isolated perfused mouse lungs. The main core consists of a double-walled, water-tempered (37°C) perspex ventilation chamber. The preparation of the lungs was performed in this chamber, all data links for ventilation and perfusion

are located in the Perspex corpus of the chamber. In order to prevent ascending bronchoalveolar liquid into the trachea, the chamber was inclined horizontally of approx. 20°.

The ventilation control module (VCM, embedded in the plugsys-unit) provides the oscillatory pressure for ventilation of the lungs. By switching a three-way valve after the preparation, the airflow created by the ventilation pump was directed to a ventury gauge (embedded into the perspex corpus). Thus, a negative pressure (Pc) was generated in the pressure chamber similar to the situation in the body. This negative pressure was detected with a pressure transducer (differential pressure transducer Validyne DP-45-24). The VCM allowed the adjusting of maximal and minimal ventilation pressure as well as the maximum pressure of the deep breaths, ventilation frequency and the temporal relationship of expiration to inspiration (90 breath · min^{-1} in all experiments).

The Timer Control Module (also embedded into the plugsys-unit) allowed the generation of deep inspiratory breaths in a defined temporal interval (here: every 5 min). The velocity of airflow was

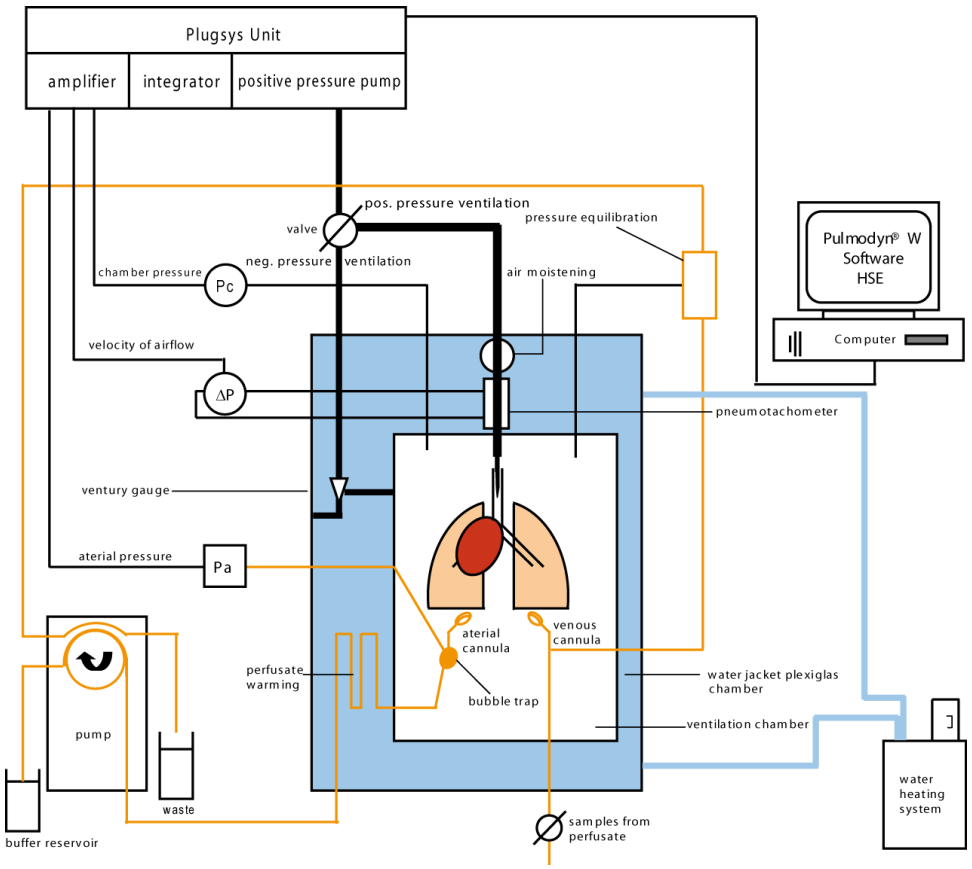

Figure 7 Set-up of the isolated perfused mouse lungs (IPL). The perfusion system is drawn in orange, the ventilation system in black. Water circulation system is marked in blue. Pc= chamber pressure, Pa= arterial pressure. According to von Bethmann *et al. 1998* [79].

detected with a pneumotachometer, connected to the tracheal cannula on the basis of the proportionality of the velocity of airflow and the pressure difference between both ends of the pneumotachometer.

Lungs were perfused in a non-recalculating fashion through the pulmonary artery at a constant flow of 1 ml · min^{-1}. The perfusion buffer was pumped via a peristaltic pump (Ismatec MS Reglo) in medical tygon tubes to the arterial catheter. In order to guarantee a buffer temperature of 37°C, the perfusate passed a warming loop inside the water jacket of the ventilation chamber. To prevent air embolisms due to CO_2 emission, bubble traps were located at the end of the warming loop before the arterial catheter. Also, the connection tube to the arterial perfusion pressure transducer ended there. Venous perfusate was collected by a tygon tube connected directly behind the venous catheter with a flow rate of 1 ml · min^{-1} into a sterile tuberculin syringe. In addition, a tygon tube for discarding the venous perfusate that was continuously generated during the experiment led to a waste bin. The perfusate flew through a pressure equilibration bin, in which the chamber pressure was added onto the venous perfusate pressure, realized by a tube connection. This bin was installed with the objective to simulate the pressure conditions in the chest, where the pressure in the left atrium varies with the inspiratory pressure. Thus, a decrease of the transpulmonary pressure in the lung vessels occur, that minimize the risk of edema formation in the lungs [80].

3.3.1.3. Electronic recording, calculating and sampling of experiment data

The following raw signals were online recorded during the experiments by analog transducers, filtered and boosted in amplifiers of the plugsys unit (Carrier Frequency Bridge Amplifier CFBA or Digital Bridge amplifier, DBA) and transmitted by the data bus-interface and the A/D-converter card for calculating and saving on a personal computer (PC). The physiologic parameters tidal volume (V_T), dynamic compliance (C_{dyn}), and resistance (R_L) were calculated by the PC from raw signals and analyzed via Pulmodyn® W software for Microsoft® Windows® 95/98/NT/XP (Hugo Sachs Electronics, March Hugstetten, Germany), as well as controlling and saving the specified and resulting experiment data online at 4 sec. intervals. Graphic presentation of the experiments was realized by GraphPad Prism 4.0 (GraphPad Software Inc., San Diego, USA) and Microsoft® Excel for Windows® XP.

Table 8 Sampled raw signals, transducer and amplifier in the isolated perfused mouse lungs (IPL).

raw signal	transducer	amplifier
Velocity of airflow	*Validyne DP 45-14*	*CFBA*
chamber pressure	*Validyne DP45-24*	*CFBA*
Pulmonary arterial pressure	*ISOTEC Healthdyne*	*DBA*

3.3.1.4. Treatment of perfusion media

As a perfusion medium we used RPMI medium lacking phenol red (37°C) and containing 4% low endotoxin grade albumin (Perfusion Buffer I; 3.2.6.1.1) or HES-Medium (37°C), containing 4% hydroxyl-ethyl starch (HES) (Perfusion Buffer II; 3.2.6.1.2). The osmolality of the buffer was adjusted with NaCl to 335-340 mOsm · kg^{-1}. After addition of all components and complete dilution of BSA, the buffer was sterile filtered and stored at 4°C for further use. Before beginning the experiment, the buffer was boiled at 37°C for at least 2 h, to facilitate the outgassing of CO_2 as complete as possible. Directly before beginning the experiment the pH of the buffer were adjusted with NaOH/HCl to 7.3. In the further process of the experiments, pH was controlled every hour and readjusted if necessary.

3.3.1.5. Extraction of perfusate and tissue samples

Venous perfusate samples were collected every 30 min with a tuberculin syringe, from the venous catheter that was located directly into the left atrium to exclude the heart as possible producer of cytokines or other mediators. Thereby 1 ml perfusate was collected during 1 min. The samples were quick-frozen directly in liquid N_2 and stored at −20°C for further use.

Lung tissue was freed from heart and trachea with sterile forceps and cutters directly after stopping the ventilation. Pulmonary lobes were equally partitioned into two sterile reaction tubes, immediately quick-frozen in liquid N_2 and stored at −80°C for further use.

3.3.1.6. Experimental design in isolated perfused mouse lungs (IPL)

Ventilation was always pressure controlled. To prevent edema formation in all experiments negative pressure ventilation was used. Experiments with TLR2 and TLR4 ligands and experiments with overventilation, compared to the TLR4 ligand LPS as stimuli were realized by using Mouse-IPL-Perfusion buffer I (3.2.6.1.1) whereas perfusion buffer II (3.2.6.1.2) was utilized for experiments with recombinant mouse amphiregulin and EGFR inhibitors.

3.3.1.6.1. Experiments with TLR2 and TLR4 ligands

Lungs were first perfused and ventilated for 60 min under control conditions with an end-inspiratory pressure (EIP) of −10 cm H_2O and an end-expiratory pressure (EEP) of -3 cm H_2O, resulting in tidal volumes of about 300 µl. Subsequently, the lungs were randomly allocated to one of the following four groups and perfused and ventilated for another 60 min: group 1 with control conditions, (-3 cmH_2O /-10 cmH_2O EEP/EIP), group 2 with addition of 160 ng · ml^{-1} Pam_3CysSK_4 into the perfusate buffer (Pam_3Cys), group 3 with 25 ng · ml^{-1} macrophage activating lipopeptide of 2 KDa into the perfusate buffer (MALP-2).

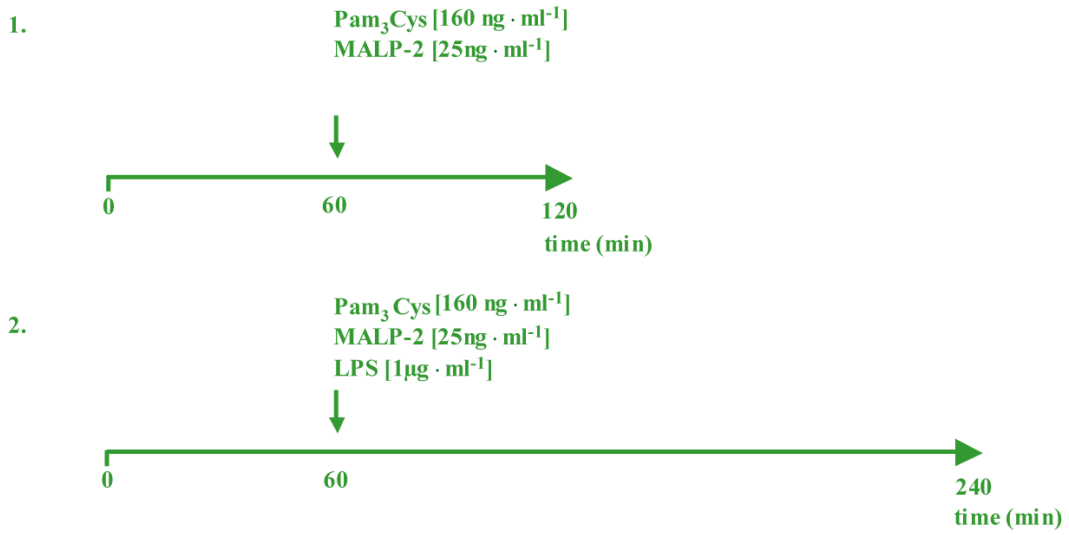

Figure 8 Experimental design of experiments with TLR2/4 ligands in isolated perfused mouse lungs (IPL). Lungs were perfused and ventilated under control conditions (-3 cmH_2O EEP and -10 cmH_2O EIP) for 60 min until they were exposed to either Pam_3Cys [160 ng · ml^{-1}], MALP-2 [25 ng · ml^{-1}] or LPS [1 µg · ml^{-1}] (Administration of substances into the perfusate buffer).

In addition, lungs were perfused and ventilated for 60 min under control conditions (-3/-10 cmH_2O EIP/EEP) and then randomly allocated to one of the following four groups and perfused and ventilated for another 180 min: group 1 with control conditions, (-3/-10 cm H_2O EEP/EIP, C), group 2 with addition of 160 ng · ml^{-1} Pam_3Cys into the perfusate buffer (Pam_3Cys) group 3 with 25 ng · ml^{-1} macrophage activating lipopeptide from 2 KDa (MALP-2) into the perfusate buffer (MALP-2) and group 4 with 1 µg · ml^{-1} lipopolysaccharide (LPS) from *S. abortus equi*. After ventilation, the surrounding tissue, the heart, and the trachea were trimmed away, subsequently lungs were flash frozen under liquid nitrogen and stored at -80 °C.

3.3.1.6.2. Experiments with lipopolysaccharide (LPS) compared to overventilation

Lungs were perfused and ventilated for 60 min under control conditions with an end-inspiratory pressure (EIP) of -10 cm H_2O and an end-expiratory pressure (EEP) of -3 cm H_2O resulting in tidal volumes of about 200 µl, until they were exposed either to overventilation (OV, 3 cm H_2O EEP and -25 cm H_2O EIP) or lipopolysaccharide (1 µg · ml^{-1} into the perfusate buffer) for further 180 min. After ventilation the lungs were treated as described in 3.3.1.6.1.

Figure 9 Experimental design of experiments with overventilation or endotoxin in isolated perfused mouse lungs (IPL). Lungs were perfused and ventilated under control conditions (-3 cmH_2O EEP/ -10 cmH_2O EIP) for 60 min until they were exposed either to overventilation (-3 cmH_2O EEP/ -25 cmH_2O EIP) or LPS [1µg · ml^{-1}] for another 180 min (Addition of substances into the perfusate buffer).

3.3.1.6.3. Experiments with recombinant mouse amphiregulin

Lungs were perfused and ventilated for 30 min or 60 min under control conditions with an end-inspiratory pressure (EIP) of -10 cm H_2O and an end-expiratory pressure (EEP) of -3 cm H_2O resulting in tidal volumes of about 300 µl, until they were exposed either to overventilation (OV,.-3 cm H_2O EEP and -25 cm H_2O EIP) or recombinant mouse amphiregulin for 30, 60 or 150 min (100 ng · ml^{-1} (AR100) or 200 ng · ml^{-1} (AR200) amphiregulin administration into the perfusate buffer). Due to the inclusion of small amounts of BSA in purchased recombinant mouse amphiregulin, IPL-mouse perfusion buffer II was completed with crystalized / lyophilized BSA ad 0.001%. After ventilation the lungs were treated as described in 3.3.1.6.1.

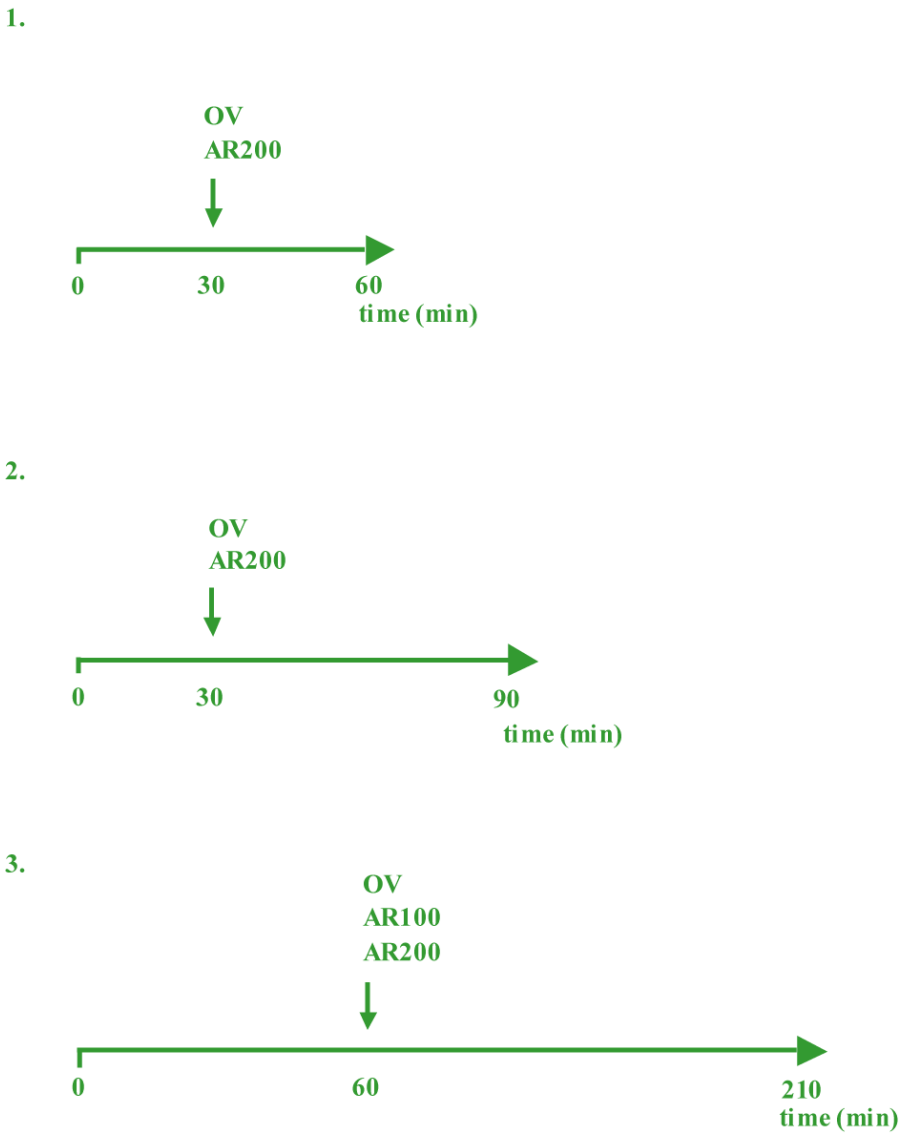

Figure 10 Experimental design of experiments with recombinant mouse amphiregulin in isolated perfused mouse lungs (IPL). Lungs were perfused and ventilated under control conditions (-3 cmH_2O EEP/-10 cmH_2O EIP) for 30 min or 60 min until they were exposed either to overventilation (OV, -3 cmH_2O EEP and –22.5 cmH_2O EIP) or amphiregulin for 30 min, 60 min or 150 min (addition of 100 ng · ml^{-1} AR or 200 ng · ml^{-1} AR into the perfusate buffer).

3.3.1.6.4. Experiments with EGFR inhibitors

Lungs were first perfused and ventilated for 60 min under control conditions as described in 3.3.1.6.1 and 3.3.1.6.3 resulting in tidal volumes of about 300 µl. Subsequently, lungs were randomly allocated to one of the following four groups and perfused and ventilated for another 150 min: Group 1 with control conditions and treatment of 0.001% DMSO from 30 min to 210 min (NVDMSO); group 2 with overventilation (OV) from 60 to 210 min and pre-treatment with

0.001% DMSO from 30 min before OV on (OVDMSO). Group 3 with OV and pre-treatment with 250 nM AG1478 dissolved in 0.001% DMSO (OVAG). Group 4 with OV and pre-treatment with.1 nM PD153035 dissolved in 0.001% DMSO (OVPD). After ventilation the lungs were treated as described in 3.3.1.6.1.

Figure 11 Experimental design of experiments with EGFR inhibitors in isolated perfused mouse lungs (IPL). Lungs were perfused and ventilated under control conditions (-3 cmH_2O EEP and -10 cmH_2O EIP) for 60 min until they were exposed to 0.001 %DMSO (NVDMSO) or overventilation (OV, -3 cmH_2O EEP and −22.5 cmH_2O EIP) + 0.001% DMSO (OVDMSO) or overventilation with the EGFR inhibitors AG1478 [250 nM] or PD301035 [1 nM] (OVAG or OVPD).

3.3.2. Enzyme linked immunosorbant assay (ELISA)

Analysis of cytokine and chemokine release from lungs into the perfusate were performed with enzyme-linked immunosorbent assays (ELISAs).

ELISA first described by van Weemen *et al.* [267] is a technique, based on the principle of the specific antibody-antibody interaction, using the fact that the amount of a specific antigen in solution can be quantitatively determined by a chromogenic conversion that can be archived by an additional antibody that is coupled to an enzyme and detects the same antigen (sandwich ELISA). ELISAs were performed in 96-well plates (Nunc-Immuno Plate F96 Maxissorp, Nunc, Langenselbold, Germany), using commercially available Kits from BD Bioscience (OptEIA™ ELISA IL6, MIP-2 and TNF-α sets) or R&D Systems (*CXCL10* DuoSet ELISA Kit). The ELISAs were performed according to the supplier's instructions. Reagents for additional solutions are listed in 3.2.7.

3.3.3. Generation of lung powder

Frozen lung tissue were ground in a mortar with a pestle in the constant presence of liquid nitrogen to a homogen powder. This generated lung powder was stored at −80°C.

3.3.4. Cell lysis

30 mg of frozen lung powder were added to 400 µl ml of complete cell lysis buffer (3.2.6.2). After incubation on ice for 30 min (with soft shaking at 10 minutes intervals), extracts were centrifuged for 10 min at 16.800 x *g*. The supernatant was aliquoted and stored at −20°C as cell lysate.

3.3.5. Protein determination

Bicinchoninic acid (BCA) Protein Assay (Pierce® BCA Protein Assay Kit, Pierce Technology, Rockford, USA) was used for determination total levels of proteins as described by Smith *et al.* [268]. This method combines the reduction of Cu^{2+} to Cu^{1+} by protein in an alkaline medium with the highly sensitive and selective colorimetric detection of the cupreous cation (Cu^{1+}) using a reagent containing bicinchoninic acid. The total protein concentration is measured by a colour change of the sample solution from green to purple in proportion to protein concentration, which can be measured by colorimetric techniques. BCA reactions were performed in 96 well plates (VWR International GmbH, Darmstadt, Germany), and realized according to manufactures instruction. Absolute concentrations were quantified by measuring the absorbance at 550 nm on an absorbance reader (GENios, Genios-Fluorescence, and absorbance Reader, Tecan, Switzerland). Serial diluted bovine serum albumin (BSA, 2 mg · ml^{-1}) (bovine albumin low endotoxin, SERVA Electrophoresis GmbH, Heidelberg, Germany) served as protein standard (ranging from 20 µg · ml^{-1} to 2 mg · ml^{-1})).

3.3.6. Sodium dodecyl sulfate polyacrylamide gel electrophoresis (SDS-PAGE)

Proteins from lung samples were separated according to their molecular weight under reducing conditions by electrophoresis as described by Laemmli *et al.* [269] in 12% discontinuous polyacrylamide-gels in the presence of 0.02% sodium-dodecyl-sulfate (SDS), realized by a standard vertical electrophoresis unit (Hoefer, SE 600 Ruby, Amersham Biosciences, Freiburg, Germany). The composition of stacking and resolving gels is listed in table 9.

Equal amounts of protein (30 $\mu g \cdot ml^{-1}$) for each sample were mixed with a reducing 4 x loading buffer (Roti®Load 1, Roth, Karlsruhe, Germany) and boiled for 5 min at 95°C. Samples were added to the stacking gel and run by 150 V for 30 min. To separate the proteins into the resolving gel the voltage was increased to 300 V for 90 min. SDS-PAGE was performed on RT in 1 x SDS-PAGE Buffer (3.2.6.3). Precision Plus Protein™ Standard (Roth, Karlsruhe, Germany) acted as marker for molecular weight.

3.3.7. Western blot analysis

Proteins were transferred to nitrocellulose transfer membranes (Schleicher and Schuell, Marienfeld, Germany) as described by Burnette *et al.* [270]. Protein transfer was performed with the TE 77 PWR Semi-Dry Transfer Unit (Amersham Biosciences, Freiburg, Germany). Blotting paper (Whatmann AG, Dassel, Germany), nitrocellulose membrane, and gel were bathed in blot

Table 9 Composition of SDS-PAGE gels. Data are for 10 ml stacking gel and 20 ml resolving gel.

Solutions	Stacking gel (4%) [ml]	Resolving gel (12%) [ml]
30% acrylamide:bis-acrylamide (37.5 :1)	1.32	8.00
1.5 M Tris-HCl pH 8.8	-	5.00
0.5 M Tris-HCl pH 6.8	2.52	-
10% SDS	0.05	0.10
H_2O bidest	6.00	6.80
10 % APS	0.05	0.20
TEMED	0.01	0.01

transfer buffer (3.2.6.4) before stacking onto the blotting apparatus. The transfer was performed at 0.8 $mV \cdot cm^{-2}$ for 90 min.

Subsequently nitrocellulose membranes were washed with TBS buffer (3.2.6.5.1.) for 2 min and blocked by Roti® Block solution (Roth, Karlsruhe, Germany) for 1 h at RT.

Afterwards protein blots were incubated overnight at 4 °C together with primary antibodies specific for the phosphorylated and non-phosphorylated form of the investigated protein, diluted in Roti® Block solution (Roth, Karlsruhe, Germany) at 1:1000. After washing with TBS-T (3.2.6.5.2) for 10 min and washing twice with TBS for 10 min, nitrocellulose membranes were incubated with both secondary infrared fluorescent conjugated antibodies (table 5) diluted in Roti® Block solution (Roth, Karlsruhe, Germany) at 1:10000 for 1 h at RT. Protein bands were pictured at 700 nm and 800 nm simultaneously in a single scan, using the Odyssey® Infrared Imaging system (LI-COR, Bad Homburg, Germany). Specific protein bands were quantified with Odyssey® imaging software.

Integrated Intensities of specified bands were expressed as ratio of the phosphorylated to the non-phosphorylated form of the detected protein and normalized to control, expressed as fold increase.

3.3.8. RNA-isolation

RNA from 30 mg lung powder was isolated with NucleoSpin® RNA II Kit (Machery Nagel, Düren, Germany) according to the manufacturer's instructions. Lung powder was suspended in 350 µl buffer, containing guanidinium thiocyanate and 1% 2-mercaptoethanol (Merck, Darmstadt, Germany). DNA were shared by passing the lysate through a 20-gauge needle. After centrifugation, the supernatant was mixed with 200 µl 70% ethanol (Merck, Darmstadt, Germany) and applied to the column. Columns were treated with DNAse, to remove all adhering genomic DNA, and subsequently washed, according to the supplier's washing protocol. To increase the yield of RNA, RNA was eluted twice with respectively 30 µl RNAse free water (Ambion, Austin, USA) to a final volume of 60 µl and stored at −80°C.

3.3.9. cDNA-generation (reverse transcriptase (RT)- reaction)

8 µl total RNA was mixed with 2 µl Oligo-(dt)-primer (Invitrogen, Karlsruhe, Germany), vortexed, briefly centrifuged and subsequently incubated at 65°C for 10 min to linearize RNA. 2 µl of this RNA-primer-mix were added to 1 µl Superscript II ™ Reverse Transcriptase (200 U · μl^{-1}) (Invitrogen, Karlsruhe, Germany), 4 µl 5 x Strand Puffer (250 mM Tris-HCL, pH 8.3, 375 mM KCl,15 mM $MgCl_2$) (Invitrogen, Kahrlsruhe), 2 µl DTT (0.1 M) (Invitrogen, Karlsruhe), 2 µl dNTP-Mix (10 mM) (peqLAB, Erlangen), 1 µl RNAseOut (40 U · μl^{-1}) (Invitrogen, Karlsruhe, Germany) and incubated for 90 min at 37 °C. After this procedure, the mixture was diluted with 30 µl RNAse free H_2O (Ambion, Austin, USA).

3.3.10. Quantitative real time polymerase chain reaction (qPCR)

Gene expression was determined online by real time quantitative polymerase chain reaction (qPCR) as described by Higuchi *et al.* [271]

Real-time PCR reactions were performed in 96 well plates (BIOplastics, Landgraaf, Netherlands) in triplets. Every reaction batch contained 1 µl of total cDNA, 200 nM forward primer, 200 nM

reverse primer, 1 x SYBR-Green I Master mix (Roche-Applied Science, Mannheim, Germany) and RNAse free water ad 10 µl. For running programs see table 10.

Plates were sealed with multiwell sealing foil (Opti-Seal Optical Disposable Adhesive, BIOplastics, Landgraaf, Netherlands) and centrifuged at 1500 x *g* for 2 min.

Real-time PCR product accumulation was monitored in LightCycler 480® (Roche-Applied Science, Mannheim, Germany) with the double-stranded DNA (dsDNA) dye SYBR Green, which accumulates into dsDNA-PCR products causing fluorescence of the dye. DNA product accumulation can be quantified due to the proportionality of cDNA accumulation and fluorescence intensity. To control heterogeneity of amplification (amplification of foreign DNA by primer dimerization or contamination) the clearness of runs was controlled by melting curves analysis. After amplification, melting curves were generated at 95°C for 5 min and subsequently 65 °C to 97 °C continuous acquisition with 5 acquisition points per sec. For amplification programs see table10. The calculation was made by using a internal standard curve of crossing point (C_T)-values against fluorescence intensity, obtained from a serially diluted sample, expressed as percent and calculated by the LC480® Software. To avoid bias, generated data were normalized to one internal control gene which did not fluctuate during treatments. Depending on the treatment, either ß-2 microglobulin (*B2m*) or tyrosine kinase 2 (*tyk2*) was used as reference gene, as indicated. Finally data were normalized to the control group, and expressed as gene expression [fold increase].

3.3.11. Statistical analysis

Data were analysed with JMP 7.0.1 for windows, and expressed as mean ± standard error (SEM). Data were always transformed by the Box-Cox transformation and examined by two-sided student's t-test. Homoscedasticity was confirmed by the Levene-test. P-values were corrected for multiple comparisons according to the false-discovery rate procedure, using R 2.8.0 [272]. $p < 0.05$ vs. control was considered significant and displayed with *, whereas ** displays $p<0.01$ vs control and ***= $p<0.001$ vs control. Cluster analysis were performed in JMP 7.0.1., using the Ward method with normalized RT-qPCR data (after Box-Cox transformation).

3.3.12. Gene expression profiling

In cooperation with T. Dolinay and A. Choi (University Pittsburgh), gene expression profiling of experiments with overventilated mouse lungs, compared to LPS stimulated lungs (3.3.1.6.2) were done. Microarray analysis (3.3.12.1), with statistics (3.3.12.2) and functional annotation (3.3.12.3) were performed by T. Dolinay.

3.3.12.1. Microarray analysis

For microarray analysis total RNA was extracted from lung tissue with Trizol (Invitrogen, Carlsbad, CA) [273]. Labeled complementary RNA was generated and hybridized to CodeLink Uniset I bio arrays as recommended by the manufacturer (General Electric (formerly Amersham Biosciences), Piscataway, NJ) and previously reported [274].

All arrays were normalized using the Cyclic Loess method [275]. For analysis, genes that did not pass the manufacturer's recommendation for quality control were filtered out. Genes were normalized to their controls and log2 base transformed. In a first set of experiments, 10K CodeLink bioarrays containing 10.500 mouse genes (n =3 replicates/group) was used. For a confirmatory analysis, 20K CodeLink bioarrays containing 20.000 mouse genes was used; n=4 biological replicates of controls, n = 4 biological replicates of LPS group, n = 3 biological replicates of OV group.

3.3.12.2. Statistical analysis for microarrays

Statistical analysis was performed by the significance analysis of microarrays (SAM, Stanford, CA) program and Scoregene software package (ScoregenePackage, available at http://compbio.cs.huji.ac.il/scoregenes/) In SAM, 200 permutations of the data were generated, and significant differences between treatment groups were determined with t-statistics ($P<0.1$). The false discovery rate method was applied to correct for multiple testing [276]. Additionally, the nonparametric threshold number of misclassification score (TNoM) was used; genes with TNoM were considered significantly changed [277]. SAM analysis were ran on each dataset separately and chose genes that were significantly changed in both datasets.

3.3.12.3. Functional annotation analysis for microarrays

LPS/C and OV/C ratios were created for 9.137 valid genes in both genesets. Genes that passed t-test ($P<0.05$) in fold change were selected using the Multiple Label Test program from the Scoregene package [278]. To obtain information about the function distribution of the genesets, the mouse gene ontology (GO) functional annotations were downloaded from the source website

(http://www.source.stanford.edu) Using Entrez Gene ID, cellular functions were matched with genes present in the genesets. Statistical significance was determined using a hyper geometric model and corrected for multiple testing using FDR methods [274]

Table 10.Programs of amplification used in RT-qPCR. Preincubation were always done at 95°C for 5 min, melting curves after amplification were always generated at 95°C for 5 min and subsequently 65 °C to 97 °C continuous acquisition with 5 acquisition points per sec.

target gen	$T_{preincubate}$ (°C)	$t_{preincubate}$ (s)	$T_{annaling}$ (°C)	$t_{annaling}$ (s)	$T_{elongate}$ (°C)	$t_{elongate}$ (s)	$T_{aquisition}$ (°C)	$t_{aquisition}$ (s)	cycles
Akap12	95	10	60	15	72	10	74	1	45
Angptl2	95	10	52	10	72	15	74	1	45
Anxa1	95	10	56	5	72	10	76	1	55
Areg	95	10	56	15	72	10	74	1	45
B2m	95	10	60	10	72	15	80	1	30
Cldn7	95	10	60	5	72	10	80	1	45
Cldn4	95	10	57	5	72	15	73	1	45
Cxcl1	95	10	60	10	72	15	74	1	45
Cxcl10	95	10	60	10	72	15	80	1	45
Cxcl2	95	10	60	10	72	15	84	1	46
Cyr61	95	10	57	10	72	15	74	1	38
Fgfbp1	95	10	57	10	72	15	78	1	45
Hbegf	95	10	53	10	72	15	45	1	45
Hprt1	95	10	58	15	72	15	74	1	45
Il11	95	10	60	15	72	10	74	1	45
Il1b	95	10	60	15	72	10	74	1	45
Il6	95	10	50	10	72	15	83	1	45
Klf5	95	10	60	10	72	15	74	1	45
Nr4a1	95	10	58	10	72	15	83	1	45
Parg	95	10	56	10	72	15	74	1	45
Ptgs2	95	10	59	15	72	10	74	1	45
Rpl32	95	10	56	7	72	15	74	1	45
Slpi	95	10	56	7	72	10	74	1	45
Tnc	95	10	57	10	72	15	74	1	45
Tnf	95	10	57	10	72	15	74	1	45
Traf	95	10	56	10	72	15	74	1	45
Tyk2	95	10	54	10	72	15	74	1	45

4.Results

4.1. Pulmonary reactions due to TLR2/4 ligand exposure

4.1.1.Pulmonary lung functions upon TLR2/4 ligand administration

In order to investigate pulmonary consequences caused by the activation of TLR2, lungs were perfused and ventilated for 120 min or 240 min with continuous administration of the TLR2/6 ligand Pam_3Cys (160 ng · ml^{-1}) or TLR1/2 ligand MALP-2 (25 ng · ml^{-1}) into the perfusate buffer from 60 min to the end of the experiment (as described in 3.3.1.6.1). Additional experiments were performed with activation of TLR4 through LPS administration (1 µg · ml^{-1}) into the perfusate buffer in the case of experiments with 240 min duration.

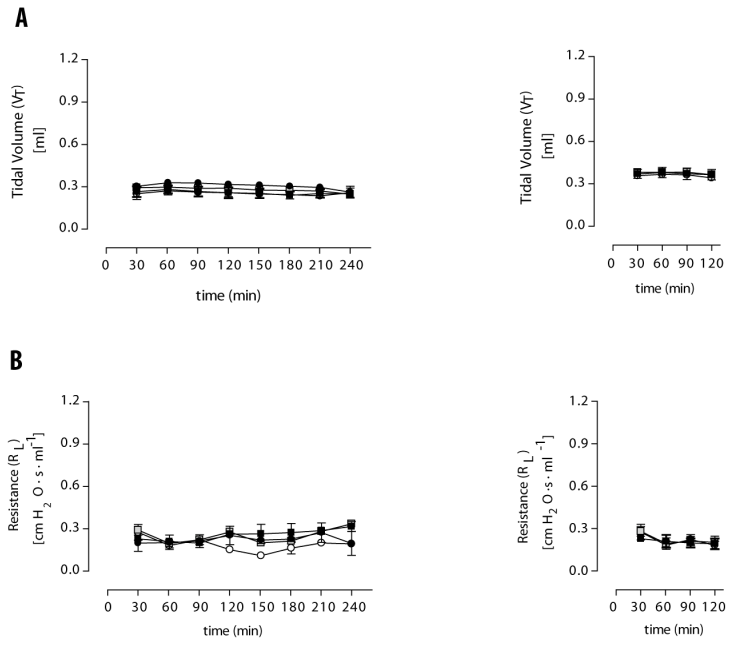

Figure 12 (A) Tidal volume and (B) pulmonary resistance of experiments with exposure to TLR4 ligand LPS, TLR1/2 ligand Pam_3Cys or TLR2/6 ligand MALP-2 from 60 min to the end of the experiment. Data are expressed as mean ± SEM. White circles indicates control lungs (n=5), grey squares indicates exposure to 25 ng · ml^{-1} MALP-2 (n=5), black squares indicates exposure to 160 ng · ml^{-1} Pam_3Cys whereas experiments with 1 µg · ml^{-1} LPS administration are displayed by black circles (n=5).

As observed before in isolated perfused mouse lungs [279], LPS administration did not change pulmonary lung functions. Also, neither MALP-2 nor Pam_3Cys administration changed tidal volume or pulmonary resistance. The values of tidal volume and pulmonary resistance remained unaltered, with values between 0.3 and 0.4 ml for tidal volume and 0.2 and 0.3 cm $H_2O \cdot s \cdot ml^{-1}$ for pulmonary resistance (Figure 12).

4.1.2. Pulmonary MAPK and AKT/protein kinase B activation upon TLR2/4 administration

To investigate the role of MAPK activation in TLR2 activated mouse lungs, experiments with TLR2 ligands were performed as described in 3.3.1.6.1. Since TLR2 is known to activate several MAPK pathways [280], the activation of ERK1/2, JNK/SAPK and p38 was analyzed after 60 min of treatment with the synthetic TLR2 ligands Pam_3Cys or MALP-2. Additional investigations were performed after 180 min treatment of ventilated lungs with both TLR2 ligands and the TLR4 ligands. Activation of MAPK was analyzed by western blot analysis in lung homogenates as described in 3.3.7.

Treatment for 60 min with both TLR2 ligands Pam_3Cys and MALP-2 increased the phosphorylation of ERK1/2 and p38 MAPK up to 1.8 fold compared to control, whereas phosphorylation of JNK/SAPK and AKT/protein kinase B were not affected (Figure 13).

Treatment for 180 min with both TLR2 ligands and with the TLR4 ligand LPS slightly increased the phosphorylation of the MAPK p38 and ERK1/2, but not in a significant manner (Figure 13).

Increased phosphorylation of JNK/SAPK and AKT/protein kinase B with TLR2 or TLR4 ligands as stimuli was not observed (Figure 13).

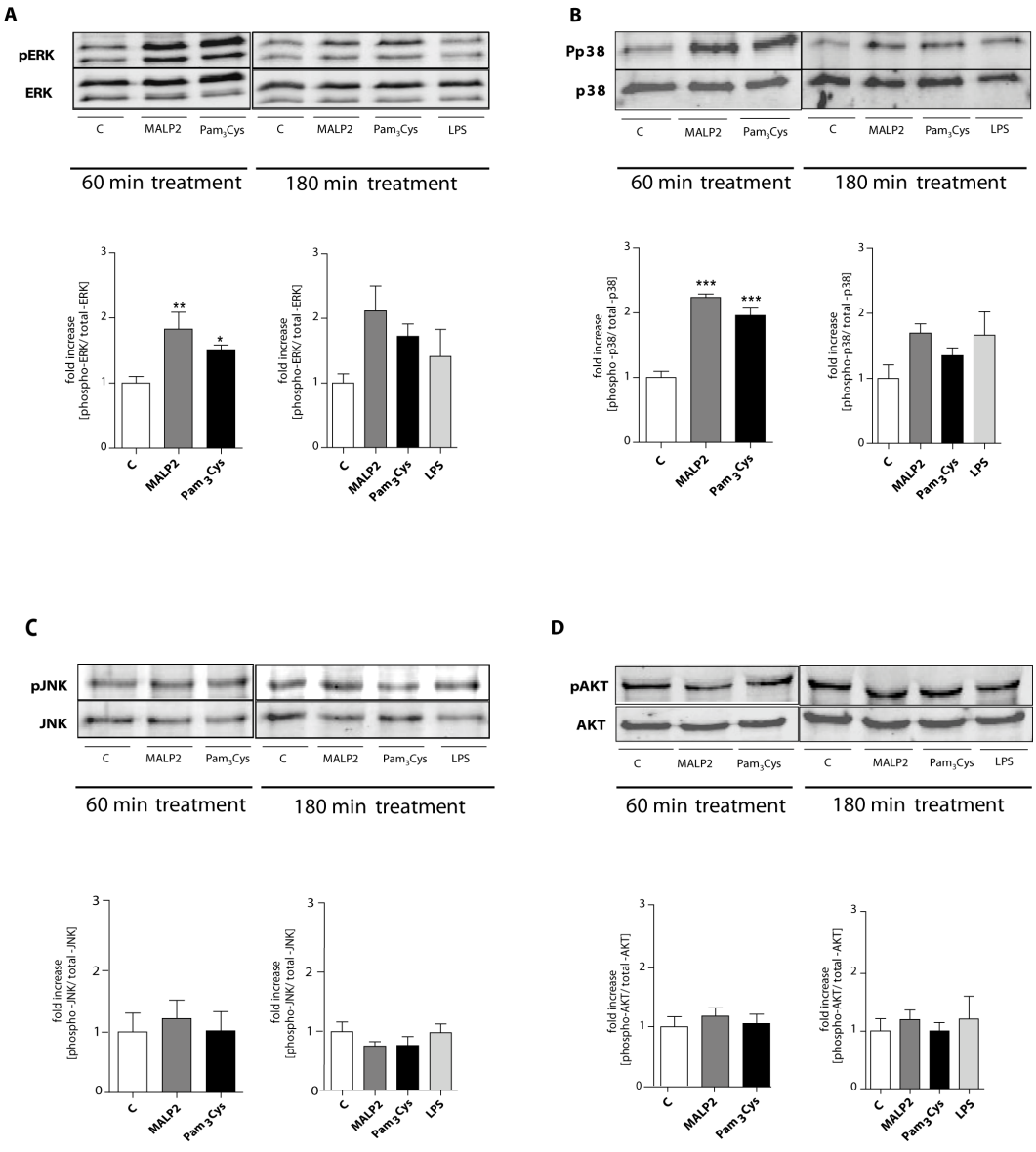

Figure 13 Mitogen activated protein kinases and AKT kinase activation. After 60 min of perfusion under baseline conditions, isolated mouse lungs were perfused for another 60 min or 180 min with Pam_3Cys (160 ng · ml^{-1}, n=5), MALP-2 (25 ng· ml^{-1}, n=5), LPS (1 µg· ml^{-1}, n=3) or under control conditions (n=5). (**A**) ERK1/2 activation of lungs after 60 min or 180 min treatment. (**B**) p38 activation of lungs after 60 min or 180 min treatment. (**C**) JNK/SAPK activation of lungs after 60 min or 180 min treatment. **(D)** AKT kinase activation of lungs after 60 min or 180 min treatment. Data were first calculated as the ratio of the phosphorylated protein to the total amount of that protein and were then referenced to the control on the same gel. Data are expressed as mean ± SEM. Pictures exemplify one representative immunoblot of 3-5 independent experiments.

4.1.3. The effects of TLR2/4 ligands on pulmonary gene transcription

4.1.3.1. Search for reference genes

Reference genes, which are often referred to as housekeeping genes or calibrator genes are frequently used to normalize RNA levels between different samples. However, since it is known, that the expression level may vary among tissues, cells and also treatment conditions, the selection of a useful reference gene is critical for gene expression studies [281].

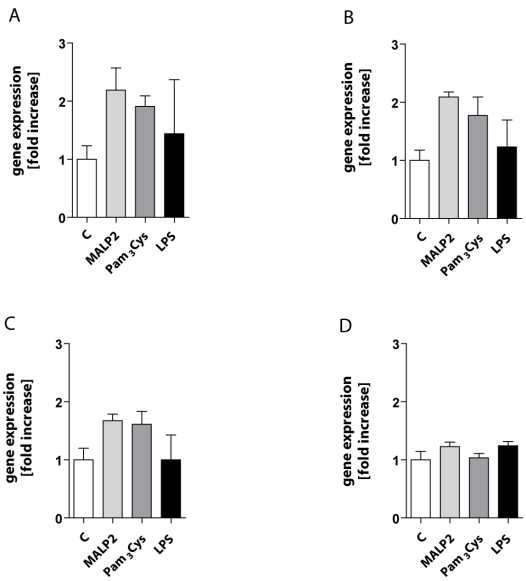

Figure 14 Reference genes for RT-qPCR experiments in isolated perfused mouse lungs. After 60 min of perfusion under baseline conditions, isolated mouse lungs were perfused for another 180 min with Pam_3Cys (160 ng · ml^{-1}, n=5), MALP-2 (25 ng · ml^{-1}, n=5), LPS (1 µg· ml^{-1}, n=3) or under control conditions (n=5). Shown are four potential calibrator genes: 2-microglobulin (*b2m*), ribosomal protein L 32 (*rpl32*), hypoxanthine phosphoribosyl transferase I (*hprt1*) or the tyrosine kinase 2 (*tyk2*). Data were normalized to the experimental control and presented as mean ± SEM.

In our studies in isolated and ventilated perfused mouse lungs, stimulated with the TLR2 ligands MALP-2 and Pam_3Cys and the TLR4 ligand LPS, we firstly investigated the expression of the 3 commonly used housekeeping genes beta 2 microglobulin (*b2m),* ribosomal protein L 32 (*rpl32*) and hypoxhantine phosphoribosyl transferase I (*hprt1*). Since we found sizable fluctuation of gene expression during treatments (up to 2 fold for experiments with TLR2 and TLR4 ligands, when compared to control), we used tyrosine kinase 2 (*tyk2*), which showed no fluctuation, as reference gene for RT-qPCR calculations in our experiments (Figure 14).

4.1.3.2. Pulmonary transcription of inflammatory and growth factor related genes upon TLR2/4 ligand administration

We investigated the regulation of 3 genes, related to growth and 10 genes involved in inflammatory processes. The genes were selected for their well known role in a wide variety of inflammatory processes in the lungs, i.e. cyclooxygenase 2 (*Ptgs2*, [282]), poly(ADP-ribose)glycohydrolase (*Parg*, [283]), secretory leukoprotease inhibitor (*Slpi*, [284]), (*Traf1*, [285]),

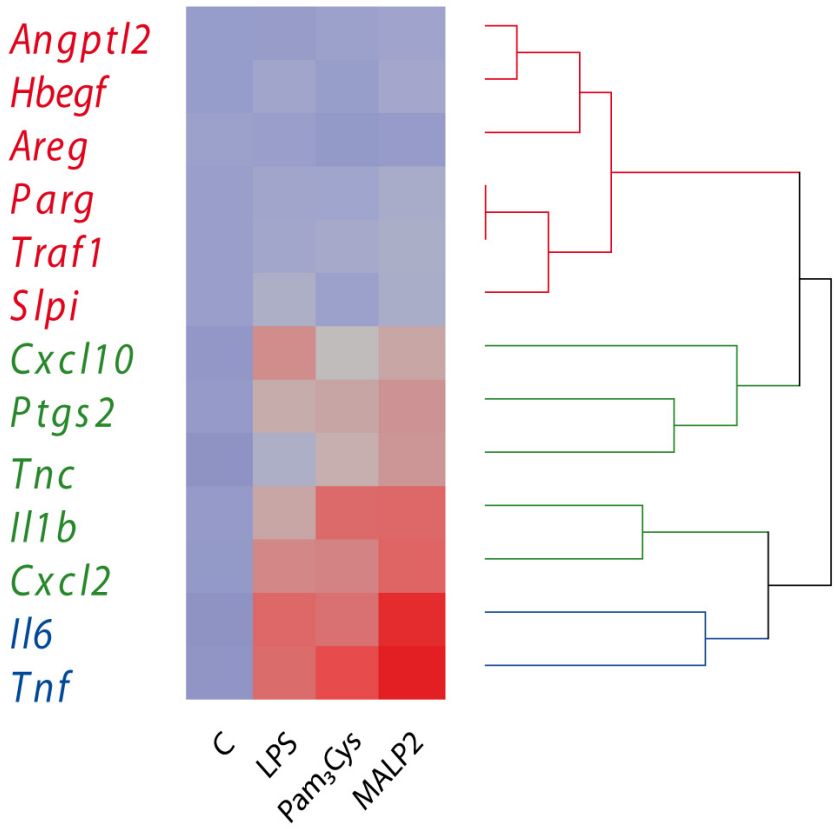

Figure 15 Cluster analysis of the gene expression data. Genes are indicated by their gene symbols and expression is colour coded: control group (blue); lighter blue and grey indicate weak upregulation; red indicates strong upregulation. The different gene symbol colours (red, green, blue) identify genes that clustered together After 60 min of perfusion under baseline conditions, isolated mouse lungs were perfused for another 180 min with Pam_3Cys (160 ng · ml^{-1}, n=5), MALP-2 (25 ng · ml^{-1}, n=5), LPS (1 µg · ml^{-1}, n=3) or under control conditions (n=5).

IP10 (*Cxcl10*, [286]), interleukin 1 (*Il1b*, [287]), MIP-2 (*Cxcl2*, [153]), interleukin-6 (*Il6*, [153]) and tumor necrosis factor (*Tnf*, [153]). Gene selection was also based on the distinction that has been made between Myd88-dependent (*Tnf*, *Il1*, *Il6*), and TRIF-dependent gene (*Traf1*, *Cxcl10*) expression [288]. Cluster analysis of RT-qPCR measurements of these genes showed, that growth factor related genes were not significantly affected by stimulation of ventilated lungs with both

TLR2 ligands or by the TLR4 ligand LPS, whether upregulation of all 11 genes involved in inflammatory processes was observed (Figure 15). The data for this measurements are shown below.

4.1.3.3. Similar pulmonary gene transcription of inflammatory genes upon TLR2/4 ligand administration

As displayed in Figure 16 A the three genes amphiregulin (*Areg*), heparin-binding EGF-like growth factor (*Hbegf*) and angiopoietin-like 2 (*Angptl2*) coding for growth factor related genes showed no

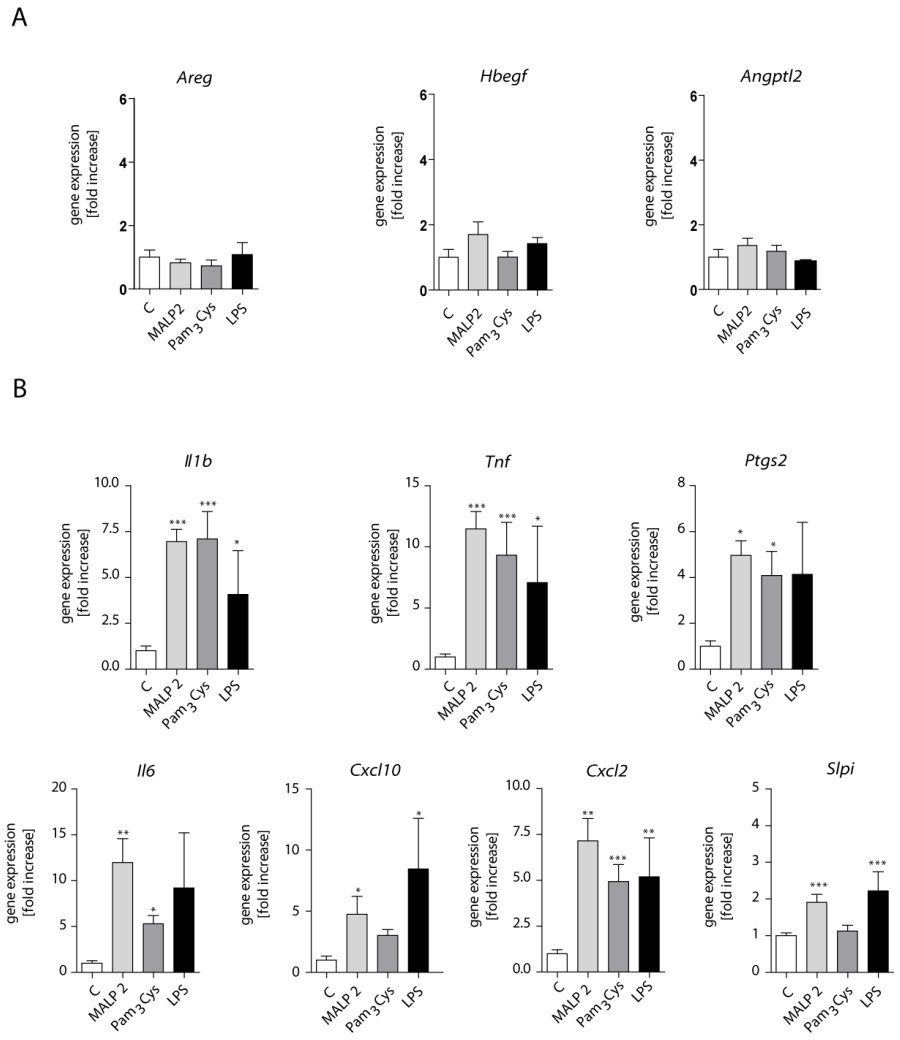

Figure 16 Expression of genes (A) encoding growth factor related proteins and (B) proteins involved in inflammatory processes. after 180 min treatment. After 60 min of perfusion under baseline conditions, isolated mouse lungs were perfused for another 180 min with Pam_3Cys (160 ng · ml^{-1}, n=5), MALP-2 (25 ng · ml^{-1}, n=5), LPS (1 µg· ml^{-1}, n=3) or under control conditions (n=5). Genes: Amphiregulin (*Areg*), heparin-binding EGF-like growth factor (*Hbegf*), angiopoietin-like 2 (*Angptl2*), interleukin 1 β (*Il1b*) macrophage inflammatory protein 2 (*Cxcl2*), tumor necrosis factor-α (*Tnf*), Prostaglandin-endoperoxide synthase 2 (*Ptgs2*), Tenascin C (*Tnc*), Interleukin-6 (*Il6*), chemokine (C-X-C motif) ligand 10 (*Cxcl10*), secretory leucocyte peptidase inhibitor (*Slpi*). Data were normalized to the experimental control and presented as mean ± SEM. *, p< 0.05 vs control; **, p< 0.01 vs control; ***, p< 0.001 vs control.

effect in mRNA expression levels of lung tissue, when lungs were treated with TLR2/4 ligands., whereas Figure 16 B shows genes, coding for typical inflammatory proteins: Interleukin 1 β (*Il1b*), macrophage inflammatory protein 2 (*Cxcl2*), tumor necrosis factor-α (*Tnf*) and prostaglandin-endoperoxide synthase 2 (*Ptgs2*) showed upregulated mRNA expression levels in lung tissue, when treated with TLR2 or TLR4 ligands, with a 7-fold increase for *Il1b*, a 5-fold increase for *Cxcl2* and *Ptgs2*, and a 10-fold increase for *Tnc* when compared to control. Stimulation of ventilated and perfused mouse lungs with the TLR2 ligand Pam_3Cys resulted in a smaller increase of mRNA levels for tenascin C (*Tnc*), interleukin-6 (*Il6*),.chemokine (C-X-C motif) ligand 10 (*Cxcl10*), and secretory leukocyte peptidase inhibitor (*Slpi*) when compared to control (*Tnc* showed 2-fold increase, *Il6* 5-fold increase, *Cxcl10* 2-fold increase and *Slpi* no regulation). Treatment of lungs with the TLR2 ligand MALP-2 increased mRNA levels comparable to mRNA levels of lungs treated with the TLR4 ligand LPS, with a fold increase of 7 for *Tnc*, 13 for *Il6*, 6 for *Cxcl10* and of 2 for *Slpi*.

4.1.3.4. TLR2 ligand MALP-2 dependent pulmonary gene transcription

mRNA levels of the inflammatory proteins poly (ADP-ribose) glycohydrolase (*Parg*) and TNF-α receptor-associated factor 1 (*Traf1)* were only increased in lung tissue of MALP-2 treated lungs (Figure 17).

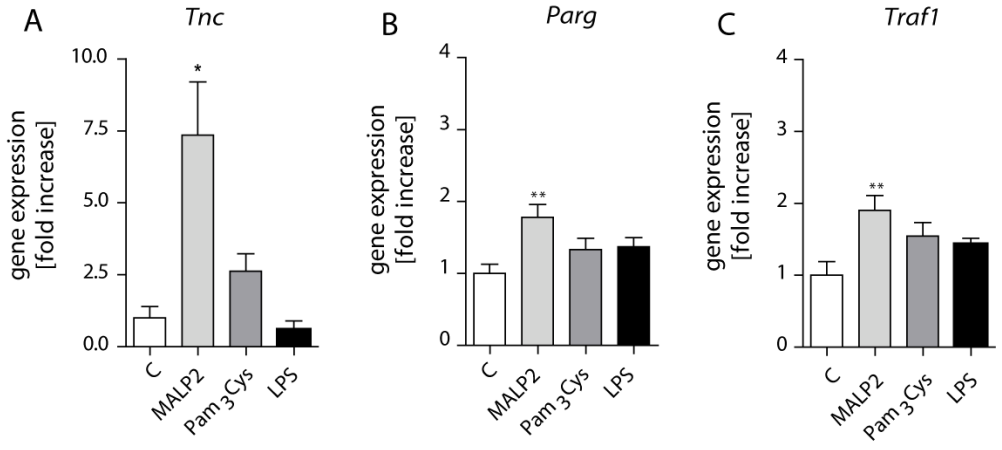

Figure 17 Expression of (A) Tenascin C (B) poly (ADP-ribose) glycohydrolase (*Parg*) and (C) TNF receptor-associated factor 1 (*Traf1*) in isolated perfused mouse lungs. After 60 min of perfusion under baseline conditions, isolated mouse lungs were perfused for another 180 min with Pam_3Cys (160 ng · ml^{-1}, n=5), MALP-2 (25 ng · ml^{-1}, n=5), LPS (1 µg · ml^{-1}, n=3) or under control conditions (n=5). Data were normalized to the experimental control and presented as mean ± SEM. *, p< 0.05 vs control; **, p< 0.01 vs control; ***, p< 0.001 vs control.

4.1.4. The effects of TLR ligands on pulmonary mediator release

4.1.4.1. Pulmonary cytokine release upon TLR2/4 ligand administration

The release of Interleukin-6 in experiments in isolated perfused mouse lungs, significantly increased from 150 min to 240 min ventilation during treatment with both TLR2 and TLR4 ligands. In addition, after 150 min ventilation TNF-α release continuously increased in lungs, treated with LPS. Smaller, but significant increase in the release of TNF-α was observed in the perfusate of lungs treated with the TLR2 ligands MALP-2 and Pam_3Cys (Figure 18).

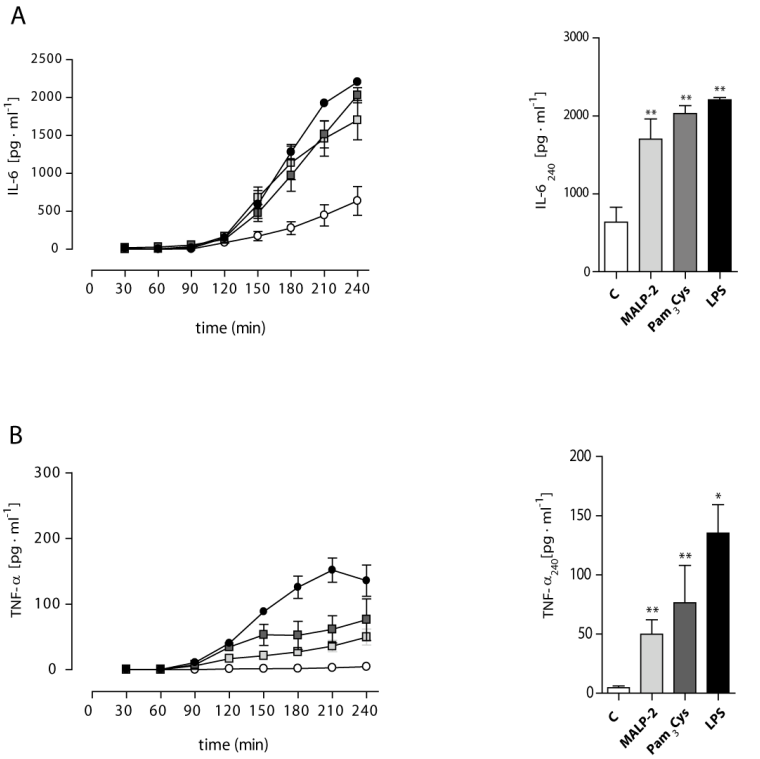

Figure 18 Cytokine release of (A) Il-6 (B) TNF-α into the perfusate buffer of lungs treated with TLR2/TLR4 ligands. Data are expressed as mean ± SEM. White circles indicates control lungs (n=5), grey squares indicates exposure to 25 ng · ml^{-1} MALP-2 (n=5), black squares indicates exposure to 160 ng · ml^{-1} Pam_3Cys whereas 1 µg · ml^{-1} LPS administration is displayed by black circles (n=5). Data are expressed as mean ± SEM. $p < 0.05$ vs control; **, $p < 0.01$ vs control; ***, $p < 0.001$ vs control.

4.1.4.2. Pulmonary chemokine release upon TLR2/4 ligand administration

The release of the chemokine macrophage inducible protein 2 (MIP-2) continuously rised up during treatment with TLR2 and TLR4 ligands, for MALP-2, Pam_3Cys and LPS compared to control as shown in Figure 19. In addition, increase of the chemokine IP-10 were observed in lungs during treatment with either TLR2 ligands MALP-2 and Pam_3Cys as well as the TLR4 ligand LPS (Figure 19.).

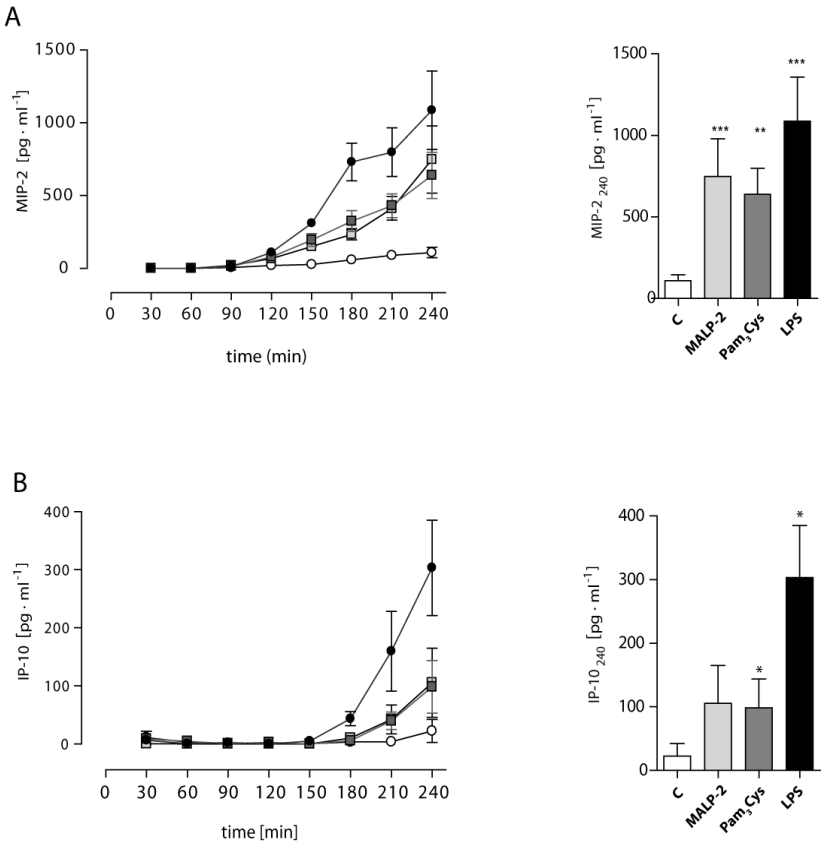

Figure 19 Chemokine release of (A) MIP-2 (B) IP-10 into the perfusate buffer of lungs treated with TLR2/TLR4 ligands. Data are expressed as mean ± SEM. White circles indicates control lungs (n=5), grey squares indicates exposure to 25 ng · ml^{-1} MALP-2 (n=5), black squares indicates exposure to 160 ng · ml^{-1} Pam_3Cys whereas 1 µg · ml^{-1} LPS administration is displayed by black circles (n=5). Data are expressed as mean ± SEM.* p< 0.05 vs control; **, p< 0.01 vs control; ***, p< 0.001 vs control.

4.2. Comparison of overventilation and LPS induced pulmonary gene transcription

4.2.1. Functional annotation analysis of gene-array measurements

In cooperation with T. Dolinay and A. Choi (University Pittsburgh), we investigated gene expression in overventilated mouse lungs compared to lungs stimulated with the TLR2 ligand LPS [103]. The gene expression patterns of animals (controls), ventilated with ~10 cmH_2O EIP, LPS-treated animals and mice (OV), ventilated with ~25 cmH_2O EIP were compared by microarray analysis using 10 k CodeLink bioarrays containing 10.500 mouse genes. To confirm the distinct gene expression profiles, the microarray experiment was repeated on a larger dataset using 20 k CodeLink bioarrays containing 20.00 mouse genes (3.3.12.1). Grouping of the 9.137 valid genes found in both genesets to cellular functions (3.3.12.3) revealed overrepresentation of genes of the immune response, receptor binding, inflammation, growth factor, apoptosis, signal transduction and cytokine activity. It should be noted, that only in the context of stretch-induced overdistension of lungs, growth factor related genes were overexpressed, a functional group of genes, not increased by endotoxin (LPS) administration, as summarized in Figure 20.

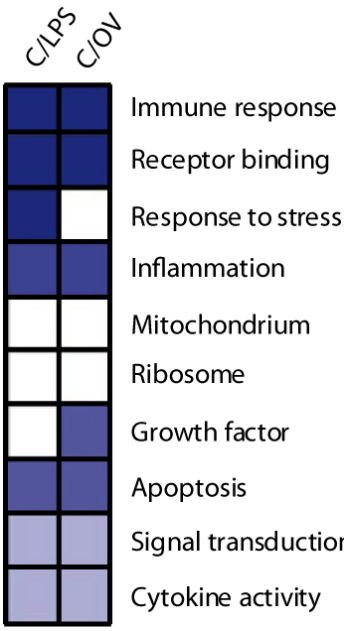

Figure 20 Functional grouping of valid genes in isolated perfused mouse lungs. Groups: Control versus lipopolysaccharide (C/LPS), Control versus overventilation (C/OV). Shades of blue represent the annotation of genes enriched in 1 cluster. Each row represents one important cellular function. Adapted from Dolinay *et al.* 2006 [103].

4.2.2. Validation of overventilation-induced candidate genes found by gene-array measurements

To find genes regulated only by overventilation in both datasets, with no significant change in the LPS treatment group, we used t-tests (3.3.12.2) and found 27 genes regulated by overstretch alone, notably involved in growth factor processes. We confirmed our gene array measurements in the case of 5 candidate genes, the EGF-like growth factor amphiregulin (*Areg*), the anchor protein 12 (*Akap12*), cystein-rich protein-61 (*Cyr61*), nuclear receptor subfamily 4, group A (*Nr4a1* also known as *Nur77*) and interleukin 11 (*IL11*) with quantitative real time PCR (RT-qPCR) and we furthermore observed increased protein expression of amphiregulin in lung tissue [103].

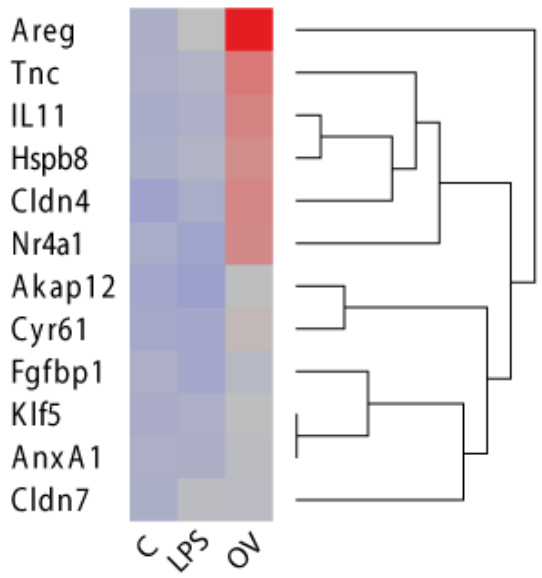

Figure 21 Cluster analysis of RT-qPCR measurements of multiple genes regulated by overventilation in isolated perfused mouse lungs after 180 min treatment. The data are normalized to the control group so that deep blue colour indicates no regulation of genes, grey colours indicates slightly upregulation of genes while red colours indicates upregulated genes. C, lungs ventilated under control conditions (-3 cmH_2O EEP/-10 cmH_2O EIP, n=4), LPS, lungs perfused with 1 $\mu g \cdot ml^{-1}$ of the TLR4 ligand LPS into the perfusate buffer (n=5), OV, lungs overventilated (-3 cmH_2O EEP/-25 cmH_2O EIP, n=3).

As mentioned above (4.2.1), for these studies, we compared gene array measurements of two independent datasets and demonstrated that the gene expression pattern of both sets matched. As the published confirmatory RT-qPCR data only deal with the mRNA of one dataset, we additionally confirmed increased gene expression of the five candidate genes in mRNA levels of the second dataset. Furthermore we studied gene expression of tenascin-C (*Tnc*), fibroblast growth factor binding protein 1 (*Fgfbp1*), heat shock protein 8 (*Hspb8*), claudin 4 (*Cldn4*), krüppel-like factor 5 (*Klf5*), annexin A1 (*Anxa1*) and claudin 7 (*Cldn7*) in the case of overventilation and LPS treatment as summarized in Figure 21.

4.2.3. Overventilation-specific pulmonary gene transcription of growth factor -and cell-extracellular matrix (ECM) related genes

mRNA levels of genes, that were increased by overventilation but not by endotoxin were first found for the five previously published genes and for tenascin c (*Tnc*), fibroblast growth factor binding protein 1 (*Fgfbp1*), heat shock protein 8 (*Hspb8*) and claudin 4 (*Cldn4*), as shown in Figure 22. mRNA levels of krüppel-like factor 5 (*Klf5*), annexin A1 (*Anxa1*) and claudin 7 (*Cldn7*) were affected neither by LPS nor by overventilation (Figure 22).

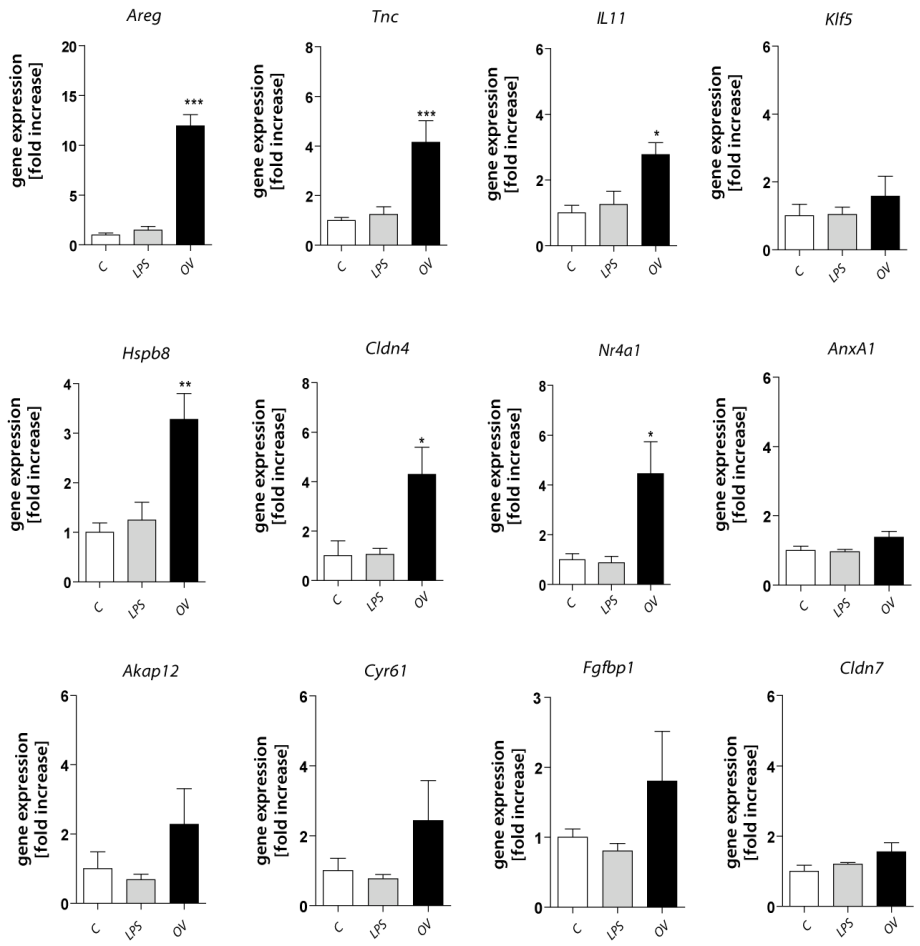

Figure 22 mRNA expression of genes, specially upregulated by overventilation but not by endotoxin after 180 min treatment in isolated perfused mouse lungs. C, lungs ventilated under control conditions (- 3 cmH_2O/-10 cmH_2O), OV, overventilated lungs (- 3 cmH_2O/- 22.5 cmH_2O). Genes: Amphiregulin (*Areg*), tenascin C (*Tnc*), interleukin11 (*Il11*), Krüppel-like zinc-finger transcription factor 5 (*Klf5*), heat shock protein 8 (*Hspb8*, claudin 4 (*Cldn4*), Nuclear receptor subfamily 4, group A, member 1 (*Nr4a1*), Annexin A1 (*AnxA1*), A kinase anchor protein 12 (*Akap12*), Cystein rich protein 61 (*Cyr61*), fibroblast growth factor binding protein 1 (*Fgfbp*1), claudin7 (*Cldn7*). Data are normalized to the experimental control and presented as mean ± SEM. *, p< 0.05 vs control; **, p< 0.01 vs control; ***, p< 0.001 vs control.

4.3. Comparison of pulmonary effects of the EGFR-ligand amphiregulin with that of overventilation

4.3.1. Pulmonary lung functions upon amphiregulin administration and overventilation

Since amphiregulin (AR) was highly expressed in overventilated mouse lungs at gene and protein levels [103], we were interested in the effects of amphiregulin in the lungs. To this end, lungs were perfused and ventilated with control ventilation (-3 cmH_2O EEP and −10 cmH_2O EIP) for 30 min before they were exposed either to 200 ng · ml^{-1} amphiregulin or overventilation (-3 cmH_2O EEP/-22.5 cmH_2O EIP) for 30 min or 60 min. In addition, lungs were perfused and ventilated for 60 min under control conditions, following amphiregulin administration (100 ng · ml^{-1} or 200 ng · ml^{-1}) or overventilation for 150 min. As shown before [151], in overventilated mouse lungs the initially elevated V_T declined, while airway resistance increased, without severe edema or gross lung damage. In all experiments neither 100 ng · ml^{-1} amphiregulin nor 200 ng · ml^{-1} amphiregulin administration significantly change tidal volume or pulmonary resistance (Figure 23).

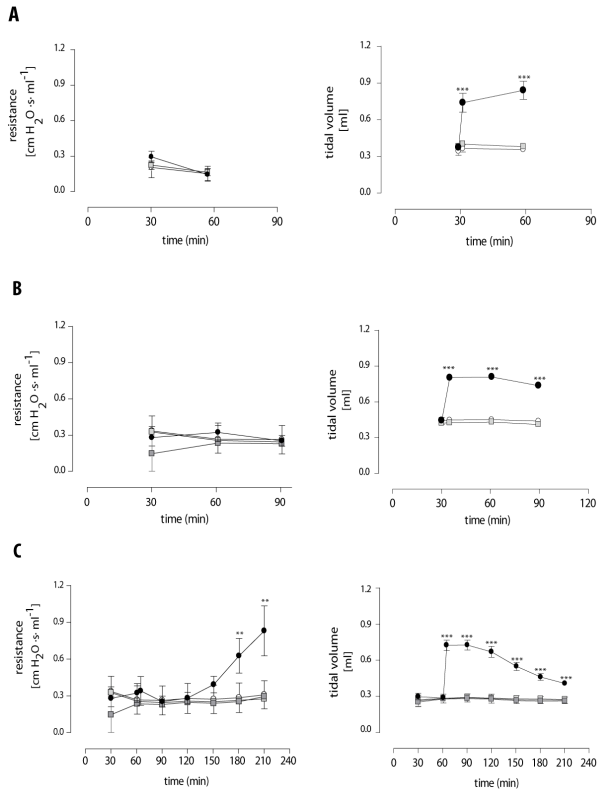

Figure 23 (A) Pulmonary tidal volumes and resistance of experiments with exposure to amphiregulin (100 ng · ml^{-1} and 200 ng · ml^{-1}) or OV for (A) 30 min (B) 60 min and (C) 150 min treatment. Data are expressed as mean ± SEM. White circles indicates control lungs (n=5), grey squares indicates exposure to 100 ng · ml^{-1} (bright) or 200 ng · ml^{-1} amphiregulin (dark) (n=5), black circles indicates exposure to OV (n=5). *, p< 0.05 vs control; **, p< 0.01 vs control; ***, p< 0.001 vs control.

4.3.2. Activation of intracellular signalling pathways upon amphiregulin administration and overventilation

To investigate whether amphiregulin changes pulmonary reactions, mouse lungs were ventilated under control conditions (-3 cmH_2O EEP/ -10 cm H_2O EIP) with additional perfusion of 200 ng · ml^{-1} amphiregulin into the perfusate buffer for 30 min, 60 min or 150 min. Additional experiments with overventilation of lungs (-3 cmH_2O EEP/ -22.5 cmH_2O EIP) were performed.

4.3.2.1. MAPK and AKT/protein kinase B activation upon amphiregulin administration and overventilation during different time points

As observed before [114], overventilation significantly increased the activation of the MAPK ERK1/2 up to 2-fold and JNK/SAPK up to 1.8-fold, compared to control after 30 min and 60 min treatment (Figure 24). Furthermore treatment with 150 min overventilation significantly increased the phosphorylation of ERK1/2 up to 4-fold compared to control, wereas at this timepoint only slight increases in JNK/SAPK phosphorylation in the case of overventilation were detected. 200 ng·

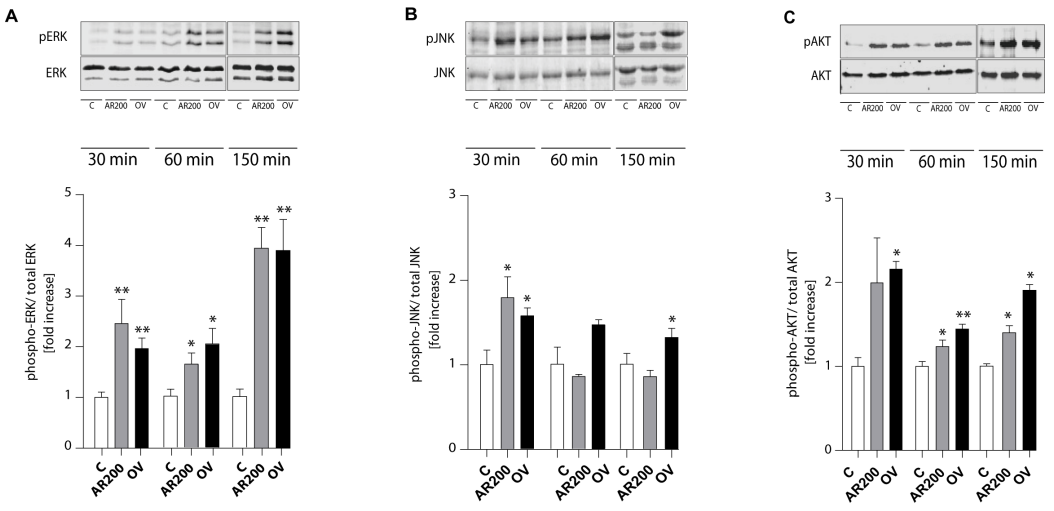

Figure 24 Time course of MAPK and AKT/protein kinase B phosphorylation assessed in lung homogenates of ventilated perfused mouse lungs stimulated with either 200 ng · ml^{-1} amphiregulin (AR) or overventilation (A) ERK1/2 activation of amphiregulin exposure (200 ng · ml^{-1} into the perfusate buffer) or overventilation after 30 min, 60 min and 150 min treatment. (B) JNK/SAPK activation of AR exposure (200 ng · ml^{-1} into the perfusate buffer) or overventilation after 30 min, 60 min and 150 min treatment (C). AKT/ protein kinase B activation of AR exposure (200 ng · ml^{-1} into the perfusate buffer) or overventilation after 30 min, 60 min and 150 min treatment C, control (-3 cmH_2O/-10 cmH_2O), AR200, treatment with 200 ng · ml^{-1} amphiregulin, OV, overventilation (-3 cmH_2O/-22.5 cmH_2O). Data are calculated as the ratio of phospho-protein to total protein, compared to control and expressed as fold increase with mean ± SEM. *, p< 0.05 vs control; **, p< 0.01 vs control. Pictures exemplify one representative immunoblot of 5 independent experiments.

ml^{-1} amphiregulin administration increased the phosphorylation of ERK1/2 with values up to 2-fold after 30 min, 1.8-fold after 60 min and 4-fold after 150 min treatment. Significant JNK/SAPK activation due to 200 ng· ml^{-1} amphiregulin administration in ventilated lungs was observed only after 30 min treatment with a 2-fold increase in phosphorylation compared to control. 200 ng· ml^{-1} amphiregulin exposure and overventilation also enhanced the phosphorylation of AKT/ protein kinase B, with a 1.5-fold increase after 60 min and 150 min amphiregulin exposure and a 2-fold increase after 60 min and 150 min overventilation (Figure 24). However, 200 ng· ml^{-1} amphiregulin exposure for 30 min to both stimuli enhanced AKT/ protein kinase B activation up to 2-fold compared to control, but only overventilation-induced AKT/ protein kinase B activation was significant for these timepoint with values up to 2.5-fold (Figure 24).

4.3.2.2. Dose-dependency of the phosphorylation state of ERK1/2 upon amphiregulin administration

In addition to AKT/proteinkinase B and MAPK investigations upon amphiregulin stiumlation with 200 ng · ml^{-1}(Figure 24), also measurements with 100 ng · ml^{-1} amphiregulin exposure for 150 min were done. Comparison of these data with that of 200 ng · ml^{-1} amphiregulin and overventilation as stimuli shows, that amphiregulin administration resulted in a concentration-dependent increase of ERK1/2 activation from 2-fold in the case of 100 ng· ml^{-1} amphiregulin administration

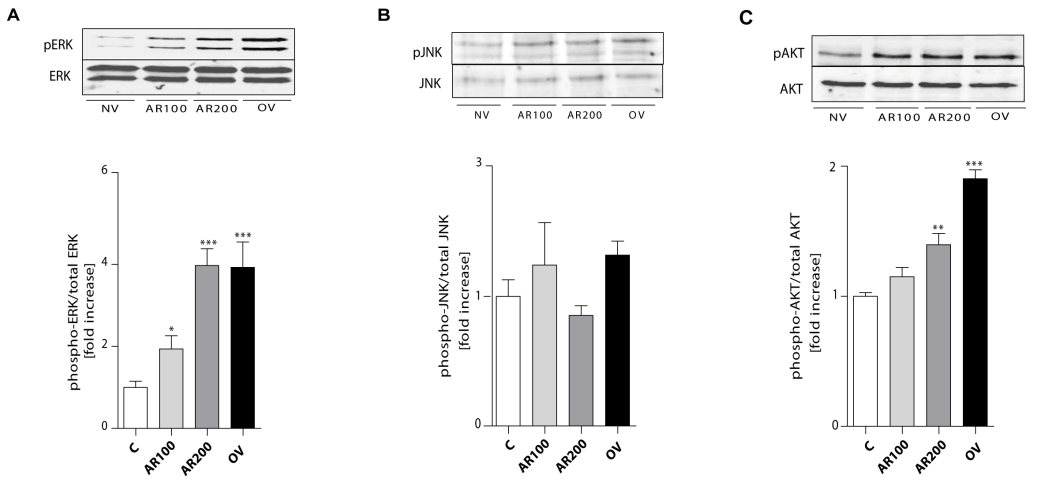

Figure 25 Overventilation –and amphiregulin-induced activation of MAP kinases ERK1/2 and JNK/SAPK and AKT/protein kinase B after 150 min treatment in isolated perfused mouse lungs. (A) ERK1/2 activation of amphiregulin exposure or overventilation after 150 min treatment. (B) JNK/SAPK activation of amphiregulin exposure or overventilation after 150 min treatment. (C) AKT/protein kinase B activation of amphiregulin exposure or overventilation after 150 min treatment. C, control (-3 cmH_2O/-10 cmH_2O), AR100, treatment with 100 ng · ml^{-1} amphiregulin, AR200, treatment with 200 ng · ml^{-1} amphiregulin, OV, overventilation (-3 cmH_2O/-22.5 cmH_2O) Data are calculated as the ratio of phospho-protein to the total amount of this protein, compared to control and expressed as fold increase with mean ± SEM. *, p< 0.05 vs control; **, p< 0.01 vs control; ***, p< 0.001 vs control. Pictures exemplify one representative immunoblot of 5 independent experiments.

to 4-fold for 200 ng· ml^{-1} amphiregulin, when compared to lungs treated under control conditions (Figure 25). Overventilation for 150 min increased phosphorylation of ERK1/2 similar to 200 ng · ml^{-1} amphiregulin administration with a 4-fold increase as shown in Figure 24 and Figure 25. However, neither overventilation nor amphiregulin administration at both concentrations affected the phosphorylation of the MAPK JNK1/2 after 150 min treatment (Figure 25). AKT/ protein kinase B activation of amphiregulin exposure was slightly but significantly increased by 200 ng · ml^{-1} amphiregulin administration after 150 min treatment, whereas no effect was observed in lungs treated with 100 ng · ml^{-1} amphiregulin. In addition, significant overventilation-induced activation of AKT/protein kinase B was observed after 150 min treatment with an 1.8-fold increase when compared to control ventilated lungs (Figure 25).

4.3.2.3. Pulmonary gene transcription upon amphiregulin administration and overventilation

In isolated and ventilated perfused mouse lungs, treated with either amphiregulin (100 ng · ml^{-1} or

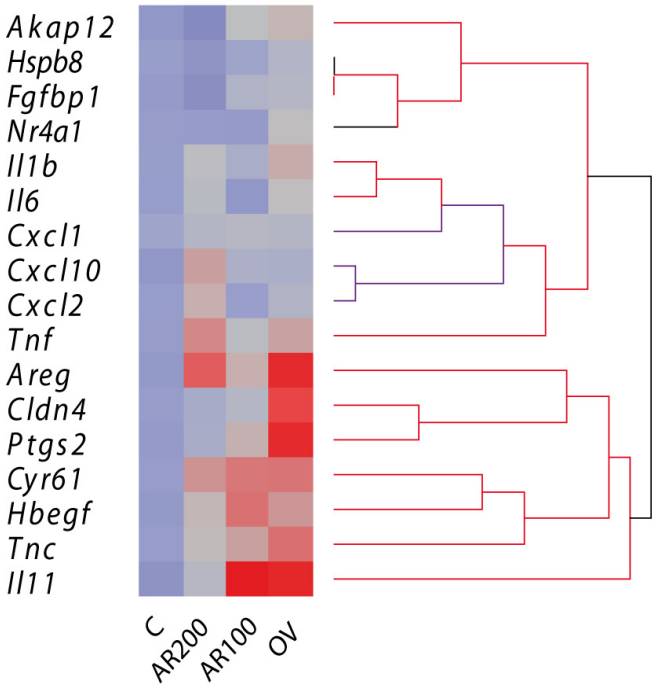

Figure 26 Cluster analysis of RT-qPCR measurements of multiple genes upregulated by overventilation or amphiregulin administration in isolated perfused mouse lungs after 180 min treatment. The data are normalized to the control group (deep blue colour), grey colours indicates slightly upregulation of genes while red colours indicates upregulated genes. Marking of lines in red indicates genes, significant increased by both overventilation and amphiregulin, violet marking indicates genes found to be more transcribed due to amphiregulin administration, whereas black marking indicates genes, significantly upregulated only during overventilation. C, lungs ventilated under control conditions (- 3 cmH_2O EEP/-10 cmH_2O EIP), AR100, lungs perfused with 100 ng · ml^{-1} of amphiregulin into the perfusate buffer, AR200, lungs perfused with 200 ng · ml^{-1} of amphiregulin into the perfusate buffer, OV, overventilated lungs (- 3 cmH_2O EEP/-22.5 cmH_2O EIP).

200 ng · ml^{-1} into the perfusate buffer) or overventilation (-3 cmH_2O EEP/-22.5 H_2O EIP), we investigated 17 genes that were previously found to be increased by overventilation, involved in inflammation, growth and extracellular matrix processes [103]. Cluster analysis (Figure 26) of RT-qPCR measurements showed increased mRNA levels for genes (i) upregulated by either overventilation alone (*Hspb8*, *Nr4a1*), (ii) upregulated by overventilation and amphiregulin administration (*Akap12*, *Fgfbp1*, *Cxcl2*, *Il6*, *Tnf*, *Areg*, *Cldn4*, *Ptgs2*, *Cyr61*, *Hbegf*, *Tnc* and *IL11*). (iii) or genes, and that are higher expressed by amphiregulin stimulation alone, when compared to overventilation (Cxcl1, Cxcl10)). (Figure 28).

4.3.2.4. Gene transcription upon amphiregulin administration and overventilation

The genes *Akap12*, *Fgfbp1*, *IL11*, *Cldn4* and *Hbegf* showed similar upregulation for overventilation and 100 ng · ml^{-1} amphiregulin administration, whereas *Il6*, *Tnf*, *Cxcl1* and *Cxcl2* showed similar upregulation for overventilation compared to 200 ng · ml-1 amphiregulin administration (Figure 28). Increases in mRNA levels for both concentrations and overventilation were observed for *Ptgs2*, *Tnc*, *Areg* and *Il1b* (Figure 28). AR failed to induce gene expression of *Nr4a1* and *Hspb8*, two genes, found to be induced via overventilation (Figure 27).

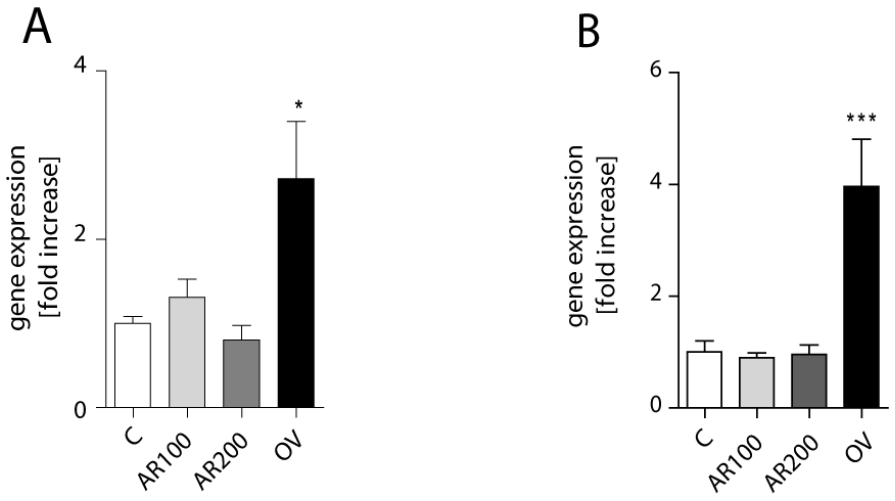

Figure 27 mRNA expression of genes, upregulated by overventilation but not by amhiregulin in isolated perfused mouse lungs. (A) heat shock protein 8 (*Hspb8*), (B) nuclear receptor subfamily 4 (*Nr4a1*). C, lungs ventilated under control conditions (- 3 cmH_2O EEP/-10 cmH_2O EIP), OV, overventilated lungs (-3 cmH_2O EEP/-22.5 cmH_2O EIP), AR100/AR200, lungs perfused with either 100 ng · ml^{-1} or 200 ng · ml^{-1} amphiregulin into the perfusate buffer. Data are normalized to the experimental control, expressed as fold increase and presented as mean ± SEM. *, p< 0.05 vs control; **, p< 0.01 vs control; ***, p< 0.001 vs control.

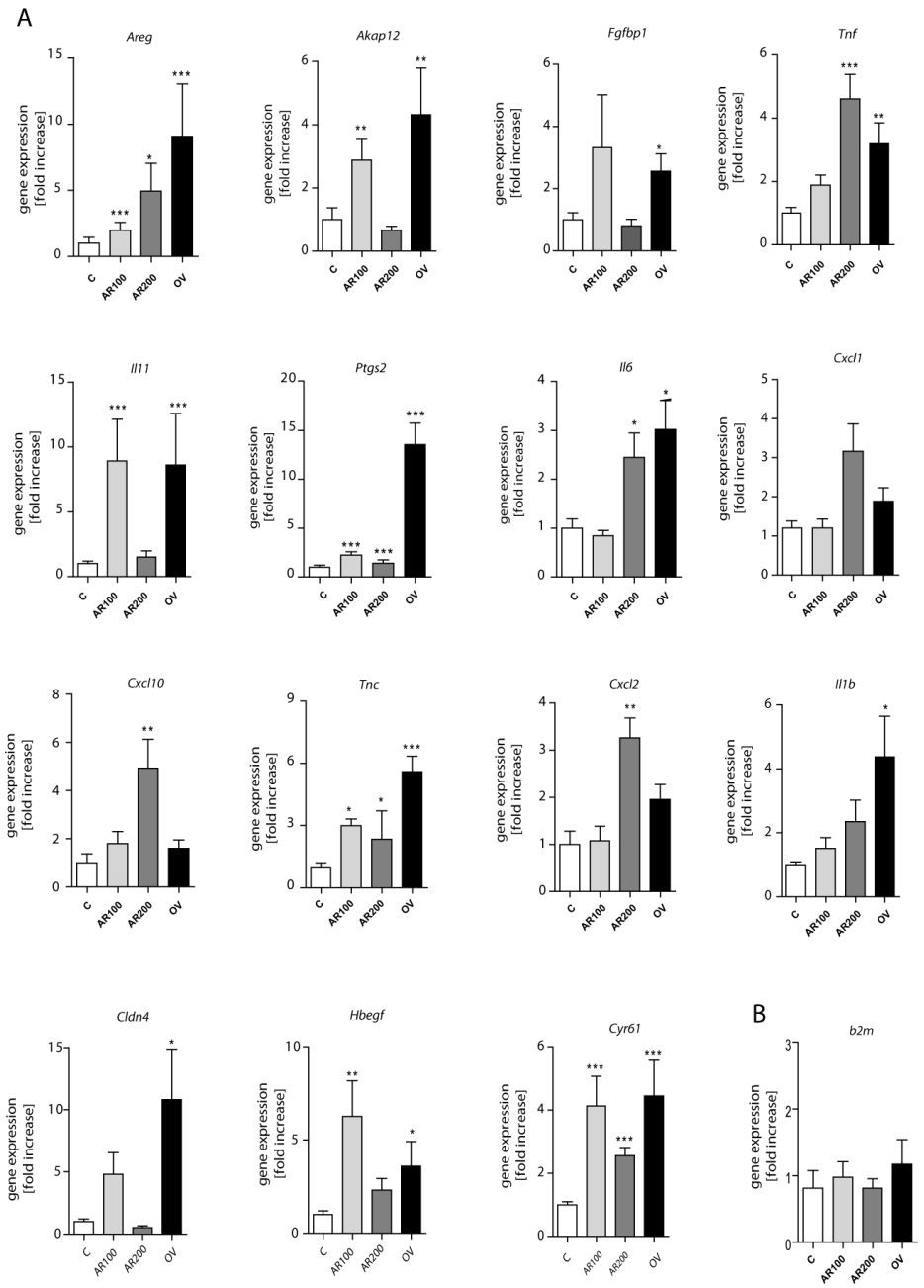

Figure 28 mRNA expression of genes (A) upregulated by overventilation or amphiregulin administration for both amphiregulin concentrations. C, lungs ventilated under control conditions (-3 cmH_2O/-10 cmH_2O), OV, overventilated lungs (-3 cmH_2O/-22.5 cmH_2O), AR100/AR200, lungs perfused with either 100 ng · ml^{-1} or 200 ng · ml^{-1} amphiregulin into the perfusate buffer. Genes: Amphiregulin (*Areg*), a kinase anchor protein 12 (*Akap12*), fibroblast growth factor binding protein 1 (*Fgfbp1*), tumor necrosis factor-α (*Tnf*), interleukin 11 (*IL11*), prostaglandin-endoperoxide synthase 2 (*Ptgs2*), interleukin 6 (*Il6*), chemokine (C-X-C motif) ligand 1 (*Cxcl1*), tenascin c (*Tnc*), MIP-2 (*Cxcl2*) claudin 4 (*Cldn4*), heparin-binding EGF-like growth factor (*Hbegf*), cystein rich protein 61 (*Cyr61*). **(B) Beta 2 microglobulin (*B2m*)** was used as reference gene. Data were normalized to the experimental control, expressed as fold increase and presented as mean ± SEM. *, p< 0.05 vs control; **, p< 0.01 vs control; ***, p< 0.001 vs control.

4.3.3. The effects of amphiregulin and overventilation on pulmonary mediator release

4.3.3.1. Cytokine release upon amphiregulin administration and overventilation

Release of interleukin-6 continuously increased following treatment with 100 ng · ml^{-1} amphiregulin, 200 ng · ml^{-1} amphiregulin or overventilation for 210 min (Figure 29). TNF-α increased only slightly during treatment with 100 ng · ml^{-1} amphiregulin or overventilation but increased significantly during treatment with 200 ng · ml^{-1} amphiregulin (Figure 29).

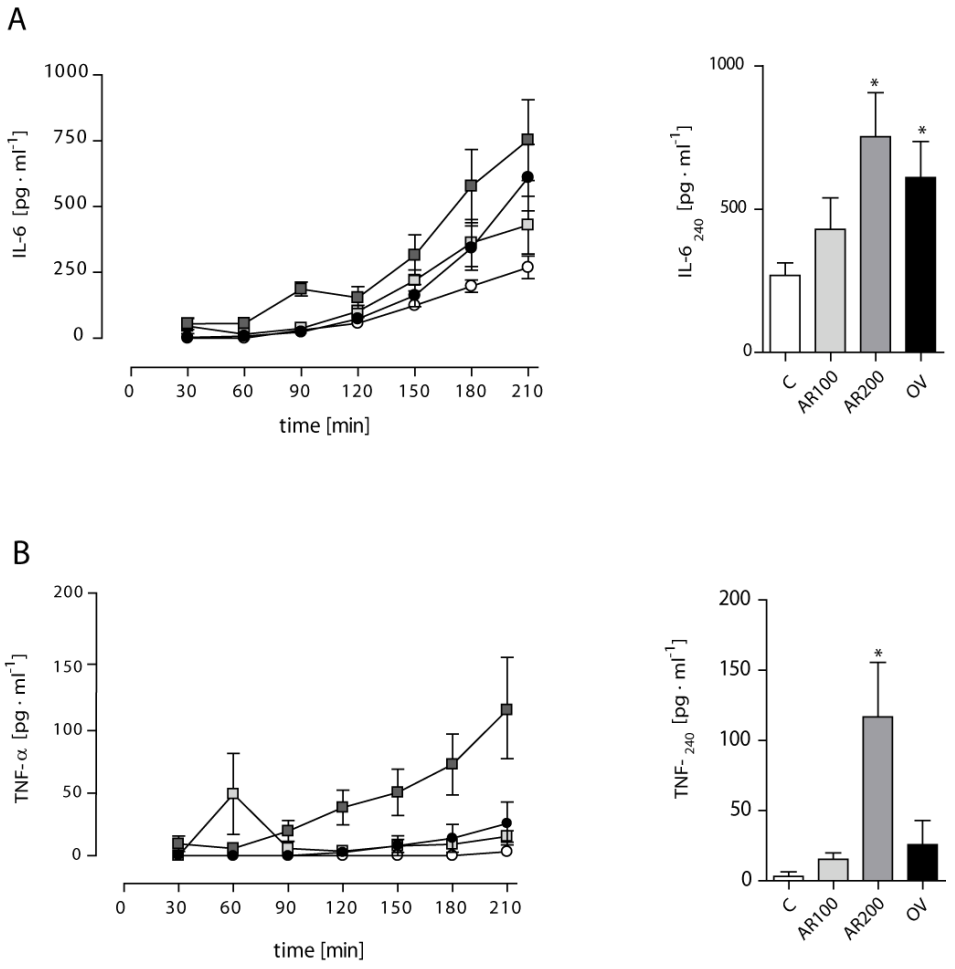

Figure 29 Overventilation-and amphiregulin-induced release of the cytokines (A) IL6 and (B) TNF-α into the perfusate buffer of isolated perfused mouse lungs White circles indicates lungs, ventilated under control conditions (-3 cmH_2O/-10 cmH_2O), (n=5), grey squares indicates exposure with 100 ng · ml^{-1} amphiregulin (n=5), deep grey squares indicates exposure to 200 ng · ml^{-1} amphiregulin whereas overventilation (-3 cmH_2O/-22.5 cmH_2O) is displayed by black circles (n=5). C, control, AR100, treatment with 100 ng · ml^{-1} amphiregulin, AR200, treatment with 200 ng · ml^{-1} amphiregulin, OV, overventilation. Data are expressed as mean ± SEM. *, p< 0.05 vs control; **, p< 0.01 vs control; ***, p< 0.001 vs control.

4.3.3.2. Pulmonary chemokine release upon amphiregulin administration and overventilation

The release of the chemokines chemokine C-X-C motif ligand 2 (MIP-2), chemokine (C-X-C motif) ligand 1 (KC) and chemokine (C-X-C motif) ligand 10.(IP10) into the perfusate buffer of mouse lungs following treatment with amphiregulin and overventilation was measured (Figure 30). Whereas MIP-2 release was only slightly enhanced following both treatment with 100 ng · ml^{-1} amphiregulin, 200 ng · ml^{-1} amphiregulin or overventilation, KC release increased in the case of 200

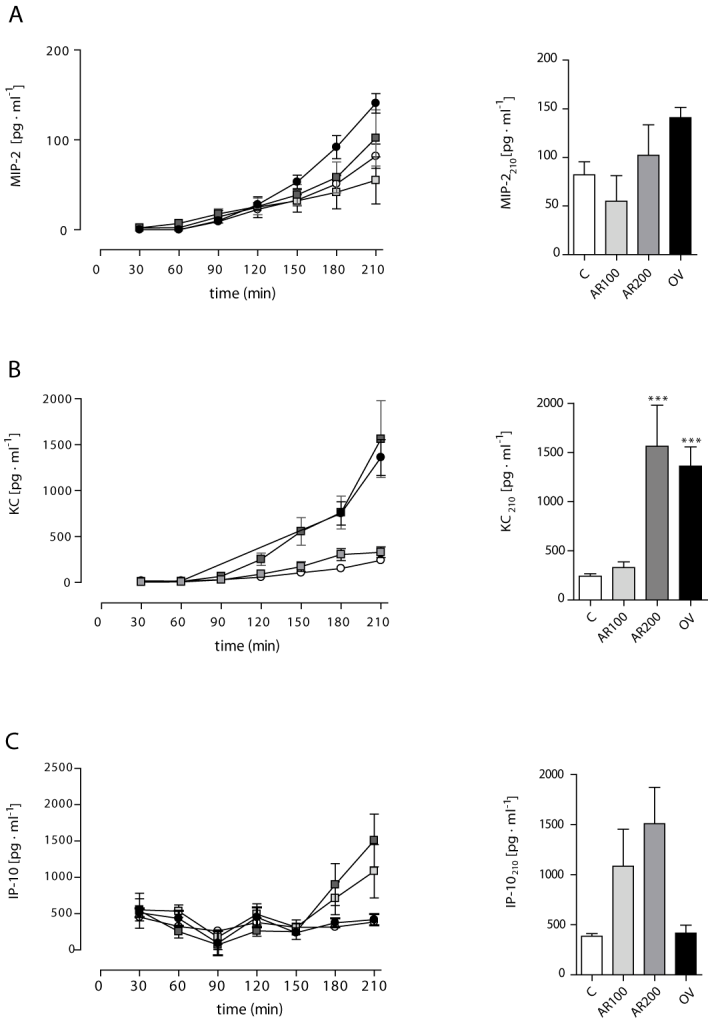

Figure 30 Overventilation–and amphiregulin-induced release of the chemokines (A) MIP-2 (B) KC and (C) IP-10 into the perfusate buffer of isolated perfused mouse lungs. White circles indicates lungs, ventilated under control conditions (-3 cmH_2O/-10 cmH_2O), (n=5), grey squares indicates exposure to 100 ng · ml^{-1} amphiregulin (n=5), deep grey squares indicates exposure to 200 ng · ml^{-1} amphiregulin whereas overventilation (-3 cmH_2O/-22.5 cmH_2O) is displayed by black circles (n=5). C, control, AR100, treatment with 100 ng · ml^{-1} amphiregulin, AR200, treatment with 200 ng · ml^{-1} amphiregulin, OV, overventilation. Data are expressed as mean ± SEM. *, p< 0.05 vs control; **, p< 0.01 vs control; ***, p< 0.001 vs control.

ng · ml^{-1} amphiregulin and overventilation (Figure 30), but showed no effect following 100 ng · ml^{-1} amphiregulin administration. Furthermore 100 ng · ml^{-1} and 200 ng · ml^{-1} amphiregulin administration into the perfusate buffer enhanced IP-10 release after 210 min treatment, whereas overventilation did not affect IP-10 release (Figure 30).

4.4. The effects of EGFR inhibitors on overventilation-induced pulmonary alterations

4.4.1. Pulmonary lung functions upon EGFR inhibitor administration

Since amphiregulin serves as ligand for the ErbB1 receptor (EGFR)(1.4.1), we investigated whether EGFR inhibitors (EGFRIs) change overventilation-induced responses of the lungs. Lungs were overventilated and additionally perfused with the ErbB inhibitors AG1478 and PD301035, which are known to block the tyrosine kinase activity of especially ErbB1 (EGFR) [289]. As mentioned above, (4.3) overventilation significantly increased tidal volume and resistance (Figure 31). Neither AG1478 nor PD301035 altered the overventilation-induced change in lung physiology (Figure 31).

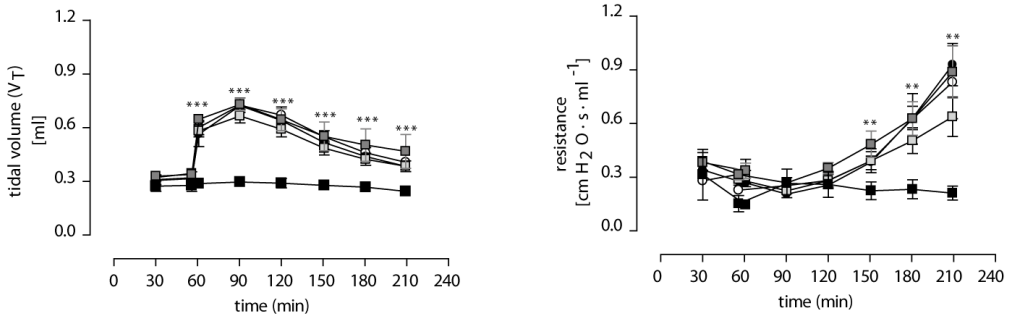

Figure 31 Tidal volume and pulmonary resistance in experiments with the EGFR inhibitors AG1478 and PD301035. White circles indicate overventilated control lungs, administered with 0.001% DMSO (n=5), grey squares indicates experiments with exposure to 250 nM (bright) AG1478 or 1 nM PD 153035 (dark) (n=5), black circles indicates exposure to OV (n=5) and black squares indicates lungs, ventilated under control conditions (-3 cmH_2O EIP/-10 cmH_2O EEP) with administration of 0.001 % DMSO. Significant changes in pulmonary lung functions were calculated for normal ventilated lungs compared to overventilated lungs with *, p< 0.05 vs control; **, p< 0.01 vs control; ***, p< 0.001 vs control. Data are expressed as mean ± SEM.

4.4.2. MAPK and AKT/protein kinase B activation upon EGFR inhibitor administration

To investigate whether EGFR inhibitors (EGFRIs) changes the overventilation-induced responses of MAPK and AKT/protein kinases B, the activation of the MAPK ERK1/2 and JNK/SAPK and that of AKT/protein kinases B were investigated after 60 min and 150 min in overventilated lungs, treated with either AG1478 or PD301035. The OV-induced activation of ERK1/2 was enhanced by AG1478, whereas PD153035 did not affected the phosphorylation of ERK1/2. Moreover, AG1478 as well as PD153035 enhanced the OV-induced activation of JNK/SAPK (Figure 32).

In contrast, AKT/ protein kinase B activation, induced by overventilation was not affected by either inhibitor (Figure 32).

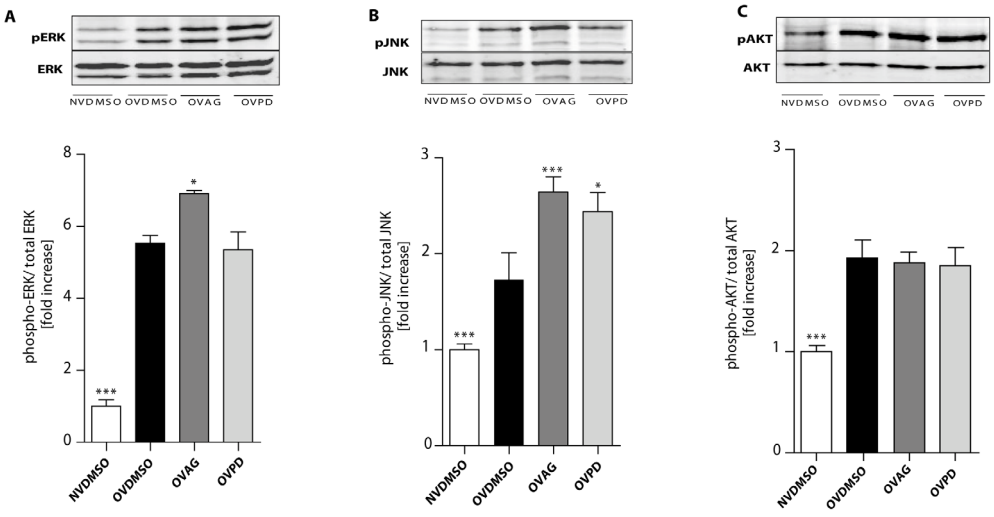

Figure 32 (A) Overventilation-induced activation of ERK1/2, JNK/SAPK and AKT/ protein kinase B after 150 min treatment in isolated perfused mouse lungs treated with the EGFR inhibitors AG1478 or PD301035. (A) ERK1/2 phosphorylation (B) JNK/SAPK phosphorylation (C) AKT/protein kinases B phosphorylation. NVDMSO indicates normal ventilated lungs (-3 cmH_2O EEP/-10 cmH_2O EIP), treated with 0.001% DMSO (n=5), OVDMSO, experiments with overventilated lungs (-3 cmH_2O EEP/-22.5 cmH_2O EIP) treated with 0.001% DMSO (n=5), OVAG, overventilated lungs with exposure to 250 nM AG1478 dissolved in 0.001% DMSO. OVDMSO, overventilated lungs with exposure to 1 nM PD301035 dissolved in 0.001% DMSO. Data are calculated as the ratio of phospho-protein to total protein, compared to control and expressed as fold increase with mean ± SEM. *, p< 0.05 vs OVDMSO; **, p< 0.01 vs OVDMSO; ***, p< 0.001 vs OVDMSO Pictures exemplify one representative immunoblot of 5 independent experiments.

4.4.3. The effects of EGFR Inhibitors on overventilation-induced gene transcription

4.4.3.1. Pulmonary transcription of overventilation-induced genes upon EGFR inhibitor administration

To investigate whether EGFR inhibitors (EGFRIs) changes the overventilation-induced gene transcription, we investigated the regulation of 16 genes, that were previously found to be upregulated by overventilation, including the five candidate genes for overstretch alone in overventilated mouse lungs treated with either 250 nM AG1478 or 1 nM PD301035.

Cluster analysis identified overventilation induced genes, that were decreased by both inhibitors

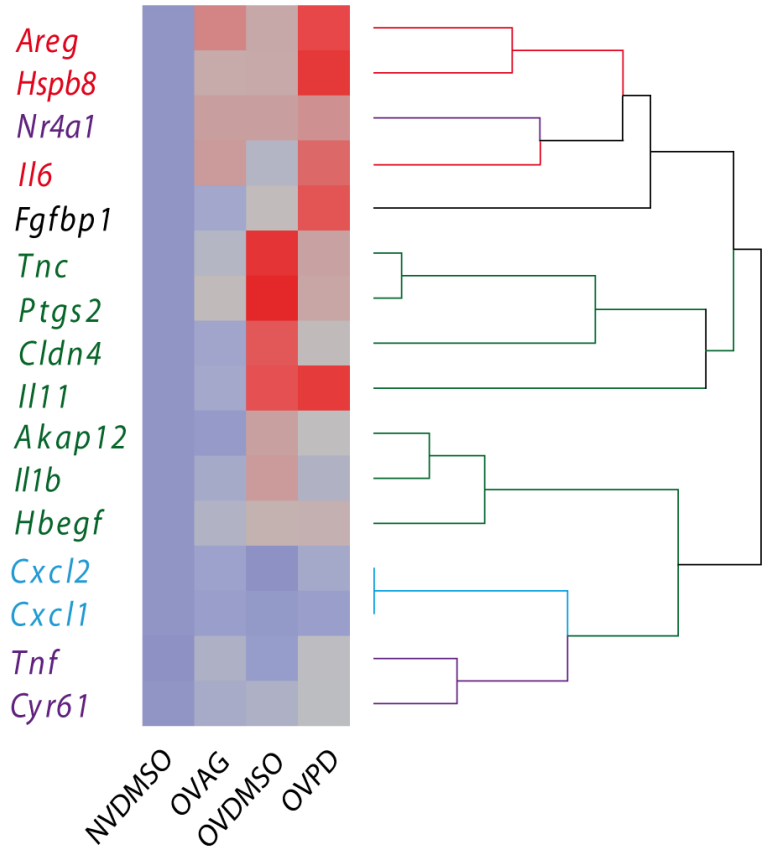

Figure 33 Cluster analysis of gene expression data. Genes are indicated by their gene symbols and expression is colour coded: control group (blue); lighter blue and grey indicate weak upregulation; red indicates strong upregulation. Green lines indicates decreased gene expression due to inhibitor administration, whereas red lines indicates genes, significant increased by inhibitor administration. Blue lines indicates genes, not significant affected. Black lines shows decrease or increase effects depending on the inhibitor, administered. After 60 min under baseline conditions, lungs were perfused for another 180 min overventilation (OVDMSO, -3 cmH_2O/-22.5 cmH_2O, n=5). In addition, isolated lungs were perfused after 30 min before OV was on with the ErbB inhibitors AG1478 (250 nM, n=5) or PD301035 (1 nM, n=5) or under control conditions with DMSO (0.001%, n=5) to the end of the experiment.

(*Tnc, Cldn4,.Akap12, Il1b, Ptgs2, IL11)* increased by both inhibitors (*Areg, Il6, Hspb8*) and overventilation induced genes that showed no effect on treatment with inhibitors (*Tnf, Cyr61, Hbegf, Nr4a1*) In addition genes that were not affected by either overventilation or inhibitor administration *(Cxcl2,* Cxcl1) were found (Figure 33).

4.4.3.1.1. *Attenuation of overventilation-induced gene transcription upon EGFR inhibitor administration*

Treatment of overventilated lungs with both EGFR inhibitors AG1478 and PD153035 resulted in decreased mRNA levels of *Tnc, Akap12, Cldn4, Il1b* and *Ptgs2*, whereas *Akap12*, *IL11* and *Cldn4* mRNA levels were decreased by AG1478, but only slightly by PD153035 (Figure 34).

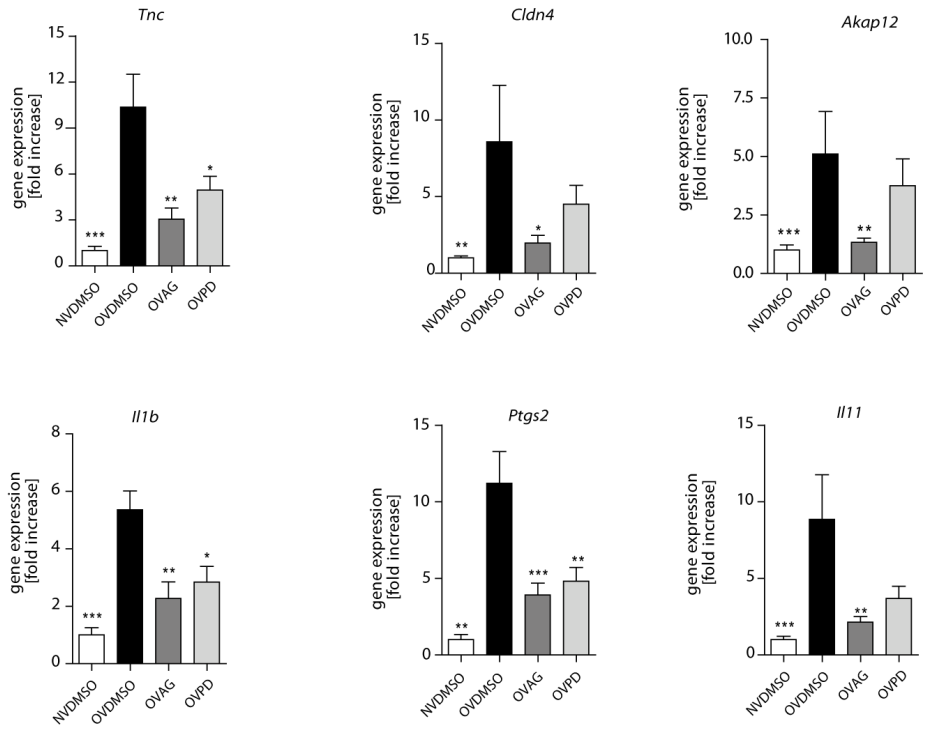

Figure 34 mRNA expression of tenascin c (*Tnc*), claudin 4 (*Cldn4*), a kinase anchor protein 12 (*Akap12*), Interleukin 1-β (*Il1b*), prostaglandin-endoperoxide synthase 2 (*Ptgs2*) and interleukin 11 (*IL11*) in overventilated lungs treated with the EGFR inhibitors AG1478 or PD153035. NVDMSO, lungs ventilated under normal conditions (- 3 cmH_2O/-10 cmH_2O) with 0.001% DMSO. OVDMSO, overventilated lungs (-3 cmH_2O/-22.5 cmH_2O) with treatment of either AG1478 or PD153035. Data are normalized to the experimental control, expressed as fold increase and presented as mean ± SEM. *, p< 0.05 vs OVDMSO; **, p< 0.01 vs OVDMSO; ***, p< 0.001 vs OVDMSO.

4.4.3.1.2. Other effects of overventilation-induced gene transcription upon EGFR inhibitor administration

The overventilation-induced increase of mRNA levels of *Tnf*, *Cyr61*, *Hbegf* and *Nr4a1* were not significantly affected by either inhibitor (Figure 35). mRNA levels of amphiregulin, interleukin-6 and heat shock protein 8 were increased by PD153035 with values up to 6 fold for *Areg* and 5 fold for *Il6* and *Hspb8* compared to overventilated controls (Figure 36 A), whereas *Cxcl1* and *Cxcl*2 were not affected by either overventilation or inhibitor administration (Figure 36 B).

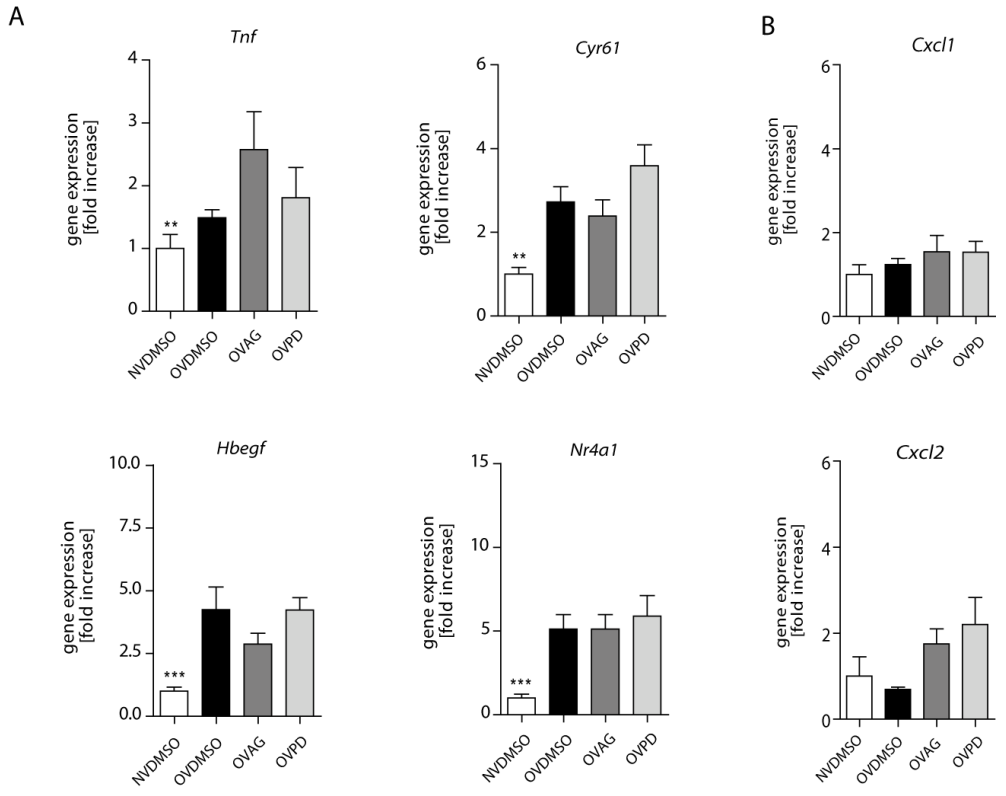

Figure 35 mRNA expression of genes in overventilated lungs treated with the EGFR inhibitors AG1478 or PD153035 (A) tumor necrosis factor alpha (*Tnf*), cystein rich protein 61 (*Cyr61*), heparin-binding EGF-like growth factor (*Hbegf*), nuclear receptor subfamily 4, group A, member 1 (*Nr4a1*) **(B)** Chemokine (C-X-C motif) ligand 10 (*Cxcl10*), Chemokine (C-X-C motif) ligand 1,(*Cxcl1*), Chemokine (C-X-C motif) ligand 2, C, lungs ventilated under control conditions (-3 cmH_2O/-10 cmH_2O) with 0.001% DMSO, OVDMSO, overventilated lungs (-3 cmH_2O/-22.5 cmH_2O),OVAG or OVPD, lungs exposed with either AG1478 or PD153035. Data are normalized to the experimental control, .expressed as fold increase and presented as mean ± SEM. *, p< 0.05 vs OVDMSO, **, p< 0.01 vs OVDMSO; ***, p< 0.001 vs OVDMSO.

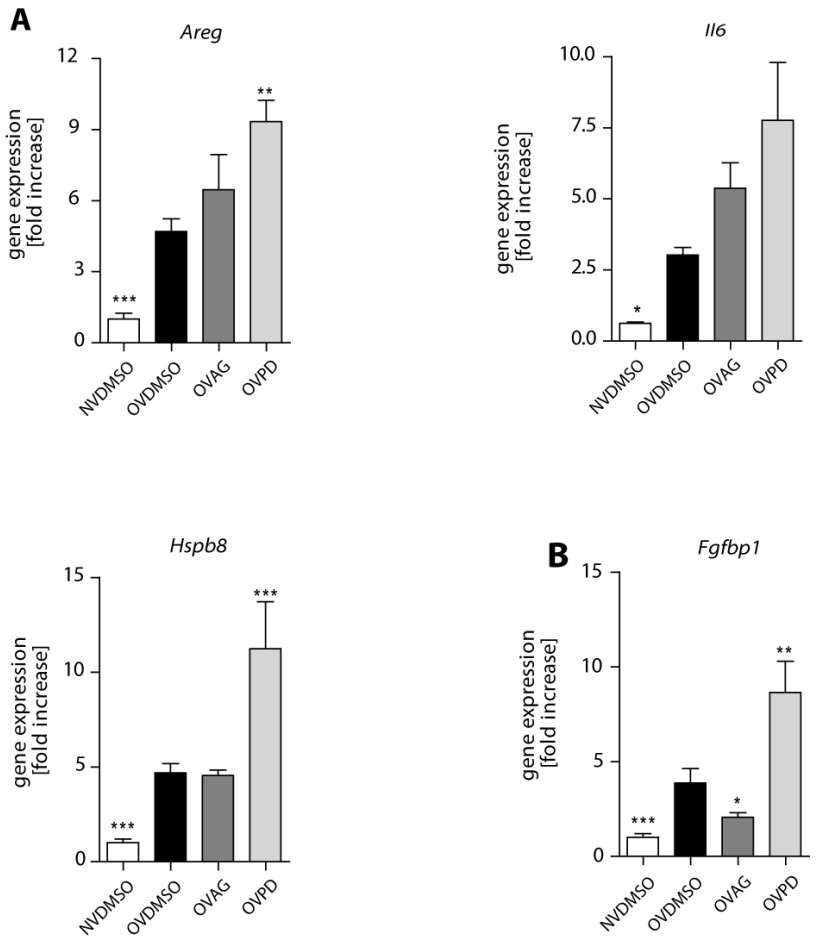

Figure 36 mRNA expression of genes (A) increased by the EGFR inhibitors AG1478 and/or PD153035. Genes: Amphiregulin (*Areg*), Interleukin-6 (*Il6*), heat shock protein 8 (*Hspb8*), (B) mRNA expression of fibroblast growth factor binding protein 1 (*Fgfbp1*) shows either inhibition (administration of AG1478) or upregulation (administration of PD153035), C, lungs ventilated under control conditions (-3 cmH_2O EEP/-10 cmH_2O EIP) with 0.001% DMSO, OVDMSO, overventilated lungs (-3 cmH_2O EEP/-22.5 cmH_2O EIP), OVAG or OVPD, with administration of either AG1478 or PD153035. Data are normalized to the experimental control, expressed as fold increase and presented as mean ± SEM. *, $p < 0.05$ vs OVDMSO; **, $p < 0.01$ vs OVDMSO, ***, $p < 0.001$ vs OVDMSO.

4.4.4. The effects of EGFR inhibitors on overventilation-induced mediator release

The overventilation-induced release of interleukin-6, was not affected by either inhibitors AG1478 or PD153035, whereas the overventilation-induced TNF-α release were diminished after 210 min ventilation for lungs treated with PD153035, but increased in lungs treated with AG1478 (Figure 37).

The overventilation-induced increase of KC was only slightly diminished by treatment with PD153035, whereas only AG1478 induced the IP-10 and MIP-2 release strongly up to 6-fold into lung perfusate during overventilation (Figure 38).

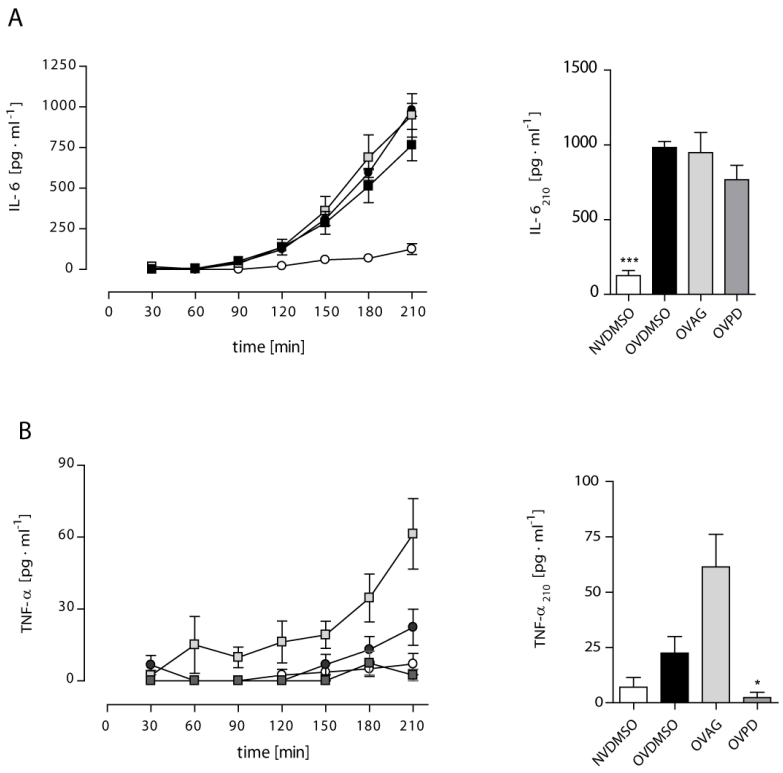

Figure 37 Release of the cytokines (A) Il-6 (B) TNF-α into the perfusate buffer of overventilated isolated perfused mouse lungs treated with the ErbB inhibitors AG1478 or PD301035. White circles indicates control lungs, (-3 cmH_2O EIP /-10 cmH_2O EEP) and administered with 0.001% DMSO (n=5), grey squares indicates experiments with exposure to 250 nM (bright) AG1478 or 1 nM PD 301035 (dark) (n=5), black circles indicates exposure to OV (-3 cmH_2O EIP /-22.5 cmH_2O EEP), n=5) with administration of 0.0001 % DMSO. NVDMSO, control, OVDMSO, overventilation and DMSO, OVAG, overventilated lungs, administered with the ErbB1 inhibitor AG1478, OVPD, overventilated lungs, administered with the ErbB1 inhibitor PD301035. Data are expressed as mean ± SEM. *, p< 0.05 vs OVDMSO, **, p< 0.01 vs OVDMSO,***, p< 0.001 vs OVDMSO.

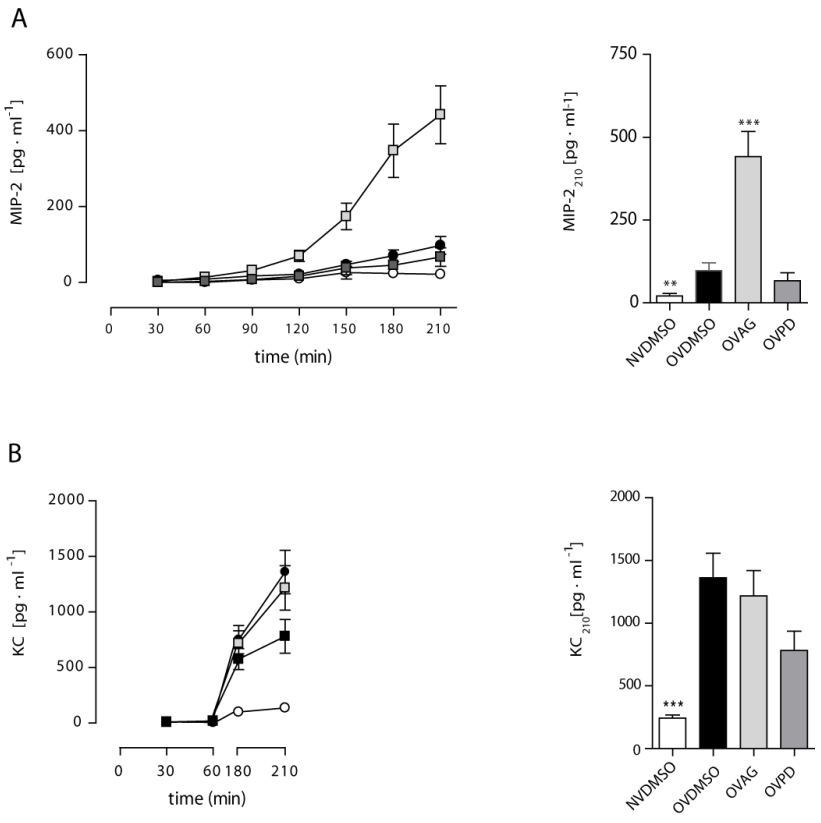

Figure 38 Release of the chemokines (A) MIP-2 (B) KC into the perfusate buffer of overventilated isolated perfused mouse lungs treated with the EGFR inhibitors AG1478 or PD301035. White circles indicates control lungs (-3 cmH_2O EIP /-10 cmH_2O EEP) and administered with 0.001% DMSO (n=5), grey squares indicates experiments with exposure to 250 nM AG1478 (bright) or 1 nM PD 153035 (dark) (n=5), black circles indicates exposure to OV (n=5) with administration of 0.001 % DMSO. NVDMSO, control, OVDMSO, overventilation, OVAG, overventilated lungs administered with the ErbB1 inhibitor AG1478, OVPD, overventilated lungs, administered with the ErbB1 inhibitor PD153035. Data are expressed as mean ± SEM. *, p< 0.05 vs OVDMSO; **, p< 0.01 vs OVDMSO; ***, p< 0.001 vs OVDMSO.

5.Discussion

5.1. Pulmonary lung responses upon TLR2/4 ligand administration

Toll-like receptors play a critical role in the recognition of pathogens by the innate immune system [290,291]. Gram-negative bacteria are recognized by TLR4 receptors, whereas Gram-positive bacteria are recognized by TLR2 receptors by their signature lipoproteins/lipopeptides [220]. Among all organs, the lungs have the highest expression of TLR2 receptors [292]. Beyond infection [293, 294, 295], TLR2-receptors may play a role in several pulmonary diseases including fibrosis [296], asthma [297], lung contusion [298] and acute lung injury [299], as suggested by studies in TLR2-deficient mice. For some time, lipoteichonic acid (LTA) was considered a relevant TLR2 receptor ligand, and most studies on TLR2 receptors in the lungs have focused on this agent [e.g. in 300,301,302,303]. However, because recent evidence indicates that LTA is not a TLR2 receptor ligand [220], now only little is known about the effects of true TLR2 ligands in the lungs. Two well defined ligands that permit studying the functions of TLR2 receptors are the lipopeptides Pam_3CysSK_4 and MALP-2, containing three and two fatty acids, respectively (1.4.2.1).
Macrophage-activating lipopeptide 2KDa (MALP-2) signals by TLR2/TLR6 dimers (1.4.2.1)). *In vivo*, MALP-2 causes increased BAL levels of several proinflammatory cytokines and chemokines as well as neutrophil and lymphocyte infiltration [304,235]. In precision-cut lung slices, it had no effect on cytokine release unless it was applied together with interferon, in whose presence it increased TNF-α and IL-1 release [305], whereas in human airway epithelial cells it induced some chemokines, but no cytokines [306]. Notably, pulmonary application of MALP-2 improved metastasis, vaccination and survival in pneumonia (1.4.2.1).
The synthetic bacterial lipopeptide analogon Pam_3Cys acts on TLR1/TLR2 dimers [220]. In intact lungs it caused cytokine and chemokine release, and in human bronchial epithelial cells (hBE) and human alveolar macrophages it stimulated the release of TNF-α, IL-1, IL-6 and IL-8 (1.4.2.1). There is evidence that TLR1 and TLR6-receptors are not redundant, since the TLR1-$_{7202G}$ mutation is associated with higher mortality rates in sepsis and hyperresponsiveness towards Pam_3Cys [307]. Thus, recent evidence is indicating that both MALP-2 [235, Il1-β, Il-10, KC and Il-12] and Pam_3Cys [308, see Table 11] can stimulate cytokine and chemokine release in intact lungs. However, as all

these studies where done *in vitro* or *in vivo* the contribution of lung parenchyma versus recruited cells to these responses remains unknown. Furthermore, as described in 1.4.2.1 Pam_3Cys and MALP-2 stimulate TLR2-receptors differently, i.e. either TLR2/TLR1 dimers (Pam_3Cys) or TLR2/TRL6 (MALP-2) dimers, but the relative potency and specificity of these agents with respect to proinflammatory responses in the lungs is unknown. Therefore, to systematically compare the effects of TLR2/TLR1 versus TLR2/TLR6 in lung tissue independent of recruited leukocytes, we used isolated blood-free perfused mouse lungs to study the effects of MALP-2 and Pam_3Cys and compared them to those of the well known TLR4 ligand lipopolysaccharide.

5.1.1. Pulmonary inflammatory mediators upon TLR2/4 ligand administration

The present observations on gene induction and cytokine/chemokine release of IL-6, MIP-2 and TNF-α confirm previous findings in mouse lungs perfused with LPS [103,153] and indicate that TLR2 receptor activation leads to similar responses as do TLR4 receptors. Together with IL-1β, these cytokines represent typical genes that are activated by the Myd88-dependent signalling pathway [288], although MIP-2 may also be activated by TRIF [309].

The increase in IP-10 gene and protein levels by TLR2 ligand administration was unexpected, since IP-10 is typically considered to depend on TRIF which are known to couple to TLR4, but not to TLR2 receptors (Figure 6). In addition, MALP-2 was even stronger than LPS in inducing another TRIF-dependent gene, namely *Traf1* (Figure 17). As an explanation, contamination of MALP-2 with LPS seems unlikely, because both MALP-2 and Pam_3Cys were synthetically produced and perfused at concentrations several times lower than LPS – concentrations at which LPS shows little effect in our system [279]. Also, it is well known that LPS is not active in the nanomolar range in the absence of lipopolysaccharide binding protein [310]. More likely explanations for the activation of IP-10 by TLR2 agonists are: (i) The release of IP-10 started later than that of the other cytokines (Figure 19) thus it seems possible that IP-10 was induced by other cytokines such as IL-1 or TNF-α [286]. (ii) There might exist some small Myd88-dependent part in MALP-2 induced activation of IP-10 [260] or another TRIF-independent pathway activated by MALP-2; (iii) Many studies on the role of TRIF in the expression of IP-10 have been performed in myeloid or fibroblast cells in culture. However, TRIF expression is particularly abundant in the lungs [292] and there are may be cell-type and organ-specific differences in the regulation of TLR-receptor signalling [311]. In fact,

MALP-2-dependent release of IP-10 had been observed before in human airway epithelial cells in culture as shown in Table 11.

Table 11 Cytokine/chemokine release and mRNA expression in lung cell lines/organ models stimulated with either LPS, MALP-2 or Pam_3Cys. ↑, slight release/upregulation,↑↑, release, upregulation, –, no release or expression, *nd*, not determined. References: [1] Chen *et al.* 2007 [240],[2] Ritter *et al.* 2005 [306], [3] Natarajan *et al.* 2009 [308],[4]This work.

LPS stimulation

	protein				gene			
cell line/organ model	**IL-6**	**(IL-8) MIP-2**	**TNF-α**	**IP-10**	***Il6***	***Cxcl2***	***Tnf***	***Cxcl10***
peripheral blood mononuclear cells [1]	↑↑	↑↑	↑↑	*nd*	↑↑	↑↑	↑↑	*nd*
human airway epithelial cells [2]	–	–	–	–	–	–	–	–
whole mouse lung in vivo[3]	↑↑	*nd*	↑↑		*nd*	*nd*	*nd*	*nd*
isolated perfused mouse lung [4]	↑↑	↑↑	↑↑	↑↑	↑	↑	↑	↑

MALP-2 stimulation

	protein				gene			
cell line/organ model	**IL-6**	**(IL-8) MIP-2**	**TNF-α**	**IP-10**	***Il6***	***Cxcl2***	***Tnf***	***Cxcl10***
peripheral blood mononuclear cells [1]	*nd*	*nd*	*nd*	*nd*	*nd*	*nd*	*nd*	*nd*
human airway epithelial cells [2]	–	↑↑	–	↑↑	*nd*	*nd*	*nd*	*nd*
isolated perfused mouse lung [4]	↑↑	↑	↑	↑	↑	↑↑	↑↑	↑↑

Pam_3Cys stimulation

	protein				gene			
cell line/organ model	**IL-6**	**(IL-8) MIP-2**	**TNF-α**	**IP-10**	***Il6***	***Cxcl2***	***Tnf***	***Cxcl10***
peripheral blood mononuclear cells [1]	↑	↑↑	↑	*nd*	↑	↑↑	↑	*nd*
human airway epithelial cells [2]	–	–	–	–	*nd*	*nd*	*nd*	*nd*
whole mouse lung in vivo [3]	↑↑	*nd*	↑↑	*nd*	*nd*	*nd*	*nd*	*nd*
isolated perfused mouse lung [4]	↑↑	↑	↑	↑	↑	↑↑	↑↑	↑↑

5.1.2. The pulmonary effects on intracellular signalling pathways upon TLR2/4 ligand exposure

The signalling pathways for both the TLR4 ligand LPS and the TLR1/2 ligands Pam_3Cys and the TLR2/6 ligand MALP-2 have been shown to depend on MyD88, leading to the activation of MAPK, including ERK1/2, JNK/SAPK and p38 (1.4.2.2).

Table 12 shows an overview of found reports, that investigated intracellular signalling proteins e.g. ERK1/2, JNK/SAPK and p38 in response to TLR4 stimulation with LPS and/or the TLR2 ligands Pam_3Cys or MALP-2 in lung tissue. Alveolar macrophages are shown to respond to both TLR4 (LPS) and TLR2 (Pam_3Cys) agonists with increased JNK/SAPK, ERK1/2 and p38 phosphorylation after 30 min treatment [240,259]. In addition, a maximal activity for ERK1/2 and p38 was found after 30 min exposure to LPS, with activity up to 60 min [312]. In line with these results, we also found increased MAPK phosphorylation of ERK1/2 and p38 after 60 min treatment for both TLR2 ligands and we also failed to detect an effect on MAPK activation after 180 min for both TLR4 ligand or TLR2 ligand exposure (Table 12).

In general, inflammatory and stressful stimuli are shown to activate JNK, p38, and ERK [313]. Phosphorylation of ERK and p38 are involved in the production of cytokines such as TNF-α, Il-6 and Il-8 (or the mouse analogon MIP-2) in response to TLR ligand stimulation [232,314,315] which are also enhanced in the model of isolated perfused mouse lungs (Table 11).

The c-Jun-NH2-terminal kinase JNK have also been reported to be an important mediator of inflammatory processes, induced by LPS [316] and JNK activity was observed after 30 min Pam_3Cys exposure (2 $\mu g \cdot ml^{-1}$) in murine alveolar macrophages [259]. In the model of isolated perfused mouse lungs, we investigated JNK activity after 60 min and 180 min agonist stimulation, and found no phosphorylation of JNK for both TLR2 and TLR4 agonist, suggesting that TLR agonist stimulation may activate JNK in a time-dependent and transient manner in the lungs (Table 12).

The serine /threonine kinase AKT/Protein kinase B plays critical roles in multiple cellular processes by inhibiting apoptosis induced by diverse stimuli (UV light, matrix detachment, DNA damage, viral infection)[317]. Recently AKT was shown to be induced via LPS in human alveolar macrophages after 5 min treatment [318]. In addition, activation of AKT within 15 min in LPS-inflamed lungs *in vivo* was observed [312]. In our model of isolated lungs, TLR2/4 ligands failed to activate AKT indicating that its activation by LPS *in vivo* might be related to AKT phosphorylation in sequestered leukocytes [319].

Table 12 MAPK/AKT protein kinase B activation in lung cell lines/organ models stimulated with either LPS, MALP-2 or Pam_3Cys. ↑, slight activation; ↑↑, activation; **–**, no significant release or expression; *nd*, not determined;^{30}, 30 min treatment;^{60}, 60 min treatment,^{180},180 min treatment. References:[1] Chen *et al.* 2007 [240], [2] Shan *et al.* 2006 [306], [3] This work., [4] Bozinowski *et al.* 2002 [312],[5] Cabanski *et al.* 2008 [259].

	LPS stimulation			
cell line/organ model	**JNK/SAPK**	**ERK1/2**	**p38**	**AKT/protein kinase B**
alveolar macrophages[1]	*nd*	*nd*	↑↑^{30}	*nd*
airway smooth muscle cells[2]	–^{30},– ^{60}	↑↑^{30}, ↑↑ ^{60}	↑↑^{30}, ↑↑^{60}	*nd*
alveolar macrophages[5]	↑^{30}	↑↑^{30}	↑↑^{30}	*nd*
whole mouse lung *in vivo*[4]	*nd*	↑↑^{30}	– ^{30}	↑^{30}
whole mouse lung (IPL)[3]	–^{180}	–^{180}	–^{180}	–^{180}

	MALP-2 stimulation			
cell line/organ model	**JNK/SAPK**	**ERK1/2**	**p38**	**AKT/protein kinase B**
whole mouse lung (IPL)[3]	–^{60}, –^{180}	↑↑^{60}, ↑^{180}	↑↑^{60}, –^{180}	–^{60}, –^{180}

	Pam_3Cys stimulation			
cell line/organ model	**JNK/SAPK**	**ERK1/2**	**p38**	**AKT/protein kinase B**
alveolar macrophages[5]	↑^{30}	↑↑^{30}	↑↑^{30}	*nd*
whole mouse lung (IPL)[3]	–^{60}, –^{180}	↑↑^{60}, –^{180}	↑↑^{60}, –^{180}	–^{60}, –^{180}

5.1.3. Pulmonary gene transcription upon TLR2/4 ligand exposure

In addition to our investigation on cytokine gene expression of *Il6, Cxcl2, Tnf and Cxcl10* (5.1.2) we investigated the regulation of 9 genes upon TLR2 and TLR4 stimulation including 3 genes that are involved in growth or related to and 6 genes, involved in inflammatory processes (Table 13). The pattern of gene transcription was very similar between the three TLR-receptor agonists studied

Table 13 Comparison of gene induction after 180 min treatment in isolated perfused mouse lungs (IPL) stimulated with either LPS, MALP-2 or Pam_3Cys. ↑, slight upregulation; ↑↑, activation; –, no significant expression; Amphiregulin (*Areg*), heparin-binding EGF-like growth factor (*Hbegf*), angiopoietin-like 2 (*Angptl2*), Prostaglandin-endoperoxide synthase 2 (*Ptgs2*), interleukin 1 beta (*Il1b*), secretory leukocyte peptidase inhibitor (*Slpi*), tenascin C (*Tnc*), TNF receptor-associated factor 1 (*Traf1*) and poly (ADP-ribose) glycohydrolase (*Parg*).

gene	stimulus		
	LPS	MALP-2	Pam_3Cys
Areg	–	–	–
Hbegf	–	–	–
Angptl2	–	–	–
Ptgs2	↑	↑	↑
Il1b	↑	↑↑	↑↑
Slpi	↑↑	↑↑	↑
Tnc	–	↑↑	↑
Traf1	–	↑↑	–
Parg	–	↑↑	–

and all of them induced several genes that are known to be involved in inflammation (Figure 15). The growth factor ligands amphiregulin (*Areg*) and heparin-binding EGF-like growth factor (*Hbegf*) that are well known to be activated by mechanical stimuli [103,100] were not affected by TLR2 or TLR4-receptor activation. This is noteworthy, because otherwise most of the genes that are activated by LPS in the lungs are also activated by mechanical ventilation [103,70,320,321], suggesting that amphiregulin and HB-EGF may be used as molecular markers to distinguish infectious from mechanical stimuli. Interestingly, there were three genes significant upregulated only upon MALP-2 stimulation: Tenascin C (*Tnc*), poly (ADP-ribose) glycohydrolase (*Parg*) and TNF receptor-associated factor 1 (*Traf1*)

Traf 1 is known to be TRIF-dependent (4.1.3.2) and form a heterodimeric complex with *Traf 2*, which is required for TNF-α mediated activation of MAPK8/JNK/SAPK and NF-kappaB and was recently suggested to play a role in facilitating allergic lung inflammation [322]. PARG is the

degrading enzyme within the metabolism of poly(ADP-ribose) (PAR). PAR homeostasis is critical for genomic stability in multicellular eukaryotes and is involved in cell cycle progression, gene transcription, cell differentiation, apoptosis and DNA repair [323].
Tensascin C as an extracellular matrix (ECM) glycoprotein within the tenascin family [324] harbours an EGF-like domain [324] and shows low but detectable action on the EGF-receptor [325]. It is highly expressed in lungs from patients with respiratory distress syndrome and bronchopulmonary dyplasia, although its role in the pathogenesis of these diseases is unknown [326]. In general, tenascins are thought to be involved in tissue remodelling after injury [327], providing a possible explanation for the beneficial effects of MALP-2 on wound healing in mice [328] and humans [329].

Because TLR1 and TLR6-receptors do not appear to be redundant [330], one aim of this study was to compare the consequences of TLR2/TLR1 vs TLR2/TRL6 receptor activation in the lungs. Therefore, we have studied Pam_3Cys that signals through TLR2/TLR1 dimers and MALP-2 that signals through TLR2/TRL6 receptors. The concentrations required for proinflammatory signalling were relatively low for perfusion experiments in intact lungs, i.e. 25 ng· ml^{-1} for MALP-2 and 160 ng · ml^{-1} for Pam_3Cys. At these concentrations, both TLR2 ligands showed a strong proinflammatory response. Overall the responses to both TLR2 ligands on MAP kinases, gene expression and mediator production were similar. However, MALP-2 was able to induce the expression of three genes that were not affected by Pam_3Cys, i.e. *Slpi*, *Tnc* and *Parg*. As these genes had not before been studied following TLR2 receptor activation, the significance of these findings remains to be shown. Others have reported in candidiasis that TLR1 deficient mice had no phenotype, whereas TLR6-deficient mice produced similar levels of TNF-α, IL-1 and IL-6, but less IFNγ and IL-10, providing further evidence that some genes may be regulated specifically by TLR2/TLR6-receptor dimers [331], although from thorough studies in cell culture others have concluded that TLR1 and TLR6 lead to identical signalling events [332].

In conclusion, despite the fact that TLR2-receptors do not couple to TRIF, the effects of TLR2/1, TLR2/6 and TLR4-receptor activation in the isolated lungs on MAPK activation, gene induction and cytokine release were largely similar. In addition to several well known proinflammatory cytokines we also demonstrate TLR2-dependent production of IP-10, a chemokine which is upregulated in acute lung injury [333], although its functions in this setting remain poorly defined. Other genes shown to be upregulated by TLR2-receptor activation were *Slpi*, tenascin C,

poly(ADP-ribose)glycohydrolase and *Traf1*. Particularly impressive and restricted to MALP-2 (TLR2/6) was the induction of tenascin C, suggesting the existence of TLR2/6-specific pathways.

5.2. Overventilation specific pulmonary gene transcription

Since intracellular signal transduction pathways initiated by mechanical ventilation and the canonical inflammation pathways activated due to microorganisms share similarities [70], we were interested in differences between microorganism-induced and overventilated induced lung reactions.

Our gene expression profiling in overventilated mouse lungs discovered genes, involved in growth factor and extracellular matrix (ECM) processes, that are regulated by overstretch, but not by endotoxin [103].

Since microarray analysis generates a huge amount of data, and hence validation is an important part of the analysis, we studied the expression pattern of 12 genes with RT-qPCR analysis and confirmed 9 genes differently regulated via overstretch alone, belonging to the group of growth factors (*Areg, Fgfbp1, Nr4a1)*, extracellular matrix proteins (*Tnc, Cyr61, Cldn4, Akap12*), heat shock proteins (*Hspb8*) and cytokines (*IL-11*), pointing to novel signalling pathways, that are activated by overventilation.

For example, nuclear orphan receptor subfamily 4 (*Nr4a1*), also known as *Nur77,* first described as a growth factor-inducible immediate-early [334] gene and also detected in a rat model of VILI [155] represents a nuclear receptor, which act as transcription factor in regulation of the expression of genes involved in numerous biological processes, including cell proliferation, differentiation, methabolism and development and notably apoptosis, where *Nr4a1* is known to have a proapoptotic role [335].

Fibroblast growth factor binding protein (*Fgfbp1*) as a second example, is a secreted binding protein that are known to enhance the activity of locally stored fibroblast growth factors (FGFs) [336]. Fibroblast growth factors (FGFs) plays critical roles in development, maintenance and repair following injury or disease in the lungs [337].

Third, *Hspb8,* also known as Crystallin c, is part of the heat shock superfamily *(sHsp),* that posses chaperone activity *in vitro* and strong evidence exists supporting their role in conformational diseases [338]. In addition, expression of other family members (e.g. *Hspb27*, *Hsp 60*, *Hsp 70* and *Hsp 32*) are well described in both whole lungs and in specific lung cells from a variety of species

and in response to a variety of stressors, where it is suggested, that they have a cytoprotective role during lung inflammation and injury [339].

Moreover our observation of the expression levels of two genes upon overventilation, that belong to the family of claudins could be interesting. We found *cldn4* upregulated during overventilation, while *cldn7* was not significant affected (Figure 21).

The family of claudins are known to play essential roles in tissue-specific barrier function of tight junctions (TJ) where it is known, that expression profiles for the claudin family member differ from tissue to tissue, resulting in the formation of tissue specific characteristics of the TJ barrier [340]. Claudin 4 and 7 were recently shown to express in normal alveolar epithelium, mainly in type II pneumocytes [341], and in line with our observation of *cldn4* expression in our mechanotransduction model, specific increase in claudin-4 mRNA and protein expression was recently shown in a model of VILI by Wray *et al.* where increase in claudin-4 expression correlated with the extent of injury [342]. Based on their study, the authors propose that the change in claudin-4 expression during lung injury could reflect an adaptive response of the alveolar epithelium, acting to protect barrier function and limit edema formation during lung injury.

In conclusion, we validate 9 genes, that we found via gene-array measurements differently regulated by overstretching alone, belonging to growth factors, extracellular matrix processes and cytokines, pointing to novel signalling pathways, activated during overventilation.

5.3. The epidermal growth factor–like ligand amphiregulin

5.3.1. Pulmonary inflammatory mediators upon amphiregulin exposure

Since we observed increased mRNA and protein expression of amphiregulin (AR) in overventilated mouse lungs [103], we examined the effects of amphiregulin stimulation in the lungs. Amphiregulin perfusion in isolated mouse lungs enhanced the release of IL-6, TNF-α , KC and IP-10 into the perfusate buffer as well as upregulation of mRNA of theses cytokines/chemokines (Figure 28, Figure 29, Figure 30).

About cytokine induction by amphiregulin nothing has been reported until 2005, where Mahtouk *et al.* observed the stimulation of Interleukin-6 and growth in bone marrow stromal cells due to amphiregulin exposure [343]. In addition, one recent study investigated the stimulatory effect of amphiregulin on cytokine production in fibroblast-like synoviocytes (FLS) and detected a concentration-dependent release of Interleukin-6, Interleukin-8 and GM-CSF [344]. In isolated lungs, IL-6 was upregulated by amphiregulin in a concentration-dependent manner and TNF-α and KC release were increased after perfusion with 200 ng $\cdot$ ml^{-1} amphiregulin.

Comparison of amphiregulin cytokine induction with overventilation-induced cytokine release showed, that IL-6, TNF-α and KC were enhanced by both, amphiregulin and overventilation. (Figure 39). Together with our findings on overventilation-induced selective amphiregulin protein and gene expression [103] we speculate that amphiregulin may contribute to some of the cytokine responses of the lungs, that we observed during overventilation (Figure 39).

5.3.2. Pulmonary gene transcription upon amphiregulin exposure and overventilation

Since nothing was known about the regulation of genes by amphiregulin in the lungs, in addition to inflammatory cytokines/chemokines, we examined the regulation of 12 genes, that we previously had found upregulated upon overventilation. Our data show induction of several genes, involved in growth, inflammation and extracellular matrix proteins by both, amphiregulin and overventilation (Figure 26).

Interestingly, the two genes *Hspb8* and *Nr4a1* that were upregulated by mechanical stretch, were not upregulated by either LPS or amphiregulin (Figure 27). This observation may be interesting in the context of overstretching of lung tissues, because our data consistently shows pulmonary upregulation of *Nr4a1* during overventilation, independent of endotoxin, amphiregulin or EGFR activation (Figure 27, Figure 35). Since amphiregulin may promote some of the proinflammatory responses of the lungs, and induction of growth factor related genes (*Areg*, *Hbegf*, *Fgfbp1*) and genes involved in ECM processes (*Tnc*, *Cyr61*), that were also found to be induced by overventilation, the activation of *Nr4a1* by overstretch may point to another signalling pathways.

5.3.3. Activation of overventilation-induced MAPK and AKT/protein kinase B upon amphiregulin exposure

MAPK (ERK1/2, JNK/SAPK) and AKT/protein kinase B phosphorylation are well known events upon ErbB activation (1.4.1) and are also known to be activated by mechanical ventilation with high tidal volume (1.3.2.1). In addition, the activation of EGFR-mediated signalling and subsequent MAP kinase activation by cyclic strain/stretch associated with MV have been demonstrated in various cell types, including lung epithelial cells, suggesting that the EGFR is involved in mechanotransduction [345,101].

Our data showed increased ERK1/2 and AKT/protein kinase B activation upon amphiregulin stimulation and overventilation at three time points: 30 min, 60 min and 150 min (Figure 24). These data are in line with findings from Papaiahgari *et al*., that the AREG-EGFR pathway is critical for regulating AKT and ERK1/2 signalling induced by cyclic stretch in lung epithelial cells [102]. Interestingly, JNK/SAPK activation due to overventilation was increased at all three time points in our study, whereas JNK/SAPK activation upon amphiregulin exposure was only found after 30 min treatment (Figure 24), suggesting that early pulmonary responses of JNK/SAPK activation could be triggered via amphiregulin (Figure 39).

In summary, our data of increased MAPK and AKT/protein kinase B activation upon amphiregulin stimulation with concomitant induction of inflammatory genes and secretion of inflammatory cytokines/chemokines in mouse lungs lead to the hypothesis, that amphiregulin may contribute to the induction of MAPK /AKT protein kinase B found by overstretch [114,108, 120].

Perhaps mechanical stretch activates amphiregulin, that in turn activates its common known receptor, the EGFR. This may lead to the activation of MAPK /AKT protein kinase B and in turn to

the regulation of several overstretch-related genes and release of related cytokines/chemokines (Figure 39).

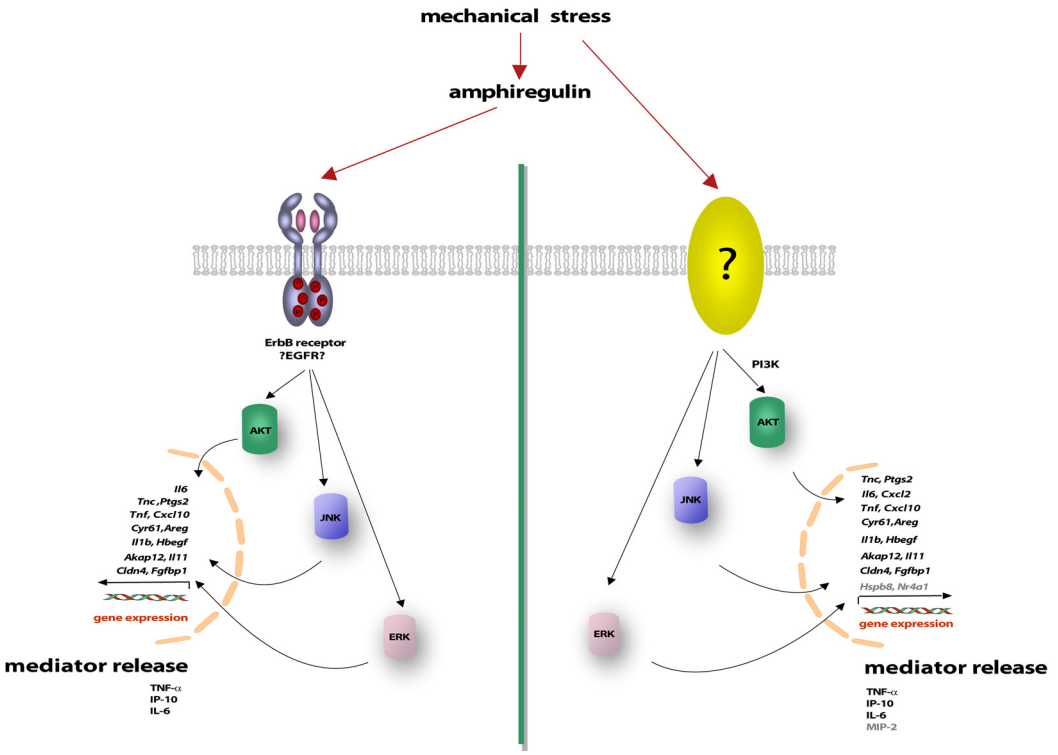

Figure 39 Amphiregulin may contribute to some of the pulmonary responses found by overstretch in the lungs. Both, mechanical stress and amphiregulin stimulation leads to the activation of AKT/protein kinase B (AKT), JNK/SAPK (JNK) and ERK1/2 (ERK), the upregulation of several genes and the release of proinflammatory mediators. Together with our findings on overventilation-induced amphiregulin protein and gene expression [103], we speculate, that amphiregulin may promote some of the stretch-induced pulmonary responses, perhaps through EGFR-signalling.

5.4. The effects of EGFR inhibitors on overventilation-induced pulmonary alterations

Amphiregulin serve as a ligand for the ErbB1 receptor (EGFR)(1.4.1.1). Since evidence suggests, that mechanical forces can activate receptor tyrosine kinases (RTKs) (1.3.1) and amphiregulin may contribute to some of the pulmonary effects that we found upon overventilation (Figure 39), we performed experiments, in which we overventilated lungs in the presence of the EGFRIs AG1478 and PD153035, two small molecule tyrosine kinase inhibitors, known to block the tyrosine kinase activity of especially EGFR.

PD153035 (AG1514) is a specific and reversible inhibitor of the EGFR tyrosine kinase family, and known to be extremely potent [289]. It blocks binding of ATP to the tyrosine kinase domain on the EGFR and suppresses tyrosine phosphorylation and receptor function. Nanomolar concentrations block EGF-mediated cellular activities, including mitogenesis, gene expression and transformation [346].

Tyrphostin AG1478 is known as a highly potent and specific inhibitor of the EGFR, with very weak action on PDGF receptor and ErbB2 kinases [347]. In addition to EGFR inhibition, AG1478 is known to block ErbB4 activation induced by radiation in cancer cells at high concentrations [348].

5.4.1. The effects on overventilation-induced MAPK and AKT/protein kinase B by EGFR inhibitors

In general, upon blocking the activity of the EGFR both EGFRIs are observed to affect cellular events via diminished phosphorylation of MAPK, with no effect on AKT/protein kinase B activation [348,349,350]. In line with that, we also found no effect on overventilation-induced AKT/protein kinase B activation upon EGFRI treatment,. Contrary to our expectations, also no inhibition of overventilation-induced activation of MAPK by either EGFRI was observed, rather both EGFRIs slightly enhanced the overventilation-induced activation of the MAPK JNK/SAPK. In addition, AG1478 enhanced slightly the overventilation-induced activation of ERK1/2 whereas PD301035 did not (Figure 32).

However, EGFRIs are considered as promising therapeutic target in cancer therapy, but are also known to have several side effects, including e.g. enhanced inflammation or alterations in attachment and migration of cells, resulting in toxic effects [351,352]. For example, Takeuchi *et al.*

2009 demonstrated in their study in PC-9 cells increased activation of JNK/SAPK by AG1478 and showed, that JNK-phosphatase MKP-1 expression is controlled by a signal downstream of EGFR and that if this signal is abolished by an inhibitor of EGFR tyrosine kinase, the decreased MKP-1 activity can result in JNK activation [353].

Therefore the increased JNK/SAPK activation during AG1478 treatment in overventilated lungs may point to the possibility, that JNK/SAPK signalling during overventilation may be also regulated downstream of the EGFR. The slight, but additive effect of overventilation-induced ERK1/2 activation in lungs treated with AG1478 also points to the possibility of regulatory proteins in an EGFR/ ERK1/2 mediated pathways during overventilation.

5.4.2. The effects on overventilation-induced gene expression by EGFR inhibitors

Treatment of overventilated lungs with both EGFRIs AG1478 and PD153035 resulted in decreased mRNA levels of *Tnc*, *Akap12*, *Cldn4*, *Il1b*, *Ptgs2* and *IL1b*, that were also found to be induced in response to amphiregulin stimulation (Figure 28, Figure 34). These data suggest a specific involvement of amphiregulin-dependent EGFR receptor activation in overventilation-induced gene transcription in both, inflammatory processes (*Ptgs2, IL-11*) and extracellular matrix processes *(Akap12*, *Tnc*, *Cldn4)*.

This idea is supported by measurements of overventilation-induced gene alterations in lungs treated with the two inhibitors of the ADAM family (a disintegrin and a metalloproteinase), GI254023X and GW280264X, [184]). ADAMs are responsible for generating soluble, and thus active forms of ErbB ligands due to limited proteolytic cleavage of their extracellular domain from integral membrane precursors (1.4.1.2). In preliminary experiments, with exception of AKAP12 (no effect upon administration of ADAM-inhibitors) inhibition of the overventilation-induced genes *Tnc*, *Cldn4*, *Il1b*, *Ptgs2* and *IL-11* was observed. Since metalloproteinase experiments in isolated perfused mouse lungs were only done with 2 lungs respectively (n=2) these data have to be confirmed with additional experiments.

Hbegf and *Cyr61*, that are shown to be induced via overventilation and amphiregulin (Figure 28) are not blocked by EGFRIs during overventilation, suggesting an EGFR-independent but amphiregulin-dependent mechanism of overventilation-induced gene transcription. This is interesting because amphiregulin is known to serve as ligand for the EGFR, and it is generally accepted, that it does not bind to other ErbB members, but recently, it was also shown, that

amphiregulin stimulation leads to an EGFR independent proliferation in XG-1 cells, that did not express ErbB1, but expressed ErbB4 and ErbB3 [343]. In addition, former studies reported that EGF and TGF-α can also activate ErbB2/ErbB4 complexes [354] and betacellulin (known to bind ErbB1/Erbb4) was able to bind Erbb2/Erbb3 [355], broaden the role of EGFR ligands in ErbB receptor signalling.

Another interesting observation was the behaviour of the expression of *Areg* itself when compared to *Il-6* mRNA expression during EGFRI treatment in overventilated lungs (Figure 28). Both genes showed upregulation due to amphiregulin stimulation and overventilation. ErbB receptors function as signal integrators cross regulating different classes of receptors, in particular the IL-6 transducer gp130 [356]. In addition, an EGFR/IL-6/STAT3 signalling cascade was discovered to be important for tumorigenesis in lung epithelial cells [357] so that a possible explanation of these similar behaviour would be a amphiregulin interaction with ErbB receptors, which in turn leads to Il-6 receptor activation in overventilated lungs, possibly in addition via ErbB2 as shown for prostate carcinoma cells [356].

Our findings of tenascin C gene expression in isolated perfused mouse lungs during different treatment conditions was also highly interesting. In our model of isolated lungs, we found tenascin C to be upregulated during overventilation (Figure 22) but not by endotoxin (Figure 22). In addition, *Tnc* was upregulated by amphiregulin (Figure 28) and overventilation-induced tenascin C gene transcription was blocked via both EGFRIs (Figure 34). As Papaiahgari *et al*. found recently a requirement of both cytoskeletal remodelling and EGFR-activated signalling for cyclic stretch-induced gene expression in lung epithelial and endothelial cells [102], our data suggest an AR-EGFR mediated role for tenascin C during mechanical stress in lungs (Figure 40).

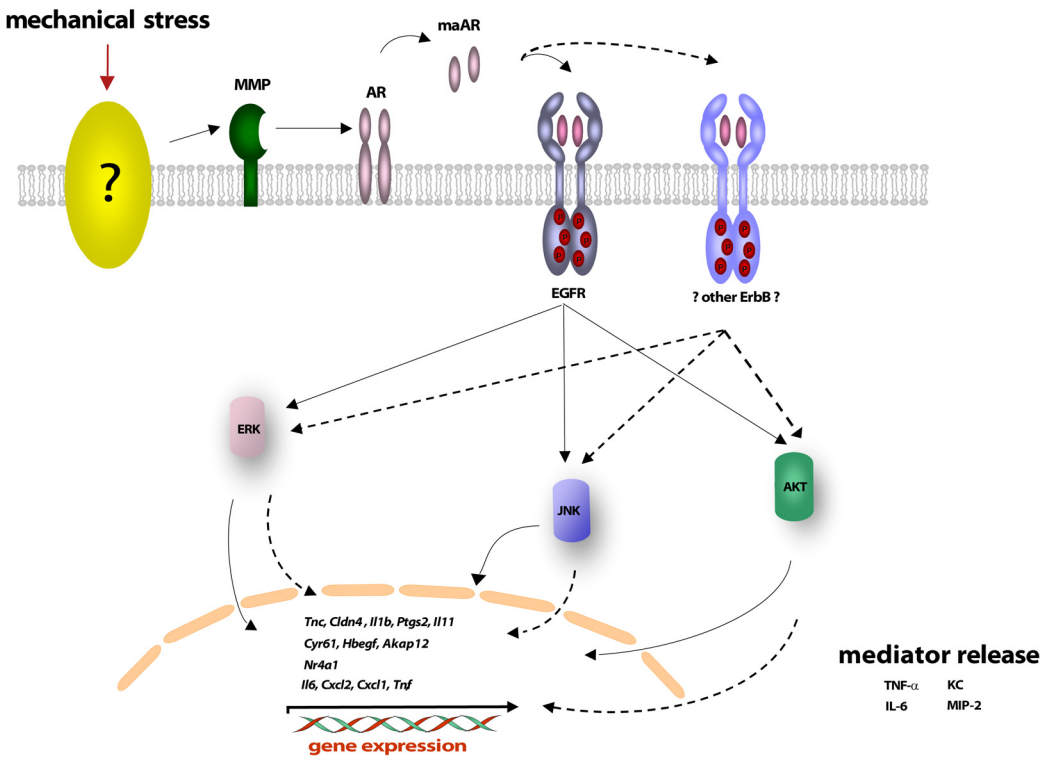

Figure 40 Hypothesis of ErbB-mediated signalling during overventilation in the lungs. Mechanical stress leads to the activation of matrix metalloproteinase (MMP, e.g. ADAM10 or ADAM17), that shed epidermal growth factor-like ligands (AR, amphiregulin), that activate ErbBs These activation of ErbBs (EGFR and perhaps other ErbBs) regulates MAPK and AKT/protein kinase B activation and leads in turn to the regulation of several inflammatory and growth factor related genes with subsequent mediator release in overventilated lungs.

5.4.3. The effects on overventilation-induced mediator release by EGFR inhibitors

Whereas neither PD301035 nor AG1478 had an effect on the overventilation-induced IL-6 release, interestingly treatment of lungs with AG1478 enhanced the pulmonary TNF-α and MIP-2 release into the perfusate, effects never observed before in isolated perfused mouse lungs, but observed before in skin epithelial cells, when treated with EGFRIs [194]. Especially IP-10 and IL-8 were found to be upregulated in cultured keratinocytes when the EGFR was effectively blocked [358,359]. Together with other findings known about the EGFR system in the skin the authors suggest that pharmacological abrogation of EGFR signalling pathways worsens skin inflammation by increasing

chemokine expression in keratinocytes, as reviewed recent by Pastore *et al.* [194]. Interestingly in our model of isolated perfused mouse lungs, the overventilation-induced TNF-α release was strongly increased by AG1478, but significant diminished in lungs treated with PD301035. In addition, PD301035 had no effect on the release of other mediators pointing to differences within the quinazolines of the tyrphostin family of EGFR inhibitors [360].
In contrast to our findings of increased mediator release upon EGFR blocking, Biermann *et al.* observed a significant decrease in MV-induced lung alveolar and vascular permeability as well as alveolar neutrophil accumulation in mice treated with the inhibitor AG1478 and suggested a role for EGFR-activated signalling in VILI [361].

However, EGFRIs are known to alter differentiation, attachment and migration and enhances inflammation, leading to well known side effects in patients, treated with EGFRIs [351] therefore studies with EGFRIs are difficult to interpret, even more so since our knowledge of the involvement of ErbB mediated signal transduction during overstretching of lungs is just in the beginning. Further investigations need to clarify the role of ErbB-dependent pathways in ventilator-induced lung injury.

Overall, these findings support the notion that amphiregulin and the EGFR mediate some of the effects of overstretch in the lungs.
Possibly, the genes induced by overventilation can be grouped in several classes: 1. Genes of the canonical inflammation pathway such as *Il6*, *Tnf*, *Cxcl1 and Cxcl2* that are induced by both endotoxin and overventilation. 2. Genes that are only induced by overventilation and which are regulated by amphiregulin (*Hbegf*, *Il11*, *Cldn4*, *Akap12*, *Cyr61*). Among these some genes appear to be upregulated by amphiregulin and hence their induction is blocked by EGFRIs (*Cldn4*, *Akap12*, *Il11*). Others are upregulated by amphiregulin but not affected by EGFRIs (*Cyr61*, *Hbegf*). 3. Genes induced by overventilation, but not by amphiregulin (*Hspb8*, *Nr4a1*).
These insights may offer the possibility to selectively interfere with the side effects of mechanical ventilation.

6. Summary

Acute lung injury (ALI) and its more severe form, the acute respiratory distress syndrome (ARDS), are devastating disorders characterized by extensive pulmonary inflammation, resulting in high mortality. In this thesis the response of the lungs to three major causes of ARDS/ALI was examined: toll-like receptor-2 (TLR2) ligands, toll-like receptor-4 (TLR4) ligands and mechanical ventilation (MV).

Gram-positive und Gram-negative bacteria are main causes of ARDS and are recognized by the innate immune system via TLR2 and TLR4, respectively. Among all organs, the lungs have the highest expression of TLR2 receptors, but little is known about the pulmonary consequences of their activation. Here we studied the effects of the TLR2/6 agonist MALP-2, the TLR2/1 agonist Pam_3Cys and the TLR4 agonist lipopolysaccharide (LPS) on proinflammatory responses in isolated lungs. TLR2 and TLR4 activation led to similar reactions in the lungs regarding MAPK and AKT/protein kinase B activation, gene induction and mediator release (IL6, TNF-α, MIP-2 and IP-10). Several novel genes were shown to be induced by TLR2 receptors such as *Cxcl10*, *Slpi*, *Tnc*, *Parg* and *Traf1*. In addition, the MALP-2 dependent induction of *Tnc* may indicate the existence of TLR2/6-specific pathways.

To identify genes that are specifically activated by mechanical stretch, we compared gene expression studies in mouse lungs exposed to either overventilation or endotoxin. We identified 9 genes selectively regulated by overstretch belonging to the group of growth factors (*Areg*, *Fgfbp1*, *Nr4a1)*, extracellular matrix proteins (*Tnc*, *Cyr61*, *Cldn4*, *Akap12)*, heat shock proteins (*Hspb8*) and cytokines (*IL-11*). These findings point to novel intracellular signalling pathways, that are activated by overventilation.
Since the upregulation of amphiregulin (AR) was remarkably strong, we further investigated the role of amphiregulin in the lungs. Amphiregulin perfusion in isolated mouse lungs enhanced the release of the inflammatory mediators interleukin-6, tumor necrosis factor-α, CXCL1/KC und IP-10. In addition, amphiregulin activated the MAP-kinases ERK1/2 and JNK/SAPK and furthermore AKT/protein kinase B. Moreover, amphiregulin and overventilation induced several genes involved in growth, inflammation and extracellular matrix proteins, such as *Ptgs2*, *Il6*, *Cyr61* and *Tnc*.

To further investigate the involvement of the EGFR receptor ligand amphiregulin, we treated overventilated mouse lungs with two EGFR inhibitors (EGFRIs) and found that some genes, that are induced by amphiregulin or overventilation where blocked by EGFRIs (*Cldn4*, *Akap12*, *Il11)* whereas others were not affected (*Cyr61*, *Hbegf*).

Overall, our investigations on gene expression in overventilated mouse lungs may point to the possibility, that genes, induced by overventilation can be grouped in 3 classes. First, genes of the canonical inflammation pathway such as *Il6*, *Tnf*, *Cxcl1 and Cxcl2* that are induced by both endotoxin and overventilation. Second, genes that are only induced by overventilation and which are regulated by amphiregulin (*Hbegf*, *Il11*, *Cldn4*, *Akap12*, *Cyr61*). Among these some genes appear to be upregulated by amphiregulin and hence their induction is blocked by EGFRIs (*Cldn4*, *Akap12*, *Il11*). Others are upregulated by amphiregulin but not affected by EGFRIs (*Cyr61*, *Hbegf*). Third, genes induced by overventilation, but not by amphiregulin (*Hspb8*, *Nr4a1*).

In summary, or findings support the notion that amphiregulin and the EGFR may mediate some of the pulmonary effects of overventilation. Finally these insights may offer the possibility to selectively interfere with the side effects of mechanical ventilation.

7. Zusammenfassung

Das akute Lungenversagen (ALI) und seine erschwerte Form ARDS (acute respiratory distress syndrome) sind durch ausgeprägte Störungen starker pulmonaler Entzündungsantworten charakterisiert und mit einer hohen Sterblichkeit verbunden. In der vorliegenden Arbeit wurde die Antwort der Lunge auf drei Hauptursachen des akuten Lungenversagens untersucht: Toll-like Rezeptor (TLR) 2 Liganden, Toll-like Rezeptor (TLR) 4 Liganden und mechanische Beatmung.

Gram-positive und Gram-negative Bakterien werden vom angeborenen Immunsystem durch Toll-like Rezeptor (TLR) 2 beziehungsweise TLR4 erkannt. Unter allen Organen verzeichnet die Lunge die höchste Genexpression des TLR2 Rezeptors, dennoch ist wenig über die pulmonalen Konsequenzen von dessen Aktivierung bekannt. Innerhalb dieser Arbeit wurden zunächst die Effekte des TLR2/6 Agonisten MALP-2, des TLR2/1 Agonisten Pam_3Cys und des TLR4 Agonisten Lipopolysaccharid (LPS) auf proentzündliche Antworten in isoliert-perfundierten Lungen untersucht. Unsere Ergebnisse zeigen, dass TLR2 und TLR4-Rezeptoren in Bezug auf die MAPK und AKT/proteinkinase B Aktivierung, die Geninduktion und Mediatorfreisetzung (IL-6, TNF-α, MIP-2 und IP-10) sehr ähnliche Wirkungen in der Lunge erzeugten. Es wurden einige Gene gefunden, von denen bisher nicht bekannt war, dass diese durch TLR2 Aktivierung induziert werden, wie beispielsweise *Cxcl10*, *Slpi*, *Tnc*, *Parg* und *Traf1*. Gleichzeitig weist die MALP-2 abhängige Hochregulierung von Tenascin C (*Tnc*) auf die Existenz TLR2/6 spezifischer Signalwege hin.

Um Gene zu identifizieren, die spezifisch durch mechanische Dehnung aktiviert werden, verglichen wir die Genexpression von Endotoxin-stimulierten Mäuselungen, mit denen, die Überdehnungsstress ausgesetzt wurden. Wir identifizierten 9 Gene, die selektiv durch Überdehnung reguliert wurden, die den Gruppen der Wachstumsfaktoren (*Areg*, *Fgfbp1*, *Nr4a1*), der extrazellularen Matrixproteine (*Tnc*, *Cyr61*, *Cldn4*, *Akap12*), der Hitzeschockproteine (*Hspb8*) und der Zytokine (*IL-11*) zugeordnet werden konnten.

Da die überdehnungsspezifische Hochregulierung von Amphiregulin (AR) besonders stark war, wurde die Reaktion der Lunge auf die Gabe von Amphiregulin untersucht. Hierbei wurde gezeigt, dass Amphiregulin die Ausschüttung der entzündlichen Mediatoren Interleukin-6, Tumor-Nekrose Faktor-α, CXCL1/KC und IP-10 erhöht. Zusätzlich aktivierte Amphiregulin die MAP-Kinasen ERK1/2 und JNK/SAPK und außerdem AKT/proteinkinase B. Sowohl Amphiregulingabe als auch Überdehnungsstress führte zur Induktion unterschiedlicher Gene, die sowohl in endzünd-

lichen- und Wachstumsprozessen, als auch innerhalb der extrazellulären Matrix eine Rolle spielen, wie beispielsweise *Ptgs2*, *Il6*, *Cyr61 und Tnc*.

Um die Beteiligung des epidermalen Wachstumsfaktor Rezeptor (EGFR) Liganden Amphiregulin zu untersuchen, wurden überdehnte Lungen mit zwei bekannten EGFR-Hemmstoffen (EGFRIs) behandelt. Hierbei zeigte sich, dass einige Gene, die durch Amphiregulin oder Überdehnung induziert werden, durch EGFRIs gehemmt wurden (*Cldn4*, *Akap12*, *Il11*) während andere Gene unberührt blieben (*Cyr61*, *Hbegf*).

Zusammenfassend lassen unsere Untersuchungen zur Genexpression in überdehnten Mauslungen den Schluss zu, dass Gene, die durch Überdehnung induziert werden, in drei Klassen eingeteilt werden können. Die erste Klasse umfasst die Gene des kanonischen Entzündungsweges, wie beispielsweise *Il6*, *Tnf*, *Cxcl1 und Cxcl2*, die sowohl durch Endotoxin-gabe als auch durch Überdehnung hochreguliert werden, während Gene, die nur durch Überdehnungsstress induziert und durch Amphiregulin reguliert werden (*Hbegf*, *Il11*, *Cldn4*, *Akap12*, *Cyr61*) einer zweiten Klasse zugeordnet werden können. Innerhalb dieser scheinen einige Gene durch Amphiregulin hochreguliert und daher ihre Induktion von EGFRIs gehemmt zu sein (*Cldn4*, *Akap12*, *Il11*). Andere Gene wiederum werden von Amphiregulin hochreguliert, ihre Induktion wird allerdings nicht von EGFRIs blockiert (*Cyr61*, *Hbegf*). Innerhalb der dritten Klasse sind die Gene zu finden, welche durch Überdehnungsstress, allerdings nicht durch Amphiregulin induziert werden (*Hspb8*, *Nr4a1*).

Zusammenfassend stützen diese Befunde die Vorstellung, dass Amphiregulin und der EGFR möglicherweise einige der pulmonalen Effekte vermitteln, die bei Überdehnungsstress beobachtet wurden. Diese Erkenntnisse könnten dazu beitragen, die Nebenwirkungen der künstlichen Beatmung selektiv zu beeinflussen.

8. References

1. **Wehner, R. Zoologie. Gehring, W and Kühn, Rüdiger. 1-954. 2007**. Georg Thieme Verlag.

2. **Mercer, R. R., M. L. Russell, V. L. Roggli, and J. D. Crapo. 1994**. Cell number and distribution in human and rat airways. *Am.J.Respir.Cell Mol.Biol.* 10:613-624.

3. **Nunn, JF. Applied respiratory physiology. 247-305. 1993**. London-Boston: Butterworth-Heinemannn.

4. **Effros, R. Anatomy, development, and physiology of the lungs**. 16-4-2006. GI Motility online nature publishing group.

5. **Lynch, PJ. Bronchial anatomy detail of alveoli and lung circulation. Jaffe, CC**. 23-12-0006. Yale University School of Medicine, Center for Advanced Instructional Media, 1987-2000. Creative Commons Attribution 2.5 License 2006.

6. **Lynch, PJ. Lungs diagram with internal details. Jaffe, CC**. 23-12-0006. Yale University School of Medicine, Center for Advanced Instructional Media, 1987-2000.Creative Commons Attribution 2.5 License 2006.

7. **James, A. and N. Carroll. 2000**. Airway smooth muscle in health and disease; methods of measurement and relation to function. *Eur.Respir.J.* 15:782-789.

8. **Levin, D. L. 1978**. Morphologic analysis of the pulmonary vascular bed in congenital left-sided diaphragmatic hernia. *J.Pediatr.* 92:805-809.

9. **Barrowcliffe, M. P. and J. G. Jones. 1987**. Solute permeability of the alveolar capillary barrier. *Thorax* 42:1-10.

10. **Brighenti, C., G. Gnudi, and G. Avanzolini. 2003**. A simulation model of the oxygen alveolo-capillary exchange in normal and pathological conditions. *Physiol Meas.* 24:261-275.

11. **Herzog, E. L., A. R. Brody, T. V. Colby, R. Mason, and M. C. Williams. 2008**. Knowns and unknowns of the alveolus. *Proc.Am.Thorac.Soc.* 5:778-782.

12. **Newman, G. R., L. Campbell, R. C. von, B. Jasani, and M. Gumbleton. 1999**. Caveolin and its cellular and subcellular immunolocalisation in lung alveolar epithelium: implications for alveolar epithelial type I cell function. *Cell Tissue Res.* 295:111-120.

13. **Wright, J. R. 1990**. Clearance and recycling of pulmonary surfactant. *Am.J.Physiol* 259:L1-12.

14. **Folkesson, H. G. and M. A. Matthay. 2006**. Alveolar epithelial ion and fluid transport: recent progress. *Am.J.Respir.Cell Mol.Biol.* 35:10-19.

15. **Verkman, A. S., M. A. Matthay, and Y. Song. 2000**. Aquaporin water channels and lung physiology. *Am.J.Physiol Lung Cell Mol.Physiol* 278:L867-L879.

16. **Adamson, I. Y. and D. H. Bowden. 1974**. The type 2 cell as progenitor of alveolar epithelial regeneration. A cytodynamic study in mice after exposure to oxygen. *Lab Invest* 30:35-42.

17. **Boitano, L. J. 2006**. Management of airway clearance in neuromuscular disease. *Respir.Care* 51:913-922.

18. **Monick, M. M. and G. W. Hunninghake. 2002**. Activation of second messenger pathways in alveolar macrophages by endotoxin. *Eur.Respir.J.* 20:210-222.

19. **Lohmann-Matthes, M. L., C. Steinmuller, and G. Franke-Ullmann. 1994**. Pulmonary macrophages. *Eur.Respir.J.* 7:1678-1689.

20. **Zhang, P., W. R. Summer, G. J. Bagby, and S. Nelson. 2000**. Innate immunity and pulmonary host defense. *Immunol.Rev.* 173:39-51.

21. **Rangel, L. B., R. Agarwal, T. D'Souza, E. S. Pizer, P. L. Alo, W. D. Lancaster, L. Gregoire, D. R. Schwartz, K. R. Cho, and P. J. Morin. 2003**. Tight junction proteins claudin-3 and claudin-4 are frequently overexpressed in ovarian cancer but not in ovarian cystadenomas. *Clin.Cancer Res.* 9:2567-2575.

22. **Grinnan, D. C. and J. D. Truwit. 2005**. Clinical review: respiratory mechanics in spontaneous and assisted ventilation. *Crit Care* 9:472-484.

23. **Slutsky, A. S.** Mechanical Ventilation. Brochard, L. 1-419. 2004. Springer Verlag.

24. **Granton, J. T. and A. S. Slutsky. 2000**. Mechanical ventilation: what's new when your patient is blue? *CMAJ.* 162:241-242.

25. **Klinke, R. Physiologie. Pape, H.-C. and Silbernagl, S. 2005**. Georg Thieme Verlag; Stuttgart, New York.

26. **Ashbaugh, D. G., D. B. Bigelow, T. L. Petty, and B. E. Levine. 1967**. Acute respiratory distress in adults. *Lancet* 2:319-323.

27. **Ware, L. B. and M. A. Matthay. 2000**. The acute respiratory distress syndrome. *N.Engl.J.Med.* 342:1334-1349.

28. **Khadaroo, R. G. and J. C. Marshall. 2002**. ARDS and the multiple organ dysfunction syndrome. Common mechanisms of a common systemic process. *Crit Care Clin.* 18:127-141.

29. **Ware, L. B. and M. A. Matthay. 2000**. The acute respiratory distress syndrome. *N.Engl.J.Med.* 342:1334-1349.

30. **Murray, J. F., M. A. Matthay, J. M. Luce, and M. R. Flick. 1988**. An expanded definition of the adult respiratory distress syndrome. *Am.Rev.Respir.Dis.* 138:720-723.

31. **Bernard, G. R., A. Artigas, K. L. Brigham, J. Carlet, K. Falke, L. Hudson, M. Lamy, J. R. LeGall, A. Morris, and R. Spragg. 1994**. Report of the American-European Consensus conference on acute respiratory distress syndrome: definitions, mechanisms, relevant outcomes, and clinical trial coordination. Consensus Committee. *J.Crit Care* 9:72-81.

32. **Fowler, A. A., R. F. Hamman, J. T. Good, K. N. Benson, M. Baird, D. J. Eberle, T. L. Petty, and T. M. Hyers. 1983**. Adult respiratory distress syndrome: risk with common predispositions. *Ann.Intern.Med.* 98:593-597.

33. **Hudson, L. D., J. A. Milberg, D. Anardi, and R. J. Maunder. 1995**. Clinical risks for development of the acute respiratory distress syndrome. *Am.J.Respir.Crit Care Med.* 151:293-301.

34. **Doyle, R. L., N. Szaflarski, G. W. Modin, J. P. Wiener-Kronish, and M. A. Matthay. 1995**. Identification of patients with acute lung injury. Predictors of mortality. *Am.J.Respir.Crit Care Med.* 152:1818-1824.

35. **Sloane, P. J., M. H. Gee, J. E. Gottlieb, K. H. Albertine, S. P. Peters, J. R. Burns, G. Machiedo, and J. E. Fish. 1992**. A multicenter registry of patients with acute respiratory distress syndrome. Physiology and outcome. *Am.Rev.Respir.Dis.* 146:419-426.

36. **Jia, X., A. Malhotra, M. Saeed, R. G. Mark, and D. Talmor. 2008**. Risk factors for ARDS in patients receiving mechanical ventilation for > 48 h. *Chest* 133:853-861.

37. **Bersten, A. D., C. Edibam, T. Hunt, and J. Moran. 2002**. Incidence and mortality of acute lung injury and the acute respiratory distress syndrome in three Australian States. *Am.J.Respir.Crit Care Med.* 165:443-448.

38. **Reynolds, H. N., M. McCunn, U. Borg, N. Habashi, C. Cottingham, and Y. Bar-Lavi. 1998**. Acute respiratory distress syndrome: estimated incidence and mortality rate in a 5 million-person population base. *Crit Care* 2:29-34.

39. **Lewandowski, K., J. Metz, C. Deutschmann, H. Preiss, R. Kuhlen, A. Artigas, and K. J. Falke. 1995**. Incidence, severity, and mortality of acute respiratory failure in Berlin, Germany. *Am.J.Respir.Crit Care Med.* 151:1121-1125.

40. **Villar, J. and A. S. Slutsky. 1989**. The incidence of the adult respiratory distress syndrome. *Am.Rev.Respir.Dis.* 140:814-816.

41. **Goss, C. H., R. G. Brower, L. D. Hudson, and G. D. Rubenfeld. 2003**. Incidence of acute lung injury in the United States. *Crit Care Med.* 31:1607-1611.

42. **Rubenfeld, G. D., E. Caldwell, E. Peabody, J. Weaver, D. P. Martin, M. Neff, E. J. Stern, and L. D. Hudson. 2005**. Incidence and outcomes of acute lung injury. *N.Engl.J.Med.* 353:1685-1693.

43. **Thomsen, G. E. and A. H. Morris. 1995**. Incidence of the adult respiratory distress syndrome in the state of Utah. *Am.J.Respir.Crit Care Med.* 152:965-971.

44. **2000**. Ketoconazole for early treatment of acute lung injury and acute respiratory distress syndrome: a randomized controlled trial. The ARDS Network. *JAMA* 283:1995-2002.

45. **Fialkow, L., S. R. Vieira, A. K. Fernandes, D. R. Silva, and M. C. Bozzetti. 2002**. Acute lung injury and acute respiratory distress syndrome at the intensive care unit of a general

university hospital in Brazil. An epidemiological study using the American-European Consensus Criteria. *Intensive Care Med.* 28:1644-1648.

46. **Gong, M. N., B. T. Thompson, P. Williams, L. Pothier, P. D. Boyce, and D. C. Christiani. 2005**. Clinical predictors of and mortality in acute respiratory distress syndrome: potential role of red cell transfusion. *Crit Care Med.* 33:1191-1198.

47. **Zambon, M. and J. L. Vincent. 2008**. Mortality rates for patients with acute lung injury/ARDS have decreased over time. *Chest* 133:1120-1127.

48. **Estenssoro, E., A. Dubin, E. Laffaire, H. Canales, G. Saenz, M. Moseinco, M. Pozo, A. Gomez, N. Baredes, G. Jannello, and J. Osatnik. 2002**. Incidence, clinical course, and outcome in 217 patients with acute respiratory distress syndrome. *Crit Care Med.* 30:2450-2456.

49. **Bellingan, G. J. 2002**. The pulmonary physician in critical care * 6: The pathogenesis of ALI/ARDS. *Thorax* 57:540-546.

50. **Ware, L. B. and M. A. Matthay. 2000**. The acute respiratory distress syndrome. *N.Engl.J.Med.* 342:1334-1349.

51. **Hudson, L. D. and C. L. Hough. 2006**. Therapy for late-phase acute respiratory distress syndrome. *Clin.Chest Med.* 27:671-677.

52. **Matthay, M. A., L. Robriquet, and X. Fang. 2005**. Alveolar epithelium: role in lung fluid balance and acute lung injury. *Proc.Am.Thorac.Soc.* 2:206-213.

53. **Berthiaume, Y. and M. A. Matthay. 2007**. Alveolar edema fluid clearance and acute lung injury. *Respir.Physiol Neurobiol.* 159:350-359.

54. **Bitterman, P. B. 1992**. Pathogenesis of fibrosis in acute lung injury. *Am.J.Med.* 92:39S-43S.

55. **Meduri, G. U., A. J. Chinn, K. V. Leeper, R. G. Wunderink, E. Tolley, H. T. Winer-Muram, V. Khare, and M. Eltorky. 1994**. Corticosteroid rescue treatment of progressive fibroproliferation in late ARDS. Patterns of response and predictors of outcome. *Chest* 105:1516-1527.

56. **Cohen, J. 2002**. The immunopathogenesis of sepsis. *Nature* 420:885-891.

57. **Puneet, P., S. Moochhala, and M. Bhatia. 2005**. Chemokines in acute respiratory distress syndrome. *Am.J.Physiol Lung Cell Mol.Physiol* 288:L3-15.

58. **Pittet, J. F., R. C. Mackersie, T. R. Martin, and M. A. Matthay. 1997**. Biological markers of acute lung injury: prognostic and pathogenetic significance. *Am.J.Respir.Crit Care Med.* 155:1187-1205.

59. **Bachofen, M. and E. R. Weibel. 1977**. Alterations of the gas exchange apparatus in adult respiratory insufficiency associated with septicemia. *Am.Rev.Respir.Dis.* 116:589-615.

60. **Guo, R. F. and P. A. Ward. 2007**. Role of oxidants in lung injury during sepsis. *Antioxid.Redox.Signal.* 9:1991-2002.

61. **Shetty, S., J. Padijnayayveetil, T. Tucker, D. Stankowska, and S. Idell. 2008**. The fibrinolytic system and the regulation of lung epithelial cell proteolysis, signaling, and cellular viability. *Am.J.Physiol Lung Cell Mol.Physiol* 295:L967-L975.

62. **Sprague, R. S., A. H. Stephenson, T. E. Dahms, and A. J. Lonigro. 1989**. Proposed role for leukotrienes in the pathophysiology of multiple systems organ failure. *Crit Care Clin.* 5:315-329.

63. **Anderson, B. O., D. D. Bensard, and A. H. Harken. 1991**. The role of platelet activating factor and its antagonists in shock, sepsis and multiple organ failure. *Surg.Gynecol.Obstet.* 172:415-424.

64. **Tasaka, S., F. Amaya, S. Hashimoto, and A. Ishizaka. 2008**. Roles of oxidants and redox signaling in the pathogenesis of acute respiratory distress syndrome. *Antioxid.Redox.Signal.* 10:739-753.

65. **Matsuo, N. 1999**. The role of intrapulmonary nitric oxide generation in the development of adult respiratory distress syndrome. *Surg.Today* 29:1068-1074.

66. **Valencia, M. and A. Torres. 2009**. Ventilator-associated pneumonia. *Curr.Opin.Crit Care* 15:30-35.

67. **Dreyfuss, D. and G. Saumon. 1998**. Ventilator-induced lung injury: lessons from experimental studies. *Am.J.Respir.Crit Care Med.* 157:294-323.

68. **Pinhu, L., T. Whitehead, T. Evans, and M. Griffiths. 2003**. Ventilator-associated lung injury. *Lancet* 361:332-340.

69. **Slutsky, A. S. 1999**. Lung injury caused by mechanical ventilation. *Chest* 116:9S-15S.

70. **Uhlig, S. and U. Uhlig. 2004**. Pharmacological interventions in ventilator-induced lung injury. *Trends Pharmacol.Sci.* 25:592-600.

71. **Santos, C. C., H. Zhang, M. Liu, and A. S. Slutsky. 2005**. Bench-to-bedside review: Biotrauma and modulation of the innate immune response. *Crit Care* 9:280-286.

72. **Uhlig, U., D. Dromann, T. Goldmann, H. Dombrowsky, E. Vollmer, P. Zabel, and S. Uhlig. 2006**. Pulmonary responses to overventilation in late multiple organ failure. *Anesthesiology* 105:1192-1200.

73. **ARDSnet 2000**. Ventilation with lower tidal volumes as compared with traditional tidal volumes for acute lung injury and the acute respiratory distress syndrome. The Acute Respiratory Distress Syndrome Network. *N.Engl.J.Med.* 342:1301-1308.

74. **Ranieri, V. M., P. M. Suter, C. Tortorella, T. R. De, J. M. Dayer, A. Brienza, F. Bruno, and A. S. Slutsky. 1999**. Effect of mechanical ventilation on inflammatory mediators in patients with acute respiratory distress syndrome: a randomized controlled trial. *JAMA* 282:54-61.

75. **Uhlig, S. 2002**. Ventilation-induced lung injury and mechanotransduction: stretching it too far? *Am.J.Physiol Lung Cell Mol.Physiol* 282:L892-L896.

76. **Halbertsma, F. J., M. Vaneker, G. J. Scheffer, and J. G. van der Hoeven. 2005**. Cytokines and biotrauma in ventilator-induced lung injury: a critical review of the literature. *Neth.J.Med.* 63:382-392.

77. **Vlahakis, N. E. and R. D. Hubmayr. 2000**. Invited review: plasma membrane stress failure in alveolar epithelial cells. *J.Appl.Physiol* 89:2490-2496.

78. **Pugin, J., I. Dunn, P. Jolliet, D. Tassaux, J. L. Magnenat, L. P. Nicod, and J. C. Chevrolet. 1998**. Activation of human macrophages by mechanical ventilation in vitro. *Am.J.Physiol* 275:L1040-L1050.

79. **von Bethmann, A. N**,B**rasch, F, Müller, K, Wendel, A, and Uhlig, S. 1996.** Prolonged hyperventilation is required for release of tumor necrosis factor alpha but not IL-6..

80. **von Bethmann, A. N., F. Brasch, R. Nusing, K. Vogt, H. D. Volk, K. M. Muller, A. Wendel, and S. Uhlig. 1998**. Hyperventilation induces release of cytokines from perfused mouse lung. *Am.J.Respir.Crit Care Med.* 157:263-272.

81. **Bonten, M. J., C. A. Gaillard, P. W. de Leeuw, and E. E. Stobberingh. 1997**. Role of colonization of the upper intestinal tract in the pathogenesis of ventilator-associated pneumonia. *Clin.Infect.Dis.* 24:309-319.

82. **Bonten, M. J., A. H. Froon, C. A. Gaillard, J. W. Greve, P. W. de Leeuw, M. Drent, E. E. Stobberingh, and W. A. Buurman. 1997**. The systemic inflammatory response in the development of ventilator-associated pneumonia. *Am.J.Respir.Crit Care Med.* 156:1105-1113.

83. **Hoare, Z. and W. S. Lim. 2006**. Pneumonia: update on diagnosis and management. *BMJ* 332:1077-1079.

84. **Lynch, J. P., III. 2001**. Hospital-acquired pneumonia: risk factors, microbiology, and treatment. *Chest* 119:373S-384S.

85. **American Thoracic Society 2005**. Guidelines for the management of adults with hospital-acquired, ventilator-associated, and healthcare-associated pneumonia. *Am.J.Respir.Crit Care Med.* 171:388-416.

86. **Fagon, J. Y., J. Chastre, Y. Domart, J. L. Trouillet, J. Pierre, C. Darne, and C. Gibert. 1989**. Nosocomial pneumonia in patients receiving continuous mechanical ventilation. Prospective analysis of 52 episodes with use of a protected specimen brush and quantitative culture techniques. *Am.Rev.Respir.Dis.* 139:877-884.

87. **Ewig, S., A. Torres, M. El-Ebiary, N. Fabregas, C. Hernandez, J. Gonzalez, J. M. Nicolas, and L. Soto. 1999**. Bacterial colonization patterns in mechanically ventilated patients with traumatic and medical head injury. Incidence, risk factors, and association with ventilator-associated pneumonia. *Am.J.Respir.Crit Care Med.* 159:188-198.

88. **Craven, D. E. and M. R. Driks. 1987**. Nosocomial pneumonia in the intubated patient. *Semin.Respir.Infect.* 2:20-33.

89. **Craven, D. E. and K. A. Steger. 1996**. Nosocomial pneumonia in mechanically ventilated adult patients: epidemiology and prevention in 1996. *Semin.Respir.Infect.* 11:32-53.

90. **Park, D. R. 2005**. The microbiology of ventilator-associated pneumonia. *Respir.Care* 50:742-763.

91. **Torres, A., M. El-Ebiary, N. Soler, C. Monton, N. Fabregas, and C. Hernandez. 1996**. Stomach as a source of colonization of the respiratory tract during mechanical ventilation: association with ventilator-associated pneumonia. *Eur.Respir.J.* 9:1729-1735.

92. **Rea-Neto, A., N. C. Youssef, F. Tuche, F. Brunkhorst, V. M. Ranieri, K. Reinhart, and Y. Sakr. 2008**. Diagnosis of ventilator-associated pneumonia: a systematic review of the literature. *Crit Care* 12:R56.

93. **Sachs, F. 1991**. Mechanical transduction by membrane ion channels: a mini review. *Mol.Cell Biochem.* 104:57-60.

94. **Parker, J. C., C. L. Ivey, and J. A. Tucker. 1998**. Gadolinium prevents high airway pressure-induced permeability increases in isolated rat lungs. *J.Appl.Physiol* 84:1113-1118.

95. **Chen, C. S., J. Tan, and J. Tien. 2004**. Mechanotransduction at cell-matrix and cell-cell contacts. *Annu.Rev.Biomed.Eng* 6:275-302.

96. **Alenghat, F. J. and D. E. Ingber. 2002**. Mechanotransduction: all signals point to cytoskeleton, matrix, and integrins. *Sci.STKE.* 2002:E6.

97. **Chen, K. D., Y. S. Li, M. Kim, S. Li, S. Yuan, S. Chien, and J. Y. Shyy. 1999**. Mechanotransduction in response to shear stress. Roles of receptor tyrosine kinases, integrins, and Shc. *J.Biol.Chem.* 274:18393-18400.

98. **Hu, Y., G. Bock, G. Wick, and Q. Xu. 1998**. Activation of PDGF receptor alpha in vascular smooth muscle cells by mechanical stress. *FASEB J.* 12:1135-1142.

99. **Liu, M., J. Liu, S. Buch, A. K. Tanswell, and M. Post. 1995**. Antisense oligonucleotides for PDGF-B and its receptor inhibit mechanical strain-induced fetal lung cell growth. *Am.J.Physiol* 269:L178-L184.

100. **Tschumperlin, D. J., G. Dai, I. V. Maly, T. Kikuchi, L. H. Laiho, A. K. McVittie, K. J. Haley, C. M. Lilly, P. T. So, D. A. Lauffenburger, R. D. Kamm, and J. M. Drazen. 2004**. Mechanotransduction through growth-factor shedding into the extracellular space. *Nature* 429:83-86.

101. **Correa-Meyer, E., L. Pesce, C. Guerrero, and J. I. Sznajder. 2002**. Cyclic stretch activates ERK1/2 via G proteins and EGFR in alveolar epithelial cells. *Am.J.Physiol Lung Cell Mol.Physiol* 282:L883-L891.

102. **Papaiahgari, S., A. Yerrapureddy, P. M. Hassoun, J. G. Garcia, K. G. Birukov, and S. P. Reddy. 2007**. EGFR-activated signaling and actin remodeling regulate cyclic stretch-induced NRF2-ARE activation. *Am.J.Respir.Cell Mol.Biol.* 36:304-312.

103. **Dolinay, T., N. Kaminski, M. Felgendreher, H. P. Kim, P. Reynolds, S. C. Watkins, D. Karp, S. Uhlig, and A. M. Choi. 2006**. Gene expression profiling of target genes in ventilator-induced lung injury. *Physiol Genomics* 26:68-75.

104. **Davis, R. J. 1993**. The mitogen-activated protein kinase signal transduction pathway. *J.Biol.Chem.* 268:14553-14556.

105. **Robinson, M. J. and M. H. Cobb. 1997**. Mitogen-activated protein kinase pathways. *Curr.Opin.Cell Biol.* 9:180-186.

106. **Sugden, P. H. and A. Clerk. 1998**. "Stress-responsive" mitogen-activated protein kinases (c-Jun N-terminal kinases and p38 mitogen-activated protein kinases) in the myocardium. *Circ.Res.* 83:345-352.

107. **Seger, R. and E. G. Krebs. 1995**. The MAPK signaling cascade. *FASEB J.* 9:726-735.

108. **Abdulnour, R. E., X. Peng, J. H. Finigan, E. J. Han, E. J. Hasan, K. G. Birukov, S. P. Reddy, J. E. Watkins, III, U. S. Kayyali, J. G. Garcia, R. M. Tuder, and P. M. Hassoun. 2006**. Mechanical stress activates xanthine oxidoreductase through MAP kinase-dependent pathways. *Am.J.Physiol Lung Cell Mol.Physiol* 291:L345-L353.

109. **Yang, K. Y., J. J. Arcaroli, and E. Abraham. 2003**. Early alterations in neutrophil activation are associated with outcome in acute lung injury. *Am.J.Respir.Crit Care Med.* 167:1567-1574.

110. **Howe, L. R., S. J. Leevers, N. Gomez, S. Nakielny, P. Cohen, and C. J. Marshall. 1992**. Activation of the MAP kinase pathway by the protein kinase raf. *Cell* 71:335-342.

111. **Yoon, S. and R. Seger. 2006**. The extracellular signal-regulated kinase: multiple substrates regulate diverse cellular functions. *Growth Factors* 24:21-44.

112. **Kito, H., E. L. Chen, X. Wang, M. Ikeda, N. Azuma, N. Nakajima, V. Gahtan, and B. E. Sumpio. 2000**. Role of mitogen-activated protein kinases in pulmonary endothelial cells exposed to cyclic strain. *J.Appl.Physiol* 89:2391-2400.

113. **Uhlig, U., H. Fehrenbach, R. A. Lachmann, T. Goldmann, B. Lachmann, E. Vollmer, and S. Uhlig. 2004**. Phosphoinositide 3-OH kinase inhibition prevents ventilation-induced lung cell activation. *Am.J.Respir.Crit Care Med.* 169:201-208.

114. **Uhlig, U., J. J. Haitsma, T. Goldmann, D. L. Poelma, B. Lachmann, and S. Uhlig. 2002**. Ventilation-induced activation of the mitogen-activated protein kinase pathway. *Eur.Respir.J.* 20:946-956.

115. **Cohen, P. 1997**. The search for physiological substrates of MAP and SAP kinases in mammalian cells. *Trends Cell Biol.* 7:353-361.

116. **Sugden, P. H. and A. Clerk. 1998**. "Stress-responsive" mitogen-activated protein kinases (c-Jun N-terminal kinases and p38 mitogen-activated protein kinases) in the myocardium. *Circ.Res.* 83:345-352.

117. **Yan, M., T. Dai, J. C. Deak, J. M. Kyriakis, L. I. Zon, J. R. Woodgett, and D. J. Templeton. 1994**. Activation of stress-activated protein kinase by MEKK1 phosphorylation of its activator SEK1. *Nature* 372:798-800.

118. **Adcock, I. M. 1997**. Transcription factors as activators of gene transcription: AP-1 and NF-kappa B. *Monaldi Arch.Chest Dis.* 52:178-186.

119. **Li, L. F., L. Yu, and D. A. Quinn. 2004**. Ventilation-induced neutrophil infiltration depends on c-Jun N-terminal kinase. *Am.J.Respir.Crit Care Med.* 169:518-524.

120. **Dolinay, T., W. Wu, N. Kaminski, E. Ifedigbo, A. M. Kaynar, M. Szilasi, S. C. Watkins, S. W. Ryter, A. Hoetzel, and A. M. Choi. 2008**. Mitogen-activated protein kinases regulate susceptibility to ventilator-induced lung injury. *PLoS.ONE.* 3:e1601.

121. **Ono, K. and J. Han. 2000**. The p38 signal transduction pathway: activation and function. *Cell Signal.* 12:1-13.

122. **Han, J., J. D. Lee, L. Bibbs, and R. J. Ulevitch. 1994**. A MAP kinase targeted by endotoxin and hyperosmolarity in mammalian cells. *Science* 265:808-811.

123. **Jiang, Y., C. Chen, Z. Li, W. Guo, J. A. Gegner, S. Lin, and J. Han. 1996**. Characterization of the structure and function of a new mitogen-activated protein kinase (p38beta). *J.Biol.Chem.* 271:17920-17926.

124. **Bode, J. G., P. Gatsios, S. Ludwig, U. R. Rapp, D. Haussinger, P. C. Heinrich, and L. Graeve. 1999**. The mitogen-activated protein (MAP) kinase p38 and its upstream activator MAP kinase kinase 6 are involved in the activation of signal transducer and activator of transcription by hyperosmolarity. *J.Biol.Chem.* 274:30222-30227.

125. **Johnson, G. L. and R. Lapadat. 2002**. Mitogen-activated protein kinase pathways mediated by ERK, JNK, and p38 protein kinases. *Science* 298:1911-1912.

126. **Tobias, P. S., J. Gegner, R. Tapping, S. Orr, J. Mathison, J. D. Lee, V. Kravchenko, J. Han, and R. J. Ulevitch. 1997**. Lipopolysaccharide dependent cellular activation. *J.Periodontal Res.* 32:99-103.

127. **Wang, Q., A. Turlington, S. Heo, A. Blanco, J. Tian, Z. Xie, B. Yan, and Y. Wan. 2005**. Extracellular matrix activity and caveolae events contribute to cell surface receptor activation that leads to MAP kinase activation in response to UV irradiation in cultured human keratinocytes. *Int.J.Mol.Med.* 15:633-640.

128. **Edlund, S., S. Bu, N. Schuster, P. Aspenstrom, R. Heuchel, N. E. Heldin, D. P. ten, C. H. Heldin, and M. Landstrom. 2003**. Transforming growth factor-beta1 (TGF-beta)-induced apoptosis of prostate cancer cells involves Smad7-dependent activation of p38 by TGF-beta-activated kinase 1 and mitogen-activated protein kinase kinase 3. *Mol.Biol.Cell* 14:529-544.

129. **Hacker, H., H. Mischak, T. Miethke, S. Liptay, R. Schmid, T. Sparwasser, K. Heeg, G. B. Lipford, and H. Wagner. 1998**. CpG-DNA-specific activation of antigen-presenting cells requires stress kinase activity and is preceded by non-specific endocytosis and endosomal maturation. *EMBO J.* 17:6230-6240.

130. **Cook, R., C. C. Wu, Y. J. Kang, and J. Han. 2007**. The role of the p38 pathway in adaptive immunity. *Cell Mol.Immunol.* 4:253-259.

131. **Symons, A., S. Beinke, and S. C. Ley. 2006**. MAP kinase kinase kinases and innate immunity. *Trends Immunol.* 27:40-48.

132. **Damarla, M., E. Hasan, A. Boueiz, A. Le, H. H. Pae, C. Montouchet, T. Kolb, T. Simms, A. Myers, U. S. Kayyali, M. Gaestel, X. Peng, S. P. Reddy, R. Damico, and P. M. Hassoun. 2009**. Mitogen activated protein kinase activated protein kinase 2 regulates actin polymerization and vascular leak in ventilator associated lung injury. *PLoS.ONE.* 4:e4600.

133. **Staal, S. P. 1987**. Molecular cloning of the akt oncogene and its human homologues AKT1 and AKT2: amplification of AKT1 in a primary human gastric adenocarcinoma. *Proc.Natl.Acad.Sci.U.S.A* 84:5034-5037.

134. **Bellacosa, A., J. R. Testa, S. P. Staal, and P. N. Tsichlis. 1991**. A retroviral oncogene, akt, encoding a serine-threonine kinase containing an SH2-like region. *Science* 254:274-277.

135. **Manning, B. D. and L. C. Cantley. 2007**. AKT/PKB signaling: navigating downstream. *Cell* 129:1261-1274.

136. **Song, G., G. Ouyang, and S. Bao. 2005**. The activation of Akt/PKB signaling pathway and cell survival. *J.Cell Mol.Med.* 9:59-71.

137. **Glass, D. J. 2005**. Skeletal muscle hypertrophy and atrophy signaling pathways. *Int.J.Biochem.Cell Biol.* 37:1974-1984.

138. **Vandenburgh, H. H., S. Hatfaludy, P. Karlisch, and J. Shansky. 1989**. Skeletal muscle growth is stimulated by intermittent stretch-relaxation in tissue culture. *Am.J.Physiol* 256:C674-C682.

139. **Bellacosa, A., C. C. Kumar, C. A. Di, and J. R. Testa. 2005**. Activation of AKT kinases in cancer: implications for therapeutic targeting. *Adv.Cancer Res.* 94:29-86.

140. **Faissner, A., N. Heck, A. Dobbertin, and J. Garwood. 2006**. DSD-1-Proteoglycan/Phosphacan and receptor protein tyrosine phosphatase-beta isoforms during development and regeneration of neural tissues. *Adv.Exp.Med.Biol.* 557:25-53.

141. **Klippel, A., W. M. Kavanaugh, D. Pot, and L. T. Williams. 1997**. A specific product of phosphatidylinositol 3-kinase directly activates the protein kinase Akt through its pleckstrin homology domain. *Mol.Cell Biol.* 17:338-344.

142. **Rameh, L. E. and L. C. Cantley. 1999**. The role of phosphoinositide 3-kinase lipid products in cell function. *J.Biol.Chem.* 274:8347-8350.

143. **Vanhaesebroeck, B., S. J. Leevers, K. Ahmadi, J. Timms, R. Katso, P. C. Driscoll, R. Woscholski, P. J. Parker, and M. D. Waterfield. 2001**. Synthesis and function of 3-phosphorylated inositol lipids. *Annu.Rev.Biochem.* 70:535-602.

144. **Ito, K., G. Caramori, and I. M. Adcock. 2007**. Therapeutic potential of phosphatidylinositol 3-kinase inhibitors in inflammatory respiratory disease. *J.Pharmacol.Exp.Ther.* 321:1-8.

145. **Guha, M. and N. Mackman. 2002**. The phosphatidylinositol 3-kinase-Akt pathway limits lipopolysaccharide activation of signaling pathways and expression of inflammatory mediators in human monocytic cells. *J.Biol.Chem.* 277:32124-32132.

146. **Kuebler, W. M., U. Uhlig, T. Goldmann, G. Schael, A. Kerem, K. Exner, C. Martin, E. Vollmer, and S. Uhlig. 2003**. Stretch activates nitric oxide production in pulmonary vascular endothelial cells in situ. *Am.J.Respir.Crit Care Med.* 168:1391-1398.

147. **Shyu, K. G. 2009**. Cellular and molecular effects of mechanical stretch on vascular cells and cardiac myocytes. *Clin.Sci.(Lond)* 116:377-389.

148. **Kippenberger, S., S. Loitsch, M. Guschel, J. Muller, Y. Knies, R. Kaufmann, and A. Bernd. 2005**. Mechanical stretch stimulates protein kinase B/Akt phosphorylation in epidermal cells via angiotensin II type 1 receptor and epidermal growth factor receptor. *J.Biol.Chem.* 280:3060-3067.

149. **Miyahara, T., K. Hamanaka, D. S. Weber, D. A. Drake, M. Anghelescu, and J. C. Parker. 2007**. Phosphoinositide 3-kinase, Src, and Akt modulate acute ventilation-induced

vascular permeability increases in mouse lungs. *Am.J.Physiol Lung Cell Mol.Physiol* 293:L11-L21.

150. **Tremblay, L., F. Valenza, S. P. Ribeiro, J. Li, and A. S. Slutsky. 1997**. Injurious ventilatory strategies increase cytokines and c-fos m-RNA expression in an isolated rat lung model. *J.Clin.Invest* 99:944-952.

151. **Dombrowsky, H. and S. Uhlig. 2007**. Steroids and histone deacetylase in ventilation-induced gene transcription. *Eur.Respir.J.* 30:865-877.

152. **Ikegami, M., S. Kallapur, J. Michna, and A. H. Jobe. 2000**. Lung injury and surfactant metabolism after hyperventilation of premature lambs. *Pediatr.Res.* 47:398-404.

153. **Held, H. D., S. Boettcher, L. Hamann, and S. Uhlig. 2001**. Ventilation-induced chemokine and cytokine release is associated with activation of nuclear factor-kappaB and is blocked by steroids. *Am.J.Respir.Crit Care Med.* 163:711-716.

154. **Berg, J. T., Z. Fu, E. C. Breen, H. C. Tran, O. Mathieu-Costello, and J. B. West. 1997**. High lung inflation increases mRNA levels of ECM components and growth factors in lung parenchyma. *J.Appl.Physiol* 83:120-128.

155. **Copland, I. B., B. P. Kavanagh, D. Engelberts, C. McKerlie, J. Belik, and M. Post. 2003**. Early changes in lung gene expression due to high tidal volume. *Am.J.Respir.Crit Care Med.* 168:1051-1059.

156. **Silverman, E. S. and T. Collins. 1999**. Pathways of Egr-1-mediated gene transcription in vascular biology. *Am.J.Pathol.* 154:665-670.

157. **Arndt, P. G., S. K. Young, J. G. Lieber, M. B. Fessler, J. A. Nick, and G. S. Worthen. 2005**. Inhibition of c-Jun N-terminal kinase limits lipopolysaccharide-induced pulmonary neutrophil influx. *Am.J.Respir.Crit Care Med.* 171:978-986.

158. **Kolb, M., P. J. Margetts, D. C. Anthony, F. Pitossi, and J. Gauldie. 2001**. Transient expression of IL-1beta induces acute lung injury and chronic repair leading to pulmonary fibrosis. *J.Clin.Invest* 107:1529-1536.

159. **Dunn, C., C. Wiltshire, A. MacLaren, and D. A. Gillespie. 2002**. Molecular mechanism and biological functions of c-Jun N-terminal kinase signalling via the c-Jun transcription factor. *Cell Signal.* 14:585-593.

160. **Tirone, F. 2001**. The gene PC3(TIS21/BTG2), prototype member of the PC3/BTG/TOB family: regulator in control of cell growth, differentiation, and DNA repair? *J.Cell Physiol* 187:155-165.

161. **Beere, H. M. and D. R. Green. 2001**. Stress management - heat shock protein-70 and the regulation of apoptosis. *Trends Cell Biol.* 11:6-10.

162. **Altemeier, W. A., G. Matute-Bello, C. W. Frevert, Y. Kawata, O. Kajikawa, T. R. Martin, and R. W. Glenny. 2004**. Mechanical ventilation with moderate tidal volumes synergistically increases lung cytokine response to systemic endotoxin. *Am.J.Physiol Lung Cell Mol.Physiol* 287:L533-L542.

163. **Gharib, S. A., W. C. Liles, G. Matute-Bello, R. W. Glenny, T. R. Martin, and W. A. Altemeier. 2006**. Computational identification of key biological modules and transcription factors in acute lung injury. *Am.J.Respir.Crit Care Med.* 173:653-658.

164. **Grigoryev, D. N., S. F. Ma, R. A. Irizarry, S. Q. Ye, J. Quackenbush, and J. G. Garcia. 2004**. Orthologous gene-expression profiling in multi-species models: search for candidate genes. *Genome Biol.* 5:R34.

165. **Haitsma, J. J., S. Uhlig, S. J. Verbrugge, R. Goggel, D. L. Poelma, and B. Lachmann. 2003**. Injurious ventilation strategies cause systemic release of IL-6 and MIP-2 in rats in vivo. *Clin.Physiol Funct.Imaging* 23:349-353.

166. **2000**. Ventilation with lower tidal volumes as compared with traditional tidal volumes for acute lung injury and the acute respiratory distress syndrome. The Acute Respiratory Distress Syndrome Network. *N.Engl.J.Med.* 342:1301-1308.

167. **Pawson, T. 2002**. Regulation and targets of receptor tyrosine kinases. *Eur.J.Cancer* 38 Suppl 5:S3-10.

168. **Franklin, W. A., R. Veve, F. R. Hirsch, B. A. Helfrich, and P. A. Bunn, Jr. 2002**. Epidermal growth factor receptor family in lung cancer and premalignancy. *Semin.Oncol.* 29:3-14.

169. **Ward, C. W., M. C. Lawrence, V. A. Streltsov, T. E. Adams, and N. M. McKern. 2007**. The insulin and EGF receptor structures: new insights into ligand-induced receptor activation. *Trends Biochem.Sci.* 32:129-137.

170. **Lemmon, M. A. 2009**. Ligand-induced ErbB receptor dimerization. *Exp.Cell Res.* 315:638-648.

171. **Citri, A. and Y. Yarden. 2006**. EGF-ERBB signalling: towards the systems level. *Nat.Rev.Mol.Cell Biol.* 7:505-516.

172. **Roskoski, R., Jr. 2004**. The ErbB/HER receptor protein-tyrosine kinases and cancer. *Biochem.Biophys.Res.Commun.* 319:1-11.

173. **Zhang, H., A. Berezov, Q. Wang, G. Zhang, J. Drebin, R. Murali, and M. I. Greene. 2007**. ErbB receptors: from oncogenes to targeted cancer therapies. *J.Clin.Invest* 117:2051-2058.

174. **Kim, A., B. Liu, D. Ordonez-Ercan, K. M. Alvarez, L. D. Jones, C. McKimmey, S. M. Edgerton, X. Yang, and A. D. Thor. 2005**. Functional interaction between mouse erbB3 and wild-type rat c-neu in transgenic mouse mammary tumor cells. *Breast Cancer Res.* 7:R708-R718.

175. **Nicodemus, K. K., A. Luna, R. Vakkalanka, T. Goldberg, M. Egan, R. E. Straub, and D. R. Weinberger. 2006**. Further evidence for association between ErbB4 and schizophrenia and influence on cognitive intermediate phenotypes in healthy controls. *Mol.Psychiatry* 11:1062-1065.

176. **Klapper, L. N., S. Glathe, N. Vaisman, N. E. Hynes, G. C. Andrews, M. Sela, and Y. Yarden. 1999**. The ErbB-2/HER2 oncoprotein of human carcinomas may function solely as a shared coreceptor for multiple stroma-derived growth factors. *Proc.Natl.Acad.Sci.U.S.A* 96:4995-5000.

177. **Guy, P. M., J. V. Platko, L. C. Cantley, R. A. Cerione, and K. L. Carraway, III. 1994**. Insect cell-expressed p180erbB3 possesses an impaired tyrosine kinase activity. *Proc.Natl.Acad.Sci.U.S.A* 91:8132-8136.

178. **Carpenter, G. 1999**. Employment of the epidermal growth factor receptor in growth factor-independent signaling pathways. *J.Cell Biol.* 146:697-702.

179. **Giaccone, G. and J. A. Rodriguez. 2005**. EGFR inhibitors: what have we learned from the treatment of lung cancer? *Nat.Clin.Pract.Oncol.* 2:554-561.

180. **Ben-Bassat, H. 2001**. Biological activity of tyrosine kinase inhibitors: novel agents for psoriasis therapy. *Curr.Opin.Investig.Drugs* 2:1539-1545.

181. **Boehrer, S., L. Ades, L. Galluzzi, N. Tajeddine, M. Tailler, C. Gardin, B. S. de, P. Fenaux, and G. Kroemer. 2008**. Erlotinib and gefitinib for the treatment of myelodysplastic syndrome and acute myeloid leukemia: a preclinical comparison. *Biochem.Pharmacol.* 76:1417-1425.

182. **Holbro, T., G. Civenni, and N. E. Hynes. 2003**. The ErbB receptors and their role in cancer progression. *Exp.Cell Res.* 284:99-110.

183. **Peles, E. and Y. Yarden. 1993**. Neu and its ligands: from an oncogene to neural factors. *Bioessays* 15:815-824.

184. **Ludwig, A., C. Hundhausen, M. H. Lambert, N. Broadway, R. C. Andrews, D. M. Bickett, M. A. Leesnitzer, and J. D. Becherer. 2005**. Metalloproteinase inhibitors for the disintegrin-like metalloproteinases ADAM10 and ADAM17 that differentially block constitutive and phorbol ester-inducible shedding of cell surface molecules. *Comb.Chem.High Throughput.Screen.* 8:161-171.

185. **Massague, J. and A. Pandiella. 1993**. Membrane-anchored growth factors. *Annu.Rev.Biochem.* 62:515-541.

186. **Sahin, U., G. Weskamp, K. Kelly, H. M. Zhou, S. Higashiyama, J. Peschon, D. Hartmann, P. Saftig, and C. P. Blobel. 2004**. Distinct roles for ADAM10 and ADAM17 in ectodomain shedding of six EGFR ligands. *J.Cell Biol.* 164:769-779.

187. **Lee, D. C., S. W. Sunnarborg, C. L. Hinkle, T. J. Myers, M. Y. Stevenson, W. E. Russell, B. J. Castner, M. J. Gerhart, R. J. Paxton, R. A. Black, A. Chang, and L. F. Jackson. 2003**. TACE/ADAM17 processing of EGFR ligands indicates a role as a physiological convertase. *Ann.N.Y.Acad.Sci.* 995:22-38.

188. **Carpenter, G. and S. Cohen. 1990**. Epidermal growth factor. *J.Biol.Chem.* 265:7709-7712.

189. **Shoyab, M., V. L. McDonald, J. G. Bradley, and G. J. Todaro. 1988**. Amphiregulin: a bifunctional growth-modulating glycoprotein produced by the phorbol 12-myristate 13-acetate-treated human breast adenocarcinoma cell line MCF-7. *Proc.Natl.Acad.Sci.U.S.A* 85:6528-6532.

190. **Shoyab, M., G. D. Plowman, V. L. McDonald, J. G. Bradley, and G. J. Todaro. 1989**. Structure and function of human amphiregulin: a member of the epidermal growth factor family. *Science* 243:1074-1076.

191. **Normanno, N., M. P. Selvam, C. F. Qi, T. Saeki, G. Johnson, N. Kim, F. Ciardiello, M. Shoyab, G. Plowman, R. Brandt, and 1994**. Amphiregulin as an autocrine growth factor for c-Ha-ras- and c-erbB-2-transformed human mammary epithelial cells. *Proc.Natl.Acad.Sci.U.S.A* 91:2790-2794.

192. **Inatomi, O., A. Andoh, Y. Yagi, S. Bamba, T. Tsujikawa, and Y. Fujiyama. 2006**. Regulation of amphiregulin and epiregulin expression in human colonic subepithelial myofibroblasts. *Int.J.Mol.Med.* 18:497-503.

193. **Piepkorn, M., C. Lo, and G. Plowman. 1994**. Amphiregulin-dependent proliferation of cultured human keratinocytes: autocrine growth, the effects of exogenous recombinant cytokine, and apparent requirement for heparin-like glycosaminoglycans. *J.Cell Physiol* 159:114-120.

194. **Pastore, S., F. Mascia, V. Mariani, and G. Girolomoni. 2008**. The epidermal growth factor receptor system in skin repair and inflammation. *J.Invest Dermatol.* 128:1365-1374.

195. **Qi, C. F., D. S. Liscia, N. Normanno, G. Merlo, G. R. Johnson, W. J. Gullick, F. Ciardiello, T. Saeki, R. Brandt, N. Kim, and 1994**. Expression of transforming growth factor alpha, amphiregulin and cripto-1 in human breast carcinomas. *Br.J.Cancer* 69:903-910.

196. **Johansson, C. C., A. Yndestad, J. M. Enserink, A. H. Ree, P. Aukrust, and K. Tasken. 2004**. The epidermal growth factor-like growth factor amphiregulin is strongly induced by the adenosine 3',5'-monophosphate pathway in various cell types. *Endocrinology* 145:5177-5184.

197. **Willmarth, N. E. and S. P. Ethier. 2008**. Amphiregulin as a novel target for breast cancer therapy. *J.Mammary.Gland.Biol.Neoplasia.* 13:171-179.

198. **Du, B., N. K. Altorki, L. Kopelovich, K. Subbaramaiah, and A. J. Dannenberg. 2005**. Tobacco smoke stimulates the transcription of amphiregulin in human oral epithelial cells: evidence of a cyclic AMP-responsive element binding protein-dependent mechanism. *Cancer Res.* 65:5982-5988.

199. **Okumura, S., H. Sagara, T. Fukuda, H. Saito, and Y. Okayama. 2005**. FcepsilonRI-mediated amphiregulin production by human mast cells increases mucin gene expression in epithelial cells. *J.Allergy Clin.Immunol.* 115:272-279.

200. **Wang, S. W., C. K. Oh, S. H. Cho, G. Hu, R. Martin, S. missie-Sanders, K. Li, M. Moyle, and Z. Yao. 2005**. Amphiregulin expression in human mast cells and its effect on the primary human lung fibroblasts. *J.Allergy Clin.Immunol.* 115:287-294.

201. **Daly, R. J. 1999**. Take your partners, please--signal diversification by the erbB family of receptor tyrosine kinases. *Growth Factors* 16:255-263.

202. **Prenzel, N., E. Zwick, M. Leserer, and A. Ullrich. 2000**. Tyrosine kinase signalling in breast cancer. Epidermal growth factor receptor: convergence point for signal integration and diversification. *Breast Cancer Res.* 2:184-190.

203. **Sweeney, C. and K. L. Carraway, III. 2004**. Negative regulation of ErbB family receptor tyrosine kinases. *Br.J.Cancer* 90:289-293.

204. **Uematsu, S. and S. Akira. 2008**. Toll-Like receptors (TLRs) and their ligands. *Handb.Exp.Pharmacol.*1-20.

205. **Akira, S. and H. Hemmi. 2003**. Recognition of pathogen-associated molecular patterns by TLR family. *Immunol.Lett.* 85:85-95.

206. **Zhang, G. and S. Ghosh. 2001**. Toll-like receptor-mediated NF-kappaB activation: a phylogenetically conserved paradigm in innate immunity. *J.Clin.Invest* 107:13-19.

207. **Dunne, A. and L. A. O'Neill. 2003**. The interleukin-1 receptor/Toll-like receptor superfamily: signal transduction during inflammation and host defense. *Sci.STKE.* 2003:re3.

208. **Akira, S. and K. Takeda. 2004**. Toll-like receptor signalling. *Nat.Rev.Immunol.* 4:499-511.

209. **Froy, O. 2005**. Regulation of mammalian defensin expression by Toll-like receptor-dependent and independent signalling pathways. *Cell Microbiol.* 7:1387-1397.

210. **Takeda, K., T. Kaisho, and S. Akira. 2003**. Toll-like receptors. *Annu.Rev.Immunol.* 21:335-376.

211. **Aliprantis, A. O., R. B. Yang, D. S. Weiss, P. Godowski, and A. Zychlinsky. 2000**. The apoptotic signaling pathway activated by Toll-like receptor-2. *EMBO J.* 19:3325-3336.

212. **Sabroe, I., S. K. Dower, and M. K. Whyte. 2005**. The role of Toll-like receptors in the regulation of neutrophil migration, activation, and apoptosis. *Clin.Infect.Dis.* 41 Suppl 7:S421-S426.

213. **Uematsu, S. and S. Akira. 2008**. Toll-Like receptors (TLRs) and their ligands. *Handb.Exp.Pharmacol.*1-20.

214. **Takeda, K. and S. Akira. 2005**. Toll-like receptors in innate immunity. *Int.Immunol.* 17:1-14.

215. **Zhang, D., G. Zhang, M. S. Hayden, M. B. Greenblatt, C. Bussey, R. A. Flavell, and S. Ghosh. 2004**. A toll-like receptor that prevents infection by uropathogenic bacteria. *Science* 303:1522-1526.

216. **Jin, M. S. and J. O. Lee. 2008**. Structures of the toll-like receptor family and its ligand complexes. *Immunity.* 29:182-191.

217. **Takeuchi, O., S. Sato, T. Horiuchi, K. Hoshino, K. Takeda, Z. Dong, R. L. Modlin, and S. Akira. 2002**. Cutting edge: role of Toll-like receptor 1 in mediating immune response to microbial lipoproteins. *J.Immunol.* 169:10-14.

218. **Takeuchi, O., T. Kawai, P. F. Muhlradt, M. Morr, J. D. Radolf, A. Zychlinsky, K. Takeda, and S. Akira. 2001**. Discrimination of bacterial lipoproteins by Toll-like receptor 6. *Int.Immunol.* 13:933-940.

219. **Barton, G. M. and R. Medzhitov. 2002**. Toll-like receptors and their ligands. *Curr.Top.Microbiol.Immunol.* 270:81-92.

220. **Zahringer, U., B. Lindner, S. Inamura, H. Heine, and C. Alexander. 2008**. TLR2 - promiscuous or specific? A critical re-evaluation of a receptor expressing apparent broad specificity. *Immunobiology* 213:205-224.

221. **Schwandner, R., R. Dziarski, H. Wesche, M. Rothe, and C. J. Kirschning. 1999**. Peptidoglycan- and lipoteichoic acid-induced cell activation is mediated by toll-like receptor 2. *J.Biol.Chem.* 274:17406-17409.

222. **Lehner, M. D., S. Morath, K. S. Michelsen, R. R. Schumann, and T. Hartung. 2001**. Induction of cross-tolerance by lipopolysaccharide and highly purified lipoteichoic acid via different Toll-like receptors independent of paracrine mediators. *J.Immunol.* 166:5161-5167.

223. **Wieland, C. W., S. Knapp, S. Florquin, A. F. de Vos, K. Takeda, S. Akira, D. T. Golenbock, A. Verbon, and P. T. van der. 2004**. Non-mannose-capped lipoarabinomannan induces lung inflammation via toll-like receptor 2. *Am.J.Respir.Crit Care Med.* 170:1367-1374.

224. **Ozinsky, A., D. M. Underhill, J. D. Fontenot, A. M. Hajjar, K. D. Smith, C. B. Wilson, L. Schroeder, and A. Aderem. 2000**. The repertoire for pattern recognition of pathogens by the innate immune system is defined by cooperation between toll-like receptors. *Proc.Natl.Acad.Sci.U.S.A* 97:13766-13771.

225. **Sato, M., H. Sano, D. Iwaki, K. Kudo, M. Konishi, H. Takahashi, T. Takahashi, H. Imaizumi, Y. Asai, and Y. Kuroki. 2003**. Direct binding of Toll-like receptor 2 to zymosan, and zymosan-induced NF-kappa B activation and TNF-alpha secretion are down-regulated by lung collectin surfactant protein A. *J.Immunol.* 171:417-425.

226. **Campos, M. A., I. C. Almeida, O. Takeuchi, S. Akira, E. P. Valente, D. O. Procopio, L. R. Travassos, J. A. Smith, D. T. Golenbock, and R. T. Gazzinelli. 2001**. Activation of Toll-like receptor-2 by glycosylphosphatidylinositol anchors from a protozoan parasite. *J.Immunol.* 167:416-423.

227. **Hashimoto, M., K. Tawaratsumida, H. Kariya, A. Kiyohara, Y. Suda, F. Krikae, T. Kirikae, and F. Gotz. 2006**. Not lipoteichoic acid but lipoproteins appear to be the dominant immunobiologically active compounds in Staphylococcus aureus. *J.Immunol.* 177:3162-3169.

228. **Hashimoto, M., M. Furuyashiki, R. Kaseya, Y. Fukada, M. Akimaru, K. Aoyama, T. Okuno, T. Tamura, T. Kirikae, F. Kirikae, N. Eiraku, H. Morioka, Y. Fujimoto, K. Fukase, K. Takashige, Y. Moriya, S. Kusumoto, and Y. Suda. 2007**. Evidence of immunostimulating lipoprotein existing in the natural lipoteichoic acid fraction. *Infect.Immun.* 75:1926-1932.

229. **Travassos, L. H., S. E. Girardin, D. J. Philpott, D. Blanot, M. A. Nahori, C. Werts, and I. G. Boneca. 2004**. Toll-like receptor 2-dependent bacterial sensing does not occur via peptidoglycan recognition. *EMBO Rep.* 5:1000-1006.

230. **Muhlradt, P. F., M. Kiess, H. Meyer, R. Sussmuth, and G. Jung. 1997**. Isolation, structure elucidation, and synthesis of a macrophage stimulatory lipopeptide from Mycoplasma fermentans acting at picomolar concentration. *J.Exp.Med.* 185:1951-1958.

231. **Hoebe, K., P. Georgel, S. Rutschmann, X. Du, S. Mudd, K. Crozat, S. Sovath, L. Shamel, T. Hartung, U. Zahringer, and B. Beutler. 2005**. CD36 is a sensor of diacylglycerides. *Nature* 433:523-527.

232. **Kaufmann, A., P. F. Muhlradt, D. Gemsa, and H. Sprenger. 1999**. Induction of cytokines and chemokines in human monocytes by Mycoplasma fermentans-derived lipoprotein MALP-2. *Infect.Immun.* 67:6303-6308.

233. **Shingu, K., C. Kruschinski, A. Luhrmann, K. Grote, T. Tschernig, S. Von Horsten, and R. Pabst. 2003**. Intratracheal macrophage-activating lipopeptide-2 reduces metastasis in the rat lung. *Am.J.Respir.Cell Mol.Biol.* 28:316-321.

234. **Luhrmann, A., T. Tschernig, R. Pabst, and S. Niewiesk. 2005**. Improved intranasal immunization with live-attenuated measles virus after co-inoculation of the lipopeptide MALP-2. *Vaccine* 23:4721-4726.

235. **Reppe, K., T. Tschernig, A. Luhrmann, L. van, V, K. Grote, M. V. Zemlin, B. Gutbier, H. C. Muller, M. Kursar, H. Schutte, S. Rosseau, R. Pabst, N. W. Suttorp, and M. Witzenrath. 2008**. Immunostimulation with Macrophage-Activating Lipopeptide-2 Increased Survival in Murine Pneumonia. *Am.J.Respir.Cell Mol.Biol.*

236. **Ziegler-Heitbrock, H. W., A. Wedel, W. Schraut, M. Strobel, P. Wendelgass, T. Sternsdorf, P. A. Bauerle, J. G. Haas, and G. Riethmuller. 1994**. Tolerance to lipopolysaccharide

involves mobilization of nuclear factor kappa B with predominance of p50 homodimers. *J.Biol.Chem.* 269:17001-17004.

237. **Petersen, B., K. D. Bloch, F. Ichinose, H. S. Shin, M. Shigematsu, A. Bagchi, W. M. Zapol, and J. Hellman. 2008**. Activation of Toll-like receptor 2 impairs hypoxic pulmonary vasoconstriction in mice. *Am.J.Physiol Lung Cell Mol.Physiol* 294:L300-L308.

238. **Natarajan, S., J. Kim, and D. G. Remick. 2009**. Chronic Pulmonary LPS Tolerance Induces Selective Immunosuppression while Maintaining the Neutrophilic Response. *Shock*.

239. **Waters, V., S. Sokol, B. Reddy, G. Soong, J. Chun, and A. Prince. 2005**. The effect of cyclosporin A on airway cell proinflammatory signaling and pneumonia 1. *Am.J.Respir.Cell Mol.Biol.* 33:138-144.

240. **Chen, H., M. J. Cowan, J. D. Hasday, S. N. Vogel, and A. E. Medvedev. 2007**. Tobacco smoking inhibits expression of proinflammatory cytokines and activation of IL-1R-associated kinase, p38, and NF-kappaB in alveolar macrophages stimulated with TLR2 and TLR4 agonists. *J.Immunol.* 179:6097-6106.

241. **Poltorak, A., X. He, I. Smirnova, M. Y. Liu, H. C. Van, X. Du, D. Birdwell, E. Alejos, M. Silva, C. Galanos, M. Freudenberg, P. Ricciardi-Castagnoli, B. Layton, and B. Beutler. 1998**. Defective LPS signaling in C3H/HeJ and C57BL/10ScCr mice: mutations in Tlr4 gene. *Science* 282:2085-2088.

242. **Kawasaki, K., S. Akashi, R. Shimazu, T. Yoshida, K. Miyake, and M. Nishijima. 2000**. Mouse toll-like receptor 4.MD-2 complex mediates lipopolysaccharide-mimetic signal transduction by Taxol. *J.Biol.Chem.* 275:2251-2254.

243. **Heine, H. and E. Lien. 2003**. Toll-like receptors and their function in innate and adaptive immunity. *Int.Arch.Allergy Immunol.* 130:180-192.

244. **da Silva, C. J., K. Soldau, U. Christen, P. S. Tobias, and R. J. Ulevitch. 2001**. Lipopolysaccharide is in close proximity to each of the proteins in its membrane receptor complex. transfer from CD14 to TLR4 and MD-2. *J.Biol.Chem.* 276:21129-21135.

245. **Smith, K. D., E. ndersen-Nissen, F. Hayashi, K. Strobe, M. A. Bergman, S. L. Barrett, B. T. Cookson, and A. Aderem. 2003**. Toll-like receptor 5 recognizes a conserved site on

flagellin required for protofilament formation and bacterial motility. *Nat.Immunol.* 4:1247-1253.

246. **Koyama, S., K. J. Ishii, C. Coban, and S. Akira. 2008**. Innate immune response to viral infection. *Cytokine* 43:336-341.

247. **Hoshino, K., O. Takeuchi, T. Kawai, H. Sanjo, T. Ogawa, Y. Takeda, K. Takeda, and S. Akira. 1999**. Cutting edge: Toll-like receptor 4 (TLR4)-deficient mice are hyporesponsive to lipopolysaccharide: evidence for TLR4 as the Lps gene product. *J.Immunol.* 162:3749-3752.

248. **Lord, K. A., B. Hoffman-Liebermann, and D. A. Liebermann. 1990**. Nucleotide sequence and expression of a cDNA encoding MyD88, a novel myeloid differentiation primary response gene induced by IL6. *Oncogene* 5:1095-1097.

249. **Horng, T., G. M. Barton, R. A. Flavell, and R. Medzhitov. 2002**. The adaptor molecule TIRAP provides signalling specificity for Toll-like receptors. *Nature* 420:329-333.

250. **Yamamoto, M., S. Sato, H. Hemmi, K. Hoshino, T. Kaisho, H. Sanjo, O. Takeuchi, M. Sugiyama, M. Okabe, K. Takeda, and S. Akira. 2003**. Role of adaptor TRIF in the MyD88-independent toll-like receptor signaling pathway. *Science* 301:640-643.

251. **Oshiumi, H., M. Matsumoto, K. Funami, T. Akazawa, and T. Seya. 2003**. TICAM-1, an adaptor molecule that participates in Toll-like receptor 3-mediated interferon-beta induction. *Nat.Immunol.* 4:161-167.

252. **Hardiman, G., N. A. Jenkins, N. G. Copeland, D. J. Gilbert, D. K. Garcia, S. L. Naylor, R. A. Kastelein, and J. F. Bazan. 1997**. Genetic structure and chromosomal mapping of MyD88. *Genomics* 45:332-339.

253. **Hofmann, K. and J. Tschopp. 1995**. The death domain motif found in Fas (Apo-1) and TNF receptor is present in proteins involved in apoptosis and axonal guidance. *FEBS Lett.* 371:321-323.

254. **Kopp, E., R. Medzhitov, J. Carothers, C. Xiao, I. Douglas, C. A. Janeway, and S. Ghosh. 1999**. ECSIT is an evolutionarily conserved intermediate in the Toll/IL-1 signal transduction pathway. *Genes Dev.* 13:2059-2071.

255. **Zhang, G. and S. Ghosh. 2002**. Negative regulation of toll-like receptor-mediated signaling by Tollip. *J.Biol.Chem.* 277:7059-7065.

256. **Didierlaurent, A., B. Brissoni, D. Velin, N. Aebi, A. Tardivel, E. Kaslin, J. C. Sirard, G. Angelov, J. Tschopp, and K. Burns. 2006**. Tollip regulates proinflammatory responses to interleukin-1 and lipopolysaccharide. *Mol.Cell Biol.* 26:735-742.

257. **Mansell, A., E. Brint, J. A. Gould, L. A. O'Neill, and P. J. Hertzog. 2004**. Mal interacts with tumor necrosis factor receptor-associated factor (TRAF)-6 to mediate NF-kappaB activation by toll-like receptor (TLR)-2 and TLR4. *J.Biol.Chem.* 279:37227-37230.

258. **Goh, K. C., M. J. deVeer, and B. R. Williams. 2000**. The protein kinase PKR is required for p38 MAPK activation and the innate immune response to bacterial endotoxin. *EMBO J.* 19:4292-4297.

259. **Cabanski, M., M. Steinmuller, L. M. Marsh, E. Surdziel, W. Seeger, and J. Lohmeyer. 2008**. PKR regulates TLR2/TLR4-dependent signaling in murine alveolar macrophages. *Am.J.Respir.Cell Mol.Biol.* 38:26-31.

260. **Kawai, T., O. Takeuchi, T. Fujita, J. Inoue, P. F. Muhlradt, S. Sato, K. Hoshino, and S. Akira. 2001**. Lipopolysaccharide stimulates the MyD88-independent pathway and results in activation of IFN-regulatory factor 3 and the expression of a subset of lipopolysaccharide-inducible genes. *J.Immunol.* 167:5887-5894.

261. **Doyle, S., S. Vaidya, R. O'Connell, H. Dadgostar, P. Dempsey, T. Wu, G. Rao, R. Sun, M. Haberland, R. Modlin, and G. Cheng. 2002**. IRF3 mediates a TLR3/TLR4-specific antiviral gene program. *Immunity.* 17:251-263.

262. **Piao, W., C. Song, H. Chen, M. A. Quevedo Diaz, L. M. Wahl, K. A. Fitzgerald, L. Li, and A. E. Medvedev. 2009**. Endotoxin tolerance dysregulates MyD88- and Toll/IL-1R domain-containing adapter inducing IFN-{beta}-dependent pathways and increases expression of negative regulators of TLR signaling.. *J.Leukoc.Biol.*

263. **Uhlig, S. and A. E. Taylor. 1998**. Methods in Pulmonary Research, 1 ed. Birkhauser, 1-541.

264. **Weisberg, S. P., D. McCann, M. Desai, M. Rosenbaum, R. L. Leibel, and A. W. Ferrante, Jr. 2003**. Obesity is associated with macrophage accumulation in adipose tissue. *J.Clin.Invest* 112:1796-1808.

265. **Hu, L., V. D. Dixit, V. de Mello-Coelho, and D. D. Taub. 2004**. Age-associated alterations in CXCL1 chemokine expression by murine B cells. *BMC.Immunol.* 5:15.

266. **Ehlers, S., J. Benini, S. Kutsch, R. Endres, E. T. Rietschel, and K. Pfeffer. 1999**. Fatal granuloma necrosis without exacerbated mycobacterial growth in tumor necrosis factor receptor p55 gene-deficient mice intravenously infected with Mycobacterium avium. *Infect.Immun.* 67:3571-3579.

267. **Van Weemen, B. K. and A. H. Schuurs. 1971**. Immunoassay using antigen-enzyme conjugates. *FEBS Lett.* 15:232-236.

268. **Smith, P. K., R. I. Krohn, G. T. Hermanson, A. K. Mallia, F. H. Gartner, M. D. Provenzano, E. K. Fujimoto, N. M. Goeke, B. J. Olson, and D. C. Klenk. 1985**. Measurement of protein using bicinchoninic acid. *Anal.Biochem.* 150:76-85.

269. **Laemmli, U. K. 1970**. Cleavage of structural proteins during the assembly of the head of bacteriophage T4. *Nature* 227:680-685.

270. **Burnette, W. N. 1981**. "Western blotting": electrophoretic transfer of proteins from sodium dodecyl sulfate--polyacrylamide gels to unmodified nitrocellulose and radiographic detection with antibody and radioiodinated protein A. *Anal.Biochem.* 112:195-203.

271. **Higuchi, R., C. Fockler, G. Dollinger, and R. Watson. 1993**. Kinetic PCR analysis: real-time monitoring of DNA amplification reactions. *Biotechnology (N.Y.)* 11:1026-1030.

272. **The R project for statistical computing** wwww.r-projekt.org. Date last accessed: August 15,2007. Date last updated: June,26:2007. 2009.

273. **Song, R., M. Kubo, D. Morse, Z. Zhou, X. Zhang, J. H. Dauber, J. Fabisiak, S. M. Alber, S. C. Watkins, B. S. Zuckerbraun, L. E. Otterbein, W. Ning, T. D. Oury, P. J. Lee, K. R. McCurry, and A. M. Choi. 2003**. Carbon monoxide induces cytoprotection in rat orthotopic lung transplantation via anti-inflammatory and anti-apoptotic effects. *Am.J.Pathol.* 163:231-242.

274. **Ning, W., C. J. Li, N. Kaminski, C. A. Feghali-Bostwick, S. M. Alber, Y. P. Di, S. L. Otterbein, R. Song, S. Hayashi, Z. Zhou, D. J. Pinsky, S. C. Watkins, J. M. Pilewski, F. C. Sciurba, D. G. Peters, J. C. Hogg, and A. M. Choi. 2004**. Comprehensive gene expression profiles reveal pathways related to the pathogenesis of chronic obstructive pulmonary disease. *Proc.Natl.Acad.Sci.U.S.A* 101:14895-14900.

275. **Wu, W., Dave, N., and Tseng, G**. Comparsion of normalization methods for CodeLink bioarray data. 2005.

276. **Tusher, V. G., R. Tibshirani, and G. Chu. 2001**. Significance analysis of microarrays applied to the ionizing radiation response. *Proc.Natl.Acad.Sci.U.S.A* 98:5116-5121.

277. **Ben-Dor, A., L. Bruhn, N. Friedman, I. Nachman, M. Schummer, and Z. Yakhini. 2000**. Tissue classification with gene expression profiles. *J.Comput.Biol.* 7:559-583.

278. **Segal, E., N. Friedman, D. Koller, and A. Regev. 2004**. A module map showing conditional activity of expression modules in cancer. *Nat.Genet.* 36:1090-1098.

279. **Held, H. D. and S. Uhlig. 2000**. Mechanisms of endotoxin-induced airway and pulmonary vascular hyperreactivity in mice. *Am.J.Respir.Crit Care Med.* 162:1547-1552.

280. **Oda, K. and H. Kitano. 2006**. A comprehensive map of the toll-like receptor signaling network. *Mol.Syst.Biol.* 2:2006.

281. **Thellin, O., W. Zorzi, B. Lakaye, B. B. De, B. Coumans, G. Hennen, T. Grisar, A. Igout, and E. Heinen. 1999**. Housekeeping genes as internal standards: use and limits. *J.Biotechnol.* 75:291-295.

282. **Uhlig, S., R. Nusing, B. A. von, R. L. Featherstone, T. Klein, F. Brasch, K. M. Muller, V. Ullrich, and A. Wendel. 1996**. Cyclooxygenase-2-dependent bronchoconstriction in perfused rat lungs exposed to endotoxin. *Mol.Med.* 2:373-383.

283. **Genovese, T., P. R. Di, P. Catalano, J. H. Li, W. Xu, E. Massuda, A. P. Caputi, J. Zhang, and S. Cuzzocrea. 2004**. Treatment with a novel poly(ADP-ribose) glycohydrolase inhibitor reduces development of septic shock-like syndrome induced by zymosan in mice 1. *Crit Care Med.* 32:1365-1374.

284. **Gipson, T. S., N. M. Bless, T. P. Shanley, L. D. Crouch, M. R. Bleavins, E. M. Younkin, V. Sarma, D. F. Gibbs, W. Tefera, P. C. McConnell, W. T. Mueller, K. J. Johnson, and P. A. Ward. 1999**. Regulatory effects of endogenous protease inhibitors in acute lung inflammatory injury. *J.Immunol.* 162:3653-3662.

285. **Pryhuber, G. S., H. L. Huyck, J. M. Roper, J. Cornejo, M. A. O'Reilly, R. H. Pierce, and E. N. Tsitsikov. 2005**. Acute tumor necrosis factor-alpha-induced liver injury in the absence of tumor necrosis factor receptor-associated factor 1 gene expression. *Am.J.Pathol.* 166:1637-1645.

286. **Neville, L. F., G. Mathiak, and O. Bagasra. 1997**. The immunobiology of interferon-gamma inducible protein 10 kD (IP-10): a novel, pleiotropic member of the C-X-C chemokine superfamily
1. *Cytokine Growth Factor Rev.* 8:207-219.

287. **Martin, C., S. Uhlig, and V. Ullrich. 2001**. Cytokine-induced bronchoconstriction in precision-cut lung slices is dependent upon cyclooxygenase-2 and thromboxane receptor activation. *Am.J.Respir.Cell Mol.Biol.* 24:139-145.

288. **Figueiredo, M. D., M. L. Vandenplas, D. J. Hurley, and J. N. Moore. 2009**. Differential induction of MyD88- and TRIF-dependent pathways in equine monocytes by Toll-like receptor agonists. *Vet.Immunol.Immunopathol.* 127:125-134.

289. **Fry, D. W., A. J. Kraker, A. McMichael, L. A. Ambroso, J. M. Nelson, W. R. Leopold, R. W. Connors, and A. J. Bridges. 1994**. A specific inhibitor of the epidermal growth factor receptor tyrosine kinase. *Science* 265:1093-1095.

290. **Iwasaki, A. and R. Medzhitov. 2004**. Toll-like receptor control of the adaptive immune responses. *Nat.Immunol.* 5:987-995.

291. **Raymond, T., M. Schaller, C. M. Hogaboam, N. W. Lukacs, R. Rochford, and S. L. Kunkel. 2007**. Toll-like receptors, Notch ligands, and cytokines drive the chronicity of lung inflammation. *Proc.Am.Thorac.Soc.* 4:635-641.

292. **Nishimura, M. and S. Naito. 2005**. Tissue-specific mRNA expression profiles of human toll-like receptors and related genes. *Biol.Pharm.Bull.* 28:886-892.

293. **Reiling, N., C. Holscher, A. Fehrenbach, S. Kroger, C. J. Kirschning, S. Goyert, and S. Ehlers. 2002**. Cutting edge: Toll-like receptor (TLR)2- and TLR4-mediated pathogen recognition in resistance to airborne infection with Mycobacterium tuberculosis 1. *J.Immunol.* 169:3480-3484.

294. **Hajishengallis, G., M. Wang, G. J. Bagby, and S. Nelson. 2008**. Importance of TLR2 in early innate immune response to acute pulmonary infection with Porphyromonas gingivalis in mice. *J.Immunol.* 181:4141-4149.

295. **Fuse, E. T., K. Tateda, Y. Kikuchi, T. Matsumoto, F. Gondaira, A. Azuma, S. Kudoh, T. J. Standiford, and K. Yamaguchi. 2007**. Role of Toll-like receptor 2 in recognition of Legionella pneumophila in a murine pneumonia model. *J.Med.Microbiol.* 56:305-312.

296. **Yang, H. Z., B. Cui, H. Z. Liu, Z. R. Chen, H. M. Yan, F. Hua, and Z. W. Hu. 2009**. Targeting TLR2 attenuates pulmonary inflammation and fibrosis by reversion of suppressive immune microenvironment. *J.Immunol.* 182:692-702.

297. **Buckland, K. F., E. O'Connor, L. A. Murray, and C. M. Hogaboam. 2008**. Toll like receptor-2 modulates both innate and adaptive immune responses during chronic fungal asthma in mice. *Inflamm.Res.* 57:379-387.

298. **Hoth, J. J., W. P. Hudson, N. A. Brownlee, B. K. Yoza, E. M. Hiltbold, J. W. Meredith, and C. E. McCall. 2007**. Toll-like receptor 2 participates in the response to lung injury in a murine model of pulmonary contusion. *Shock* 28:447-452.

299. **Jiang, D., J. Liang, J. Fan, S. Yu, S. Chen, Y. Luo, G. D. Prestwich, M. M. Mascarenhas, H. G. Garg, D. A. Quinn, R. J. Homer, D. R. Goldstein, R. Bucala, P. J. Lee, R. Medzhitov, and P. W. Noble. 2005**. Regulation of lung injury and repair by Toll-like receptors and hyaluronan. *Nat.Med.* 11:1173-1179.

300. **Knapp, S., A. S. von, M. Leendertse, I. Haslinger, C. Draing, D. T. Golenbock, and P. T. van der. 2008**. Lipoteichoic acid-induced lung inflammation depends on TLR2 and the concerted action of TLR4 and the platelet-activating factor receptor. *J.Immunol.* 180:3478-3484.

301. **Hattar, K., U. Grandel, A. Moeller, L. Fink, J. Iglhaut, T. Hartung, S. Morath, W. Seeger, F. Grimminger, and U. Sibelius. 2006**. Lipoteichoic acid (LTA) from Staphylococcus aureus

stimulates human neutrophil cytokine release by a CD14-dependent, Toll-like-receptor-independent mechanism: Autocrine role of tumor necrosis factor-[alpha] in mediating LTA-induced interleukin-8 generation. *Crit Care Med.* 34:835-841.

302. **Liu, K., G. P. Anderson, and S. Bozinovski. 2008**. DNA vector augments inflammation in epithelial cells via EGFR-dependent regulation of TLR4 and TLR2. *Am.J.Respir.Cell Mol.Biol.* 39:305-311.

303. **Hoogerwerf, J. J., A. F. de Vos, P. Bresser, J. S. van der Zee, J. M. Pater, B. A. de, M. Tanck, D. L. Lundell, C. Her-Jenh, C. Draing, A. S. von, and P. T. van der. 2008**. Lung inflammation induced by lipoteichoic acid or lipopolysaccharide in humans. *Am.J.Respir.Crit Care Med.* 178:34-41.

304. **Pabst, R., D. Durak, A. Roos, A. Luhrmann, and T. Tschernig. 2009**. TLR2/6 stimulation of the rat lung: effects on lymphocyte subsets, natural killer cells and dendritic cells in different parts of the air-conducting compartments and at different ages. *Immunology* 126:132-139.

305. **Henjakovic, M., K. Sewald, S. Switalla, D. Kaiser, M. Muller, T. Z. Veres, C. Martin, S. Uhlig, N. Krug, and A. Braun. 2008**. Ex vivo testing of immune responses in precision-cut lung slices..*Toxicol.Appl.Pharmacol.* 231:68-76.

306. **Ritter, M., D. Mennerich, A. Weith, and P. Seither. 2005**. Characterization of Toll-like receptors in primary lung epithelial cells: strong impact of the TLR3 ligand poly(I:C) on the regulation of Toll-like receptors, adaptor proteins and inflammatory response. *J.Inflamm.(Lond)* 2:16.

307. **Wurfel, M. M., A. C. Gordon, T. D. Holden, F. Radella, J. Strout, O. Kajikawa, J. T. Ruzinski, G. Rona, R. A. Black, S. Stratton, G. P. Jarvik, A. M. Hajjar, D. A. Nickerson, M. Rieder, J. Sevransky, J. P. Maloney, M. Moss, G. Martin, C. Shanholtz, J. G. Garcia, L. Gao, R. Brower, K. C. Barnes, K. R. Walley, J. A. Russell, and T. R. Martin. 2008**. Toll-like receptor 1 polymorphisms affect innate immune responses and outcomes in sepsis.. *Am.J.Respir.Crit Care Med.* 178:710-720.

308. **Natarajan, S., J. Kim, and D. G. Remick. 2009**. Chronic Pulmonary LPS Tolerance Induces Selective Immunosuppression while Maintaining the Neutrophilic Response. *Shock*.

309. **De, F. K., R. B. Henderson, M. Laschinger, and N. Hogg. 2008**. Neutrophil chemokines KC and macrophage-inflammatory protein-2 are newly synthesized by tissue macrophages using distinct TLR signaling pathways. *J.Immunol.* 180:4308-4315.

310. **Freudenberg, M. A., S. Tchaptchet, S. Keck, G. Fejer, M. Huber, N. Schutze, B. Beutler, and C. Galanos. 2008**. Lipopolysaccharide sensing an important factor in the innate immune response to Gram-negative bacterial infections: benefits and hazards of LPS hypersensitivity. *Immunobiology* 213:193-203.

311. **Andreakos, E., S. M. Sacre, C. Smith, A. Lundberg, S. Kiriakidis, T. Stonehouse, C. Monaco, M. Feldmann, and B. M. Foxwell. 2004**. Distinct pathways of LPS-induced NF-kappa B activation and cytokine production in human myeloid and nonmyeloid cells defined by selective utilization of MyD88 and Mal/TIRAP. *Blood* 103:2229-2237.

312. **Bozinovski, S., J. E. Jones, R. Vlahos, J. A. Hamilton, and G. P. Anderson. 2002**. Granulocyte/macrophage-colony-stimulating factor (GM-CSF) regulates lung innate immunity to lipopolysaccharide through Akt/Erk activation of NFkappa B and AP-1 in vivo. *J.Biol.Chem.* 277:42808-42814.

313. **Kyriakis, J. M. and J. Avruch. 2001**. Mammalian mitogen-activated protein kinase signal transduction pathways activated by stress and inflammation. *Physiol Rev.* 81:807-869.

314. **Means, T. K., R. P. Pavlovich, D. Roca, M. W. Vermeulen, and M. J. Fenton. 2000**. Activation of TNF-alpha transcription utilizes distinct MAP kinase pathways in different macrophage populations. *J.Leukoc.Biol.* 67:885-893.

315. **Berndt, A., F. J. Derksen, P. J. Venta, W. Karmaus, S. Ewart, V. Yuzbasiyan-Gurkan, and N. E. Robinson. 2009**. Expression of toll-like receptor 2 mRNA in bronchial epithelial cells is not induced in RAO-affected horses. *Equine Vet.J.* 41:76-81.

316. **Hambleton, J., S. L. Weinstein, L. Lem, and A. L. DeFranco. 1996**. Activation of c-Jun N-terminal kinase in bacterial lipopolysaccharide-stimulated macrophages. *Proc.Natl.Acad.Sci.U.S.A* 93:2774-2778.

317. **Franke, T. F., D. R. Kaplan, and L. C. Cantley. 1997**. PI3K: downstream AKTion blocks apoptosis. *Cell* 88:435-437.

318. **Monick, M. M., R. K. Mallampalli, A. B. Carter, D. M. Flaherty, D. McCoy, P. K. Robeff, M. W. Peterson, and G. W. Hunninghake. 2001**. Ceramide regulates lipopolysaccharide-induced phosphatidylinositol 3-kinase and Akt activity in human alveolar macrophages. *J.Immunol.* 167:5977-5985.

319. **Yum, H. K., J. Arcaroli, J. Kupfner, R. Shenkar, J. M. Penninger, T. Sasaki, K. Y. Yang, J. S. Park, and E. Abraham. 2001**. Involvement of phosphoinositide 3-kinases in neutrophil activation and the development of acute lung injury 1. *J.Immunol.* 167:6601-6608.

320. **dos Santos, C. C., B. Han, C. F. Andrade, X. Bai, S. Uhlig, R. Hubmayr, M. Tsang, M. Lodyga, S. Keshavjee, A. S. Slutsky, and M. Liu. 2004**. DNA microarray analysis of gene expression in alveolar epithelial cells in response to TNFalpha, LPS, and cyclic stretch. *Physiol Genomics* 19:331-342.

321. **Wurfel, M. M., A. C. Gordon, T. D. Holden, F. Radella, J. Strout, O. Kajikawa, J. T. Ruzinski, G. Rona, R. A. Black, S. Stratton, G. P. Jarvik, A. M. Hajjar, D. A. Nickerson, M. Rieder, J. Sevransky, J. P. Maloney, M. Moss, G. Martin, C. Shanholtz, J. G. Garcia, L. Gao, R. Brower, K. C. Barnes, K. R. WALLEY, J. A. Russell, and T. R. Martin. 2008**. Toll-like receptor 1 polymorphisms affect innate immune responses and outcomes in sepsis. *Am J Respir Crit Care Med* 178:710-720.

322. **Oyoshi, M. K., P. Bryce, S. Goya, M. Pichavant, D. T. Umetsu, H. C. Oettgen, and E. N. Tsitsikov. 2008**. TNF receptor-associated factor 1 expressed in resident lung cells is required for the development of allergic lung inflammation. *J.Immunol.* 180:1878-1885.

323. **Cortes, U., W. M. Tong, D. L. Coyle, M. L. Meyer-Ficca, R. G. Meyer, V. Petrilli, Z. Herceg, E. L. Jacobson, M. K. Jacobson, and Z. Q. Wang. 2004**. Depletion of the 110-kilodalton isoform of poly(ADP-ribose) glycohydrolase increases sensitivity to genotoxic and endotoxic stress in mice. *Mol.Cell Biol.* 24:7163-7178.

324. **Hsia, H. C. and J. E. Schwarzbauer. 2005**. Meet the tenascins: multifunctional and mysterious. *J.Biol.Chem.* 280:26641-26644.

325. **Iyer, A. K., K. T. Tran, C. W. Borysenko, M. Cascio, C. J. Camacho, H. C. Blair, I. Bahar, and A. Wells. 2007**. Tenascin cytotactin epidermal growth factor-like repeat binds epidermal growth factor receptor with low affinity. *J.Cell Physiol* 211:748-758.

326. **Kaarteenaho-Wiik, R., V. L. Kinnula, R. Herva, Y. Soini, R. Pollanen, and P. Paakko. 2002**. Tenascin-C is highly expressed in respiratory distress syndrome and bronchopulmonary dysplasia. *J.Histochem.Cytochem.* 50:423-431.

327. **Brellier, F., R. P. Tucker, and R. Chiquet-Ehrismann. 2009**. Tenascins and their implications in diseases and tissue mechanics. *Scand.J.Med.Sci.Sports*.

328. **Deiters, U., J. Barsig, B. Tawil, and P. F. Muhlradt. 2004**. The macrophage-activating lipopeptide-2 accelerates wound healing in diabetic mice. *Exp.Dermatol.* 13:731-739.

329. **Niebuhr, M., P. F. Muhlradt, M. Wittmann, A. Kapp, and T. Werfel. 2008**. Intracutaneous injection of the macrophage-activating lipopeptide-2 (MALP-2) which accelerates wound healing in mice--a phase I trial in 12 patients. *Exp.Dermatol.* 17:1052-1056.

330. **Wurfel, M. M., A. C. Gordon, T. D. Holden, F. Radella, J. Strout, O. Kajikawa, J. T. Ruzinski, G. Rona, R. A. Black, S. Stratton, G. P. Jarvik, A. M. Hajjar, D. A. Nickerson, M. Rieder, J. Sevransky, J. P. Maloney, M. Moss, G. Martin, C. Shanholtz, J. G. Garcia, L. Gao, R. Brower, K. C. Barnes, K. R. WALLEY, J. A. Russell, and T. R. Martin. 2008**. Toll-like receptor 1 polymorphisms affect innate immune responses and outcomes in sepsis. *Am J Respir Crit Care Med* 178:710-720.

331. **Netea, M. G., d. van, V, I. Verschueren, J. W. Van der Meer, and B. J. Kullberg. 2008**. Role of TLR1 and TLR6 in the host defense against disseminated candidiasis 1. *FEMS Immunol.Med.Microbiol.* 52:118-123.

332. **Farhat, K., S. Riekenberg, H. Heine, J. Debarry, R. Lang, J. Mages, U. Buwitt-Beckmann, K. Roschmann, G. Jung, K. H. Wiesmuller, and A. J. Ulmer. 2008**. Heterodimerization of TLR2 with TLR1 or TLR6 expands the ligand spectrum but does not lead to differential signaling. *J.Leukoc.Biol.* 83:692-701.

333. **Abdullah, F., P. Ovadia, G. Feuerstein, L. F. Neville, R. Morrison, G. Mathiak, M. Whiteford, and R. Rabinovici. 1997**. The novel chemokine mob-1: involvement in adult respiratory distress syndrome. *Surgery* 122:303-312.

334. **Davis, I. J., T. G. Hazel, and L. F. Lau. 1991**. Transcriptional activation by Nur77, a growth factor-inducible member of the steroid hormone receptor superfamily. *Mol.Endocrinol.* 5:854-859.

335. **Brady, S. F., M. M. Wagenaar, M. P. Singh, J. E. Janso, and J. Clardy. 2000**. The cytosporones, new octaketide antibiotics isolated from an endophytic fungus. *Org Lett.* 2:4043-4046.

336. **Kurtz, A., A. Aigner, R. H. Cabal-Manzano, R. E. Butler, D. R. Hood, R. B. Sessions, F. Czubayko, and A. Wellstein. 2004**. Differential regulation of a fibroblast growth factor-binding protein during skin carcinogenesis and wound healing. *Neoplasia.* 6:595-602.

337. **Newman, D. R., E. Walsh, K. B. Apparao, and P. L. Sannes. 2007**. Fibroblast growth factor-binding protein and N-deacetylase/N-sulfotransferase-1 expression in type II cells is modulated by heparin and extracellular matrix. *Am.J.Physiol Lung Cell Mol.Physiol* 293:L1314-L1320.

338. **Carra, S., M. Sivilotti, A. T. Chavez Zobel, H. Lambert, and J. Landry. 2005**. HspB8, a small heat shock protein mutated in human neuromuscular disorders, has in vivo chaperone activity in cultured cells. *Hum.Mol.Genet.* 14:1659-1669.

339. **Wheeler, D. S. and H. R. Wong. 2007**. Heat shock response and acute lung injury. *Free Radic.Biol.Med.* 42:1-14.

340. **Tsukita, S. and M. Furuse. 2002**. Claudin-based barrier in simple and stratified cellular sheets. *Curr.Opin.Cell Biol.* 14:531-536.

341. **Kaarteenaho-Wiik, R. and Y. Soini. 2009**. Claudin-1, -2, -3, -4, -5, and -7 in usual interstitial pneumonia and sarcoidosis. *J.Histochem.Cytochem.* 57:187-195.

342. **Wray, C., Y. Mao, J. Pan, A. Chandrasena, F. Piasta, and J. A. Frank. 2009**. Claudin-4 augments alveolar epithelial barrier function and is induced in acute lung injury. *Am.J.Physiol Lung Cell Mol.Physiol* 297:L219-L227.

343. **Mahtouk, K., D. Hose, T. Reme, V. J. De, M. Jourdan, J. Moreaux, G. Fiol, M. Raab, E. Jourdan, V. Grau, M. Moos, H. Goldschmidt, M. Baudard, J. F. Rossi, F. W. Cremer, and**

B. Klein. 2005. Expression of EGF-family receptors and amphiregulin in multiple myeloma. Amphiregulin is a growth factor for myeloma cells. *Oncogene* 24:3512-3524.

344. **Yamane, S., S. Ishida, Y. Hanamoto, K. Kumagai, R. Masuda, K. Tanaka, N. Shiobara, N. Yamane, T. Mori, T. Juji, N. Fukui, T. Itoh, T. Ochi, and R. Suzuki. 2008**. Proinflammatory role of amphiregulin, an epidermal growth factor family member whose expression is augmented in rheumatoid arthritis patients. *J.Inflamm.(Lond)* 5:5.

345. **Tschumperlin, D. J. 2004**. EGFR autocrine signaling in a compliant interstitial space: mechanotransduction from the outside in. *Cell Cycle* 3:996-997.

346. **Bos, M., J. Mendelsohn, Y. M. Kim, J. Albanell, D. W. Fry, and J. Baselga. 1997**. PD153035, a tyrosine kinase inhibitor, prevents epidermal growth factor receptor activation and inhibits growth of cancer cells in a receptor number-dependent manner. *Clin.Cancer Res.* 3:2099-2106.

347. **Levitzki, A. and A. Gazit. 1995**. Tyrosine kinase inhibition: an approach to drug development. *Science* 267:1782-1788.

348. **Bowers, G., D. Reardon, T. Hewitt, P. Dent, R. B. Mikkelsen, K. Valerie, G. Lammering, C. Amir, and R. K. Schmidt-Ullrich. 2001**. The relative role of ErbB1-4 receptor tyrosine kinases in radiation signal transduction responses of human carcinoma cells. *Oncogene* 20:1388-1397.

349. **MacLaine, N. J., M. D. Wood, J. C. Holder, R. W. Rees, and J. Southgate. 2008**. Sensitivity of normal, paramalignant, and malignant human urothelial cells to inhibitors of the epidermal growth factor receptor signaling pathway. *Mol.Cancer Res.* 6:53-63.

350. **Beier, I., R. Dusing, H. Vetter, and U. Schmitz. 2008**. Epidermal growth factor stimulates Rac1 and p21-activated kinase in vascular smooth muscle cells. *Atherosclerosis* 196:92-97.

351. **Lacouture, M. E. 2006**. Mechanisms of cutaneous toxicities to EGFR inhibitors. *Nat.Rev.Cancer* 6:803-812.

352. **Brockstein, B., M. Lacouture, and M. Agulnik. 2008**. The role of inhibitors of the epidermal growth factor in management of head and neck cancer. *J.Natl.Compr.Canc.Netw.* 6:696-706.

353. **Takeuchi, K., T. Shin-ya, K. Nishio, and F. Ito. 2009**. Mitogen-activated protein kinase phosphatase-1 modulated JNK activation is critical for apoptosis induced by inhibitor of epidermal growth factor receptor-tyrosine kinase. *FEBS J.* 276:1255-1265.

354. **Wang, L. M., A. Kuo, M. Alimandi, M. C. Veri, C. C. Lee, V. Kapoor, N. Ellmore, X. H. Chen, and J. H. Pierce. 1998**. ErbB2 expression increases the spectrum and potency of ligand-mediated signal transduction through ErbB4. *Proc.Natl.Acad.Sci.U.S.A* 95:6809-6814.

355. **Alimandi, M., L. M. Wang, D. Bottaro, C. C. Lee, A. Kuo, M. Frankel, P. Fedi, C. Tang, M. Lippman, and J. H. Pierce. 1997**. Epidermal growth factor and betacellulin mediate signal transduction through co-expressed ErbB2 and ErbB3 receptors. *EMBO J.* 16:5608-5617.

356. **Qiu, Y., L. Ravi, and H. J. Kung. 1998**. Requirement of ErbB2 for signalling by interleukin-6 in prostate carcinoma cells. *Nature* 393:83-85.

357. **Gao, S. P., K. G. Mark, K. Leslie, W. Pao, N. Motoi, W. L. Gerald, W. D. Travis, W. Bornmann, D. Veach, B. Clarkson, and J. F. Bromberg. 2007**. Mutations in the EGFR kinase domain mediate STAT3 activation via IL-6 production in human lung adenocarcinomas. *J.Clin.Invest* 117:3846-3856.

358. **Mascia, F., V. Mariani, G. Girolomoni, and S. Pastore. 2003**. Blockade of the EGF receptor induces a deranged chemokine expression in keratinocytes leading to enhanced skin inflammation. *Am.J.Pathol.* 163:303-312.

359. **Pastore, S., F. Mascia, F. Mariotti, C. Dattilo, V. Mariani, and G. Girolomoni. 2005**. ERK1/2 regulates epidermal chemokine expression and skin inflammation. *J.Immunol.* 174:5047-5056.

360. **Levitzki, A. and E. Mishani. 2006**. Tyrphostins and other tyrosine kinase inhibitors. *Annu.Rev.Biochem.* 75:93-109.

361. **Bierman, A., A. Yerrapureddy, N. M. Reddy, P. M. Hassoun, and S. P. Reddy. 2008**. Epidermal growth factor receptor (EGFR) regulates mechanical ventilation-induced lung injury in mice. *Transl.Res.* 152:265-272.